

**SPECTRUM SENSING USING SUB-NYQUIST  
RATE SAMPLING**

BY

**ZAHID SALEEM**

A Thesis Presented to the  
DEANSHIP OF GRADUATE STUDIES

**KING FAHD UNIVERSITY OF PETROLEUM & MINERALS**  
DHAHRAN, SAUDI ARABIA

In Partial Fulfillment of the  
Requirements for the Degree of

**MASTER OF SCIENCE**

In

**ELECTRICAL ENGINEERING**

MAY 2012

**KING FAHD UNIVERSITY OF PETROLEUM & MINERALS**  
**DHAHRAN, SAUDI ARABIA**

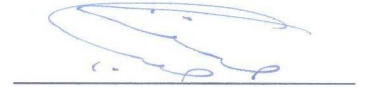
**DEANSHIP OF GRADUATE STUDIES**

This thesis, written by Zahid Saleem under the direction of his thesis advisor and approved by his thesis committee, has been presented to and accepted by the Dean of Graduate Studies, in partial fulfillment of the requirements for the degree of **MASTER OF SCIENCE** in **ELECTRICAL ENGINEERING**.

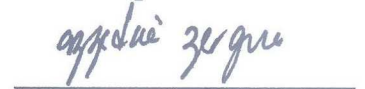
Thesis Committee



Thesis Advisor  
**Dr. Samir Al-Ghadhban**



Co-advisor  
**Dr. Tareq Y. Al-Naffouri**



Member  
**Dr. Azzedine Zerguine**



Member  
**Dr. Abdelmalek Zidouri**



Member  
**Dr. Ali Ahmad Al-Shaikhi**



Department Chairman  
**Dr. Ali Ahmad Al-Shaikhi**



Dean of Graduate Studies  
**Dr. Salam A. Zummo**

20/5/12

Date



*This thesis is dedicated to most loving,*

*caring and beautiful family I have...*

*Love you all!*

## ***ACKNOWLEDGEMENT***

*In the name of ALLAH, the Beneficent the Most Merciful*

All honor and grandeur goes to Allah Almighty who gave me the strength and endurance to carry out this work.

First of all I would like to show my gratitude to esteemed university, **King Fahd University of Petroleum and Minerals**, and its learned faculty members for providing me with quality education that paved my way through my Master's studies and thesis work.

I would like to pay my immense regard and appreciation to my thesis advisor **Dr. Samir Al-Ghadhban** for his consistent guidance, motivation and feedback during the course of this research work. Beside research work, he is always there to provide me advice on shaping up my career and future goals.

I would like to express my appreciation to Dr. Tareq Y. Al-Naffouri for helping me with my research work. I am heartily thankful to the efforts he put in while encouraging and mentoring me. I extend my deepest gratitude to my thesis committee members Dr. Azzedine Zerguine, Dr. Abdelmalek Zidouri and Dr. Ali Ahmad Al-Shaikh who gave insightful comments and reviewed my work.

I owe thanks to my seniors Ahmed Abdul Quadeer, Muhammad Saqib Sohail, Raza Umar and Dr. Muhammad Omer Bin Saeed whose consistent guidance and support helped me during the course of Master's studies and research work. I would also like to thanks all my friends here at KFUPM who made my stay at KFUPM pleasant.

I would also like to thanks my (always there friends) friends Rana Umer Sadaqat, Waqas Asif and Zohaib Tanveer whose consistent support and encouragement made my stay at Saudi Arabia a lot pleasant. Thanks guys, you were always there for me.

Last, but most important, I thank my family: my father Muhammad Aslam Saleem and my mother Naseem Akhtar for indescribable support, love and confidence they provided during course of my foreign studies. My sister Nazia Riaz , Sobia Khaleeq and Faiza Saleem for being always there to listen to me, encouraging me, motivating me and standing up for me. My brothers Shahid Saleem, Riaz Ahmad Bashir and Khaleeq Hassan for mentoring me and giving me immense support and motivation. My nephews and nieces whom love always kept me happy and feel good.

*May Allah help us in following Islam according to Quran and Sunnah (Ameen)*

# TABLE OF CONTENTS

TABLE OF CONTENTS .....	VI
LIST OF TABLES .....	X
LIST OF FIGURES .....	XI
TABLE OF NOTATIONS .....	XIII
TABLE OF ABBREVIATIONS .....	XIV
THESIS ABSTRACT (ENGLISH) .....	XV
THESIS ABSTRACT (ARABIC) .....	XVI
CHAPTER 1 INTRODUCTION .....	1
1.1 COGNITIVE RADIO .....	4
1.1.1 COGNITIVE RADIO CHARACTERISTICS .....	4
1.1.1.1 Cognitive Capability .....	5
1.1.1.2 Reconfigurability .....	8
1.1.2 SPECTRUM SENSING .....	8
1.1.2.1 Key Challenges in Spectrum Sensing .....	8
1.2 SCOPE OF WORK .....	11
1.3 CONTRIBUTIONS OF THE THESIS .....	12
CHAPTER 2 FUNDAMENTAL CONCEPTS .....	13
2.1 COMPRESSIVE SENSING .....	13
2.1.1 HISTORY .....	14
2.1.2 MOTIVATION .....	14

2.1.3 THEORY OF COMPRESSIVE SENSING .....	15
2.1.3.1 The Sensing Problem .....	17
2.1.3.2 Sparse Signal Recovery .....	20
2.2 BLIND SOURCE SEPARATION .....	21
2.2.1 MIXING MODELS FOR BSS TECHNIQUES .....	22
2.3 CONCLUSION .....	25
<b>CHAPTER 3 LITERATURE SURVEY .....</b>	<b>26</b>
3.1 SPECTRUM SENSING TECHNIQUES FOR COGNITIVE RADIO .....	26
3.1.1 ENERGY DETECTION .....	26
3.1.2 WAVEFORM BASED SENSING .....	27
3.1.3 CYCLOSTATIONARITY-BASED SENSING .....	28
3.1.4 MATCHED FILTERING .....	28
3.2 SPECTRUM SENSING USING COMPRESSIVE SENSING .....	29
3.3 DRAWBACKS OF COMPRESSIVE SENSING APPROACH .....	35
3.3.1 COMPUTATIONAL COMPLEXITY .....	36
3.3.2 STRUCTURE OF SENSING MATRIX .....	37
3.3.3 EVALUATION OF PERFORMANCE .....	37
3.3.4 USAGE OF APRIORI INFORMATION .....	37
3.3.5 Bottleneck on Performance .....	38
3.4 STRUCTURE BASED BAYESIAN SPARSE RECONSTRUCTION .....	38
3.4.1 ESTIMATION OF SPARSE SIGNAL .....	40
3.4.2 EVALUATION OVER $S$ .....	42
3.4.3 SIGNAL RECONSTRUCTION METHODOLOGY USING SBBSR .....	44
3.4.3.1 Correlation of Signal and Sensing Matrix .....	44
3.4.3.2 Semi-Orthogonal Cluster Formulation .....	45

3.4.3.3 Find Supports and Likelihoods.....	46
3.4.3.4 Evaluate MAP Estimate .....	46
3.5 CONCLUSION .....	46
<b>CHAPTER 4 BLIND SOURCE SEPERATION BASED THRESHOLD CALCULATION .....</b>	<b>47</b>
4.1 SYSTEM MODEL .....	48
4.2 PROBLEM STATEMENT.....	49
4.3 BLIND SOURCE SEPARATION APPROACH TO EDGE DETECTION .....	53
4.4 SIMULATION .....	57
4.5 CONCLUSION .....	60
<b>CHAPTER 5 SPECTRUM SENSING USING SBBSR APPROACH .....</b>	<b>61</b>
5.1 SBBSR APPROACH FOR SPECTRUM SENSING .....	62
5.2 SIGNAL MODEL FOR SIMULATION .....	68
5.3 SIMULATION RESULTS.....	70
<i>5.3.1 TRANSMITTED SIGNAL DISTRIBUTION IS KNOWN .....</i>	<i>71</i>
5.3.1.1 Case 1 .....	72
5.3.1.2 Case 2 .....	76
5.3.1.3 Case 3 .....	80
<i>5.3.2 TRANSMITTED SIGNAL DISTRIBUTION IS UNKNOWN .....</i>	<i>83</i>
5.3.2.1 Case1 .....	84
5.3.2.2 Case 2 .....	85
5.3.2.3 Case3 .....	87
5.4 CONCLUSION .....	89
<b>CHAPTER 6 SPECIAL CASE: OFDM SIGNAL.....</b>	<b>90</b>
6.1 DIGITAL VIDEO BROADCASTING-TERRESTRIAL OFDM SYSTEM .....	90
6.2 SIMULATION RESULTS.....	95



6.2.1 SPECTRUM SENSING USING SBBSR ALGORITHM .....	95
6.2.2 PRIMARY USER SIGNAL DISTRIBUTION IS KNOWN .....	97
6.2.2.1 Case 1 .....	99
6.2.2.2 Case 2 .....	101
6.2.3 PRIMARY USER SIGNAL DISTRIBUTION IS UN-KNOWN .....	103
6.2.3.1 Case1 .....	104
6.2.3.2 Case 2 .....	105
6.3 CONCLUSION .....	106
<b>CHAPTER 7 CONCLUSION AND FUTURE WORK .....</b>	<b>107</b>
7.1 CONCLUSION .....	107
7.2 FUTURE WORK .....	108
<b>REFERENCES .....</b>	<b>109</b>
<b>VITA .....</b>	<b>114</b>

# LIST OF TABLES

TABLE 5-1: CLUSTER INFORMATION .....	65
TABLE 5-2: MAP ESTIMATES FOR CORRESPONDING SUPPORT SIZES.....	67
TABLE 5-3: REQUIRED VALUES BY SBBSR ALGORITHMS FOR CASE 1.....	74
TABLE 5-4: WORKING RANGE FOR KNOWN PRIMARY USER DISTRIBUTION - CASE 1.....	76
TABLE 5-5: REQUIRED VALUES BY SBBSR ALGORITHMS FOR CASE 2.....	78
TABLE 5-6: WORKING RANGE FOR KNOWN PRIMARY USER DISTRIBUTION - CASE 2.....	80
TABLE 5-7: REQUIRED VALUES BY SBBSR ALGORITHMS FOR CASE 3.....	82
TABLE 5-8: WORKING RANGE FOR KNOWN PRIMARY USER DISTRIBUTION - CASE 2.....	83
TABLE 5-9: WORKING RANGE FOR UN-KNOWN PRIMARY USER DISTRIBUTION - CASE 1 .....	85
TABLE 5-10: WORKING RANGE FOR UN-KNOWN PRIMARY USER DISTRIBUTION - CASE 2 .....	87
TABLE 5-11: WORKING RANGE FOR UN-KNOWN PRIMARY USER DISTRIBUTION - CASE 3 .....	89
TABLE 6-1: DESCRIPTION OF VARIABLES FOR GENERALIZED DVB-T SYSTEM .....	92
TABLE 6-2: NUMERICAL VALUES FOR OFDM SYMBOL IN DVB-T $2k$ MODE .....	93
TABLE 6-3: SIMULATED OFDM SYMBOL IN DVB-T $2k$ MODE .....	94
TABLE 6-4: CLUSTER INFORMATION FOR DVB-T SYSTEM .....	97
TABLE 6-5: MAP ESTIMATES FOR CORRESPONDING SUPPORT SIZES - DVB-T SYSTEM.....	98
TABLE 6-6: REQUIRED VALUES BY SBBSR ALGORITHM – DVB-T CASE 1.....	101
TABLE 6-7: REQUIRED VALUES BY SBBSR ALGORITHM – DVB-T CASE 2.....	102

# LIST OF FIGURES

FIGURE 1.1: NTIA'S FREQUENCY ALLOCATION CHART .....	2
FIGURE 1.2: MEASURED SPECTRUM UTILIZATION VS. FREQUENCY FOR THE MEASUREMENTS RECORDED IN ANNAPOLIS.....	3
FIGURE 1.3: OPPORTUNISTIC ACCESS FOR COGNITIVE RADIO.....	5
FIGURE 1.4: A) TEMPORAL SPECTRUM HOLE DETECTION B) SPATIAL SPECTRUM HOLE DETECTION .....	6
FIGURE 1.5: COGNITIVE CYCLE .....	7
FIGURE 1.6: HIDDEN PRIMARY USER PROBLEM IN CR .....	10
FIGURE 2.1: EXAMPLE OF MRI A) IN SPACE DOMAIN B) IN FREQUENCY DOMAIN .....	16
FIGURE 2.2: COMPRESSIVE SENSING MEASUREMENT PROCESS .....	18
FIGURE 2.3: A) 1 MEGAPIXEL IMAGE B) WAVELET COEFFICIENTS.....	18
FIGURE 2.4: BLOCK DIAGRAM FOR BLIND SOURCE SEPARATION.....	22
FIGURE 2.5: BLOCK DIAGRAM ILLUSTRATING BSS SYSTEM .....	23
FIGURE 3.1: ENERGY DETECTION USING WELCH'S PERIODOGRAM.....	27
FIGURE 3.2: PSD OF ASSUMED SIGNAL .....	30
FIGURE 3.3: A PARALLEL STRUCTURE FOR SPECTRUM SENSING BASED ON CS.....	33
FIGURE 3.4: FLOW CHART OF ORTHOGONAL CLUSTERING ALGORITHM .....	45
FIGURE 4.1: (A) INCOMING SIGNAL PSD; (B) OUTPUT OF EDGE DETECTION TECHNIQUE.....	51
FIGURE 4.2: (A) INCOMING SIGNAL PSD; (B) OUTPUT OF EDGE DETECTION TECHNIQUE.....	52
FIGURE 4.3: FLOWCHART OF PROPOSED ALGORITHM .....	58
FIGURE 4.4: SUCCESS RATIO VERSUS SNR.....	59
FIGURE 4.5: PROBABILITY OF DETECTION VERSUS SNR.....	59
FIGURE 5.1: RECEIVED SIGNAL AT CR.....	63
FIGURE 5.2: CORRELATION AMONG COLUMNS OF SENSING MATRIX .....	64

FIGURE 5.3: CORRELATION OF OBSERVED SIGNAL WITH SENSING MATRIX .....	64
FIGURE 5.4: RECOVERED SPECTRUM.....	68
FIGURE 5.5: ASSUMED WIDEBAND SIGNAL – FLAT PSD .....	70
FIGURE 5.6: ASSUMED WIDEBAND SIGNAL - NON FLAT PSD .....	71
FIGURE 5.7: FLOW CHART OF MODIFIED SBBSR ALGORITHM .....	74
FIGURE 5.8: PROBABILITY OF DETECTION FOR KNOWN PRIMARY USER DISTRIBUTION - CASE 1.....	75
FIGURE 5.9: SBBSR ALGORITHM FOR APRIORI LENGTH KNOWLEDGE .....	78
FIGURE 5.10: PROBABILITY OF DETECTION FOR KNOWN PRIMARY USER DISTRIBUTION - CASE 2.....	79
FIGURE 5.11: PROBABILITY OF DETECTION FOR KNOWN PRIMARY USER DISTRIBUTION - CASE 3.....	82
FIGURE 5.12: PROBABILITY OF DETECTION FOR UN-KNOWN PRIMARY USER DISTRIBUTION - CASE 1.....	84
FIGURE 5.13: PROBABILITY OF DETECTION FOR UN-KNOWN PRIMARY USER DISTRIBUTION - CASE 2.....	86
FIGURE 5.14: PROBABILITY OF DETECTION FOR UN-KNOWN PRIMARY USER DISTRIBUTION - CASE 3.....	88
FIGURE 6.1: OFDM SIGNAL GENERATION .....	95
FIGURE 6.2: OBSERVED SPECTRUM .....	96
FIGURE 6.3: RECONSTRUCTION OF SPECTRUM - DVB-T SYSTEM .....	99
FIGURE 6.4: OBSERVED SPECTRUM WITH MULTIPLE PRIMARY USERS – DVB-T SYSTEM.....	100
FIGURE 6.5: PROBABILITY OF DETECTION FOR KNOWN PRIMARY USER DISTRIBUTION – DVB-T CASE 1 .....	101
FIGURE 6.6: PROBABILITY OF DETECTION FOR KNOWN PRIMARY USER DISTRIBUTION – DVB-T CASE 2 .....	103
FIGURE 6.7: PROBABILITY OF DETECTION FOR UN-KNOWN PRIMARY USER DISTRIBUTION – DVB-T CASE 1 .....	104
FIGURE 6.8: PROBABILITY OF DETECTION FOR UN-KNOWN PRIMARY USER DISTRIBUTION – DVB-T CASE 2 .....	105

## TABLE OF NOTATIONS

Symbol	Explanation
$y$	Observed Signal
$x$	Transmitted Signal
$n$	Additive White Gaussian Noise
$\Psi$	Basis Matrix
$\Phi$	Sensing Matrix
$\rho_s$	Wavelet Transformed Signal
$\hat{y}$	Correlation Vector Between Observed Signal and $\Theta$
$W$	Un-mixing Matrix
$\Theta$	Sensing Matrix times Basis Matrix
$F$	Discrete Fourier Transform Matrix
Scalars	Represented by Upper Case Letter e.g. N
Vectors	Represented by Bold Face Small Case Letter e.g. $y$
Matrices	Represented by Bold Face Small Case Letter e.g. $W$

## TABLE OF ABBREVIATIONS

Abbreviation	Explanation
ADC	Analog to Digital Converter
BSS	Blind Source Separation
CR	Cognitive Radio
CS	Compressive Sensing
DFT	Discrete Fourier Transform
DTV	Digital Terrestrial Television
DVB-T	Digital Video Broadcasting-Terrestrial
FCC	Federal Communications Commission
IDFT	Inverse Discrete Fourier Transform
MAP	Maximum A posteriori Probability
PSD	Power Spectral Density
SBBSR	Structure Based Bayesian Sparse Recovery
SDR	Software Defined Radio
SNR	Signal to Noise Ratio

## THESIS ABSTRACT (ENGLISH)

**NAME:** Zahid Saleem

**TITLE OF STUDY:** Spectrum Sensing Using Sub-Nyquist Rate Sampling

**MAJOR FIELD:** Electrical Engineering

**DATE OF DEGREE:** May, 2012

This thesis proposes solution for two different problems. One it provide solution to extract the frequency band boundaries information efficiently from the observed spectrum. Second it performs spectrum sensing on the signal acquired at less than Nyquist rate samples. Applying wavelet transform on the observed wideband spectrum generates edges (peaks) which contain information regarding frequency band locations. In the presence of noise, the wavelet transform generates a mixture of true peaks and noisy peaks. A threshold value is proposed for extracting the true peak information. Sensing the wideband spectrum puts constraints on hardware. Spectrum sensing is a time dependent process. Sampling a wideband signal based on Nyquist sampling theorem may require more time than given sensing duration. To solve this problem, observed spectrum is acquired at less than (required) Nyquist rate samples. Spectrum sensing is performed using the structure based Bayesian sparse reconstruction algorithm. Comparison of results with the techniques present in literature showed considerable improvement.

## THESIS ABSTRACT (ARABIC)

### ملخص الرسالة

الاسم: زاهد سليم

: إستشعار الطيف بواسطة عينات أقل من عينات نايكوست المطلوبه عنوان البحث

مجال التخصص : قسم الهندسة الكهربائية

مايو، : 2012 التاريخ على درجة

هذه الرسالة تفتح حلولاً لمشكلتين مختلفتين. الأولى هي توفير معلومات عن حدود نطاق التردد بكفاءة عالية من الطيف الملاحظ. والثانية هي القيام بأداء الإستشعار عن الطيف بإشارات ذات معدل أقل من عينات نايكويست. تطبيق تحويل ويفليت يولد قمم تدل على حدود النطاق الترددي. وفي وجود الضوضاء، تحويل الموجات يولد مزيجاً من قمم حقيقيه وصاخبة. نقترح في هذه الرسالة استخدام عتبة فاصله تساعد في استخراج القمم الحقيقية. كما أننا نقوم بإستخدام عينات من الإشاره المستقبلة أقل بكثير من عينات نايكوست وهذا يساعد على تقليل كمية المعالجة المطلوبة. إضافة إلى ما ذكر سابقاً، فإننا نستخدم تقنية جديده لإعاده الإشاره المظغوطه مبنية على اساس بايسان. نتائج البحث تشير إلى وجود تحسن كبير في أداء الإستشعار المظغوط مقارنة مع الطرق المعروضه في هذا المجال سابقاً.



# **CHAPTER 1**

## **INTRODUCTION**

Radio frequency spectrum is a limited natural resource. Modern wireless service providers aim to provide high data rate applications to numerous customers simultaneously. These high data rate applications require more radio frequency spectrum. Licenses are usually required for operation on certain frequency bands. Government agencies provide licenses to wireless service providers for use of certain frequency band. Over past years fixed spectrum allocation scheme was working fine but with the dramatic increase in requirement of more spectrum reinforces the scarcity mindset. National telecommunications and information administration's (NTIA) frequency allocation chart, as shown in Figure 1.1, shows unavailability of the spectrum for future wireless service providers [1].

Federal communications commission (FCC) carried out various surveys to investigate the spectrum scarcity. Observed rationale behind the spectrum scarcity was underutilization of spectrum rather than the unavailability of spectrum [2]. Underutilization of spectrum leads us to think of the spectrum holes i.e. primary user is

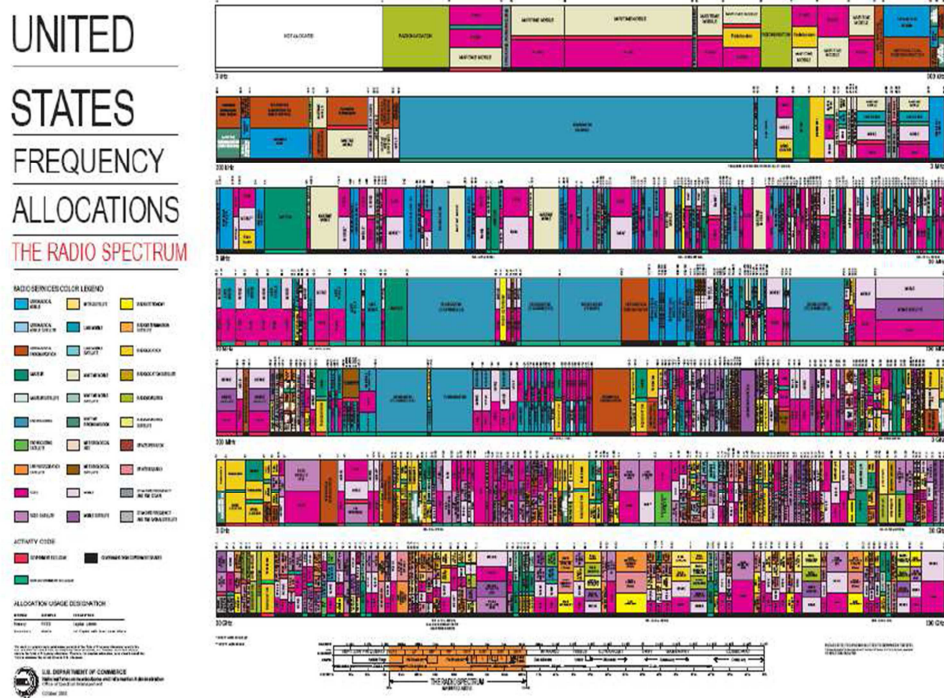


Figure 1.1: NTIA's Frequency Allocation Chart

not using the available radio spectrum all the time. Figure 1.2 shows typical usage of the frequency spectrum in Annapolis, United States [3].

According to FCC [2], the spectrum utilization varies from 15% to 85% with high variance in time and space. Spectrum occupancy measurement project concluded that the average spectrum occupancy over multiple locations is 5.2%, with a maximum of 13.1% [4]. These statistics raises the question on appropriateness of the current regulatory regime. Solving this question leads to solution of the spectrum scarcity.

Developing a new spectrum allocation chart (as shown in Figure 1.1) could be one of the possible solutions. But is this a practical or implementable solution for current and

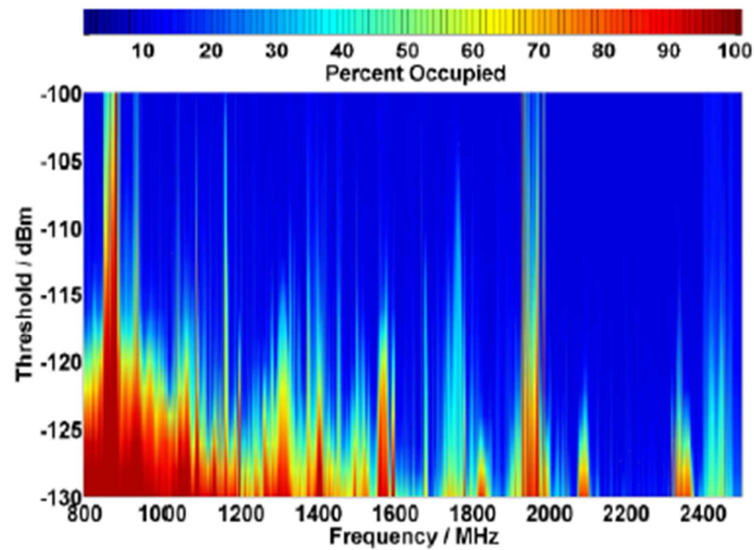


Figure 1.2: Measured spectrum utilization vs. frequency for the measurements  
recorded in Annapolis

future wireless systems? Of course not! Future wireless communication systems cannot be predicted. Agitating spectrum allocation scheme of the current wireless service providers is not a good option.

Dynamic Spectrum Access (DSA) is proposed as a solution to solve the spectrum scarcity versus underutilization phenomena. In DSA unlicensed users (or secondary user) are allowed to utilize the vacant bands of licensed (or primary user) users provided interference is minimal. Cognitive Radio (CR) is the enabling technology behind opportunistic access of licensed user's spectrum.

## 1.1 COGNITIVE RADIO

CR is the evolution of Software Defined Radio (SDR). SDR has capability to operate in different standards (air interfaces) with different frequency bands and leads to development of multiband base stations [5]. CR is an intelligent wireless communication system which upon interaction with the environment exploits any available spectrum opportunities. In 1991, J. Mitola introduces the notation of SDR. In 1999, J. Mitola with G. Maguire used the term CR for the first time [6]. FCC has defined CR as [7]

*“A **Cognitive Radio** is a radio that can change its transmitter parameters based on interaction with the environment in which it operates.”*

Based on the above definition, in contrast to traditional radio, CR is an intelligent radio that changes its parameters on the go. CR keeps track of the spectrum and accomplishes opportunistic accesses whenever possible. Primary goal of any CR is to utilize the spectrum efficiently. Figure 1.3 [6], pictorially explains aforementioned discussion. Assume that green blocks represent the spectrum occupancy by primary user (or licensed user). The spaces (or spectrum holes) between these blocks point the opportunity for CR.

### **1.1.1 COGNITIVE RADIO CHARACTERISTICS**

Cognitive functionality is achieved by two main characteristics of CR i.e. cognitive

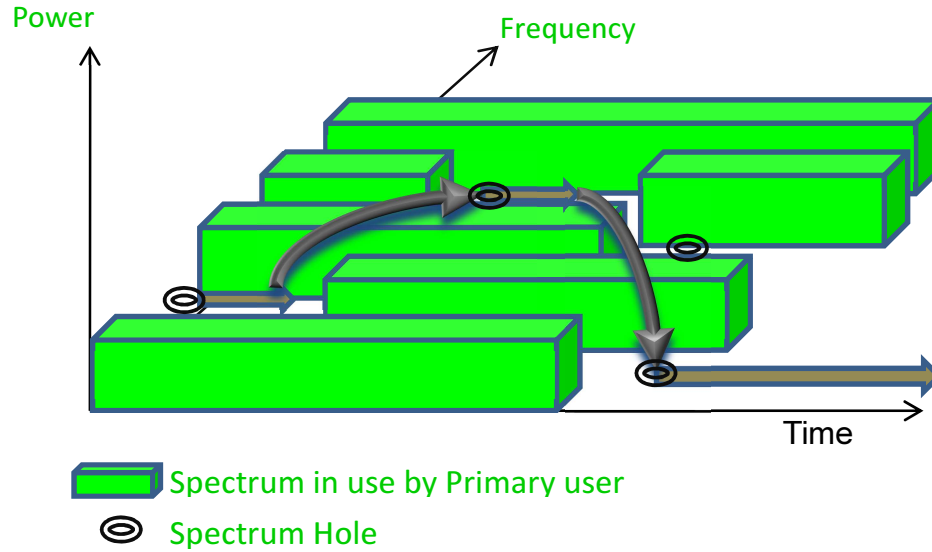


Figure 1.3: Opportunistic Access for Cognitive Radio

capability and reconfigurability.

#### 1.1.1.1 Cognitive Capability

Cognitive capability refers to ability of CR to interact with the surrounding environment and acquire the information of vacant bands or spectrum holes in the corresponding spectrum [8]. Spectrum holes can be classified in two categories: temporal spectrum holes and spatial spectrum holes.

##### **1- Temporal Spectrum Hole**

Temporal spectrum hole refers to the situation where no primary user activity is observed over corresponding spectrum and hence CR can avail spectrum during current time slot. Figure 1.4a [9], depicts the scenario of temporal spectrum hole detection. Secondary user lies in the same coverage area of primary transmission. Sensing in this case is relatively easy as the CR requires similar detection sensitivity as primary receiver.

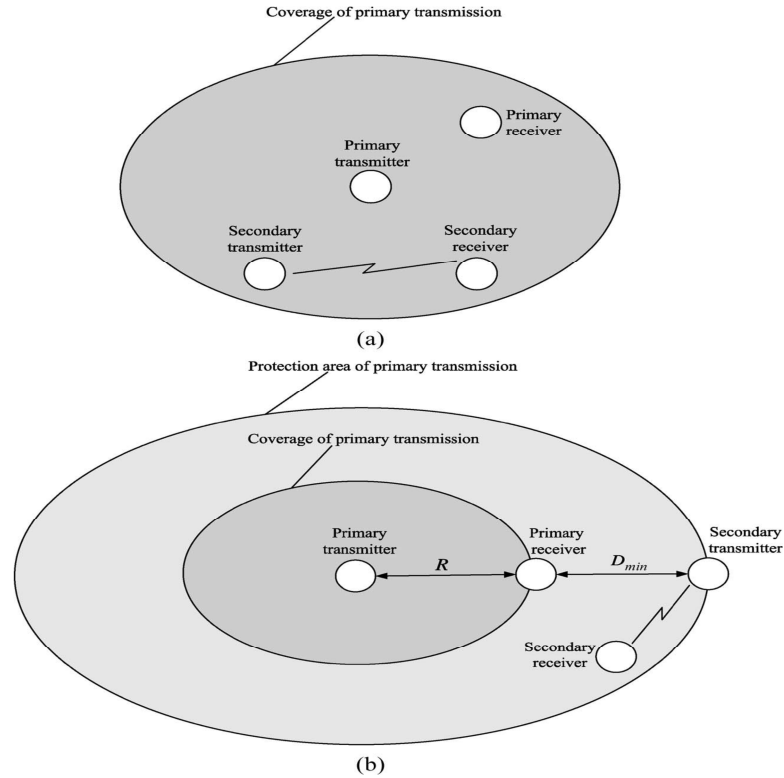


Figure 1.4: a) Temporal Spectrum Hole Detection b) Spatial Spectrum Hole Detection

## 2- Spatial Spectrum Hole

Spatial spectrum hole exists when the secondary user resides outside the coverage area of primary user and still can access corresponding spectrum. This is depicted in Figure 1.4b [9]. Secondary user can use the available spectrum provided there is no interference to primary user. In such scenario, detection sensitivity of the secondary user must be higher than that of primary user. Also the secondary user must be at considerable distance from primary receiver so that chance of interference between secondary user and primary communication is negligible.

Figure 1.5 shows the cognitive radio operation also called as “Cognitive cycle” [8], [10]. Cognitive cycle involves

**Spectrum Sensing** is the most important task of cognitive cycle. CR has to detect the spectrum hole on which it will transmit its data.

**Spectrum Analysis** helps CR to predict the available channel capacity in spectrum hole for secondary user.

**Spectrum Decision** chooses the best available spectrum hole to meet user requirements.

Hence, cognitive capability ensures the availability of best available spectrum for secondary user.

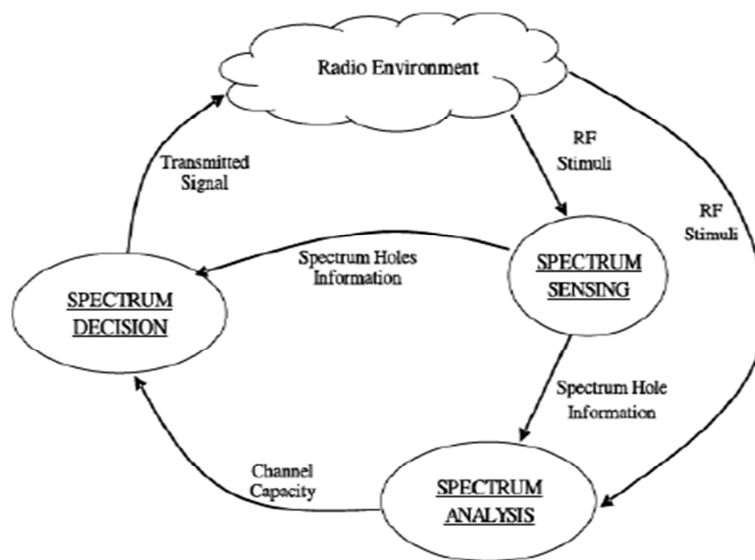


Figure 1.5: Cognitive Cycle

### 1.1.1.2 Reconfigurability

Reconfigurability adds adaptive capability in a CR, making it an example of feedback communication system [8]. When primary user starts transmission, CR has to leave that band and has to shift to a new band (or spectrum hole). Reconfigurability ensures that CR transmission parameters must be changed accordingly so that CR again chooses the best available spectrum for secondary user.

## **1.1.2 SPECTRUM SENSING**

Spectrum sensing is the essence of CR. As soon CR starts its functioning, its first and most basic operation is to detect spectrum holes. Spectrum holes detection is done using spectrum sensing. Efficient performance of spectrum sensing is necessary so that whenever there is a vacant band CR makes full use of it.

### 1.1.2.1 Key Challenges in Spectrum Sensing

Spectrum sensing enables a CR to scan wide range of frequencies to efficiently use any vacant band. In order to analyze spectrum sensing problem, it is appropriate to first investigate the practical challenges associated with it. Some of the key challenges faced by spectrum sensing are discussed below.

#### **1- Restricted Sensing Ability**

CR has no information regarding the primary user. CR has to scan a multidimensional environment with limited scanning ability. These issues makes spectrum sensing a challenging task.



Possible solution to this problem could be usage of cooperative communication between secondary users.

## **2- Hardware Requirements**

CR has to sense multiple frequency bands for identification of spectrum holes. This comes with additional cost on the wideband antennas, power amplifier, high sampling rate analog to digital converters etc.

In [11], it is suggested to allow a CR to scan only a limited range of frequency band. This solution leads to usage of multiple CRs for multiple frequency bands.

## **3- Primary User Detection Sensitivity Requirement**

Shadowing and severe fading effects can decrease the sensitivity of CR to detect primary user. This problem has been shown in Figure 1.6 [12]. Poor CR sensing ability can cause interference with the primary user.

Cooperative sensing approach can be used in this respect [13]. In cooperative sensing multiple CRs cooperate with each other in a given geographical area and try to improve overall sensing performance.

## **4- Detecting Spread Spectrum Primary User**

Primary users some time incorporate the spread spectrum techniques for establishment of a secure communication. In such situation, primary user spreads the power over whole frequency range. It is difficult for the CR to detect the primary user in

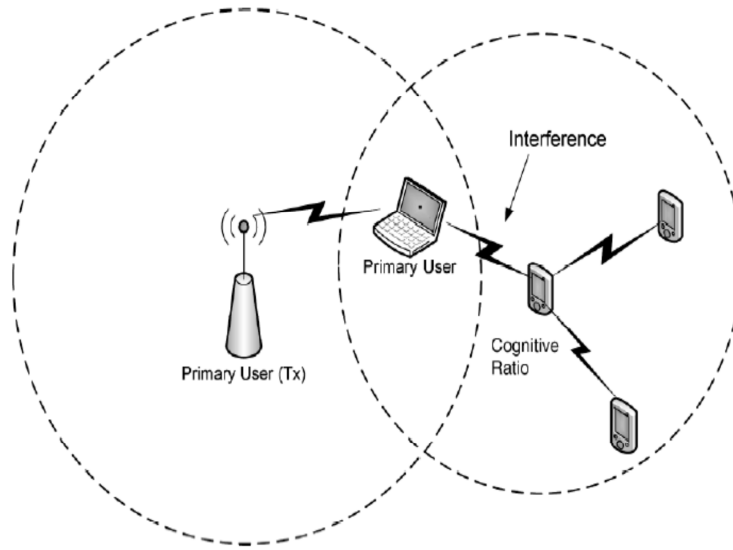


Figure 1.6: Hidden Primary User Problem in CR

the presence of such patterns. Without apriori knowledge of the hopping patterns and synchronization pulses CR cannot detect such signals [14].

### 5- Sensing Duration and Frequency

Sensing duration is related to the efficiency of a CR. Efficient CR uses less time for sensing but they have to pay price on sensing reliability. Sensing frequency depends on how often a CR has to perform the sensing operation. Optimum values of these parameters depend upon the CR abilities and primary user temporal characteristic in the radio environment [12].

### 6- Security

In multiuser environment, there is a possibility that, a secondary user may act as a primary user by intruding its data. This scenario is discussed in [15] and is called Primary user Emulation Attack (PUE).

## 1.2 SCOPE OF WORK

As described in section 1.1.2.1, spectrum sensing has some challenges associated with its implementation. Performing spectrum sensing in the wideband regime is a major challenge. In the wideband regime, CR has to sense a wide range of frequency band. To completely recover an analog signal from its samples the Nyquist sampling theorem has been followed i.e. sampling frequency must be twice the maximum frequency ( $f_s \geq 2 f_{max}$ ). In order to sense a wideband signal following two approaches have been proposed in the literature [16].

- 1- Radio front end can be designed to have a bank of narrowband (tunable) band pass filters to search multiple narrow frequency bands (at a time). This scheme requires lots of RF components; and tuning range of each filter is predefined.
- 2- Radio front end can have the wideband circuitry followed by high speed digital signal processor which search over multiple bands concurrently.

In the wideband regime, Nyquist sampling theorem requires huge amount of samples. Spectrum sensing is a time dependent process. Due to timing constraints there is a possibility that small number of samples (as compared to required) are acquired. This amount of information may not be sufficient to perform spectrum sensing efficiently.

If a signal is sparse in some domain, it can be acquired (at sub-Nyquist sampling rate) and reconstructed using the compressive sensing technique. As a result of this, sub-Nyquist sampling rate solutions can be provided for the observed problems. In spectrum

sensing, the observed spectrum is sparse in frequency domain (as shown in Figure 1.2). Compressive sensing technique can be used to perform spectrum sensing on the signal that is acquired at sub-Nyquist sampling rate.

### **1.3 CONTRIBUTIONS OF THE THESIS**

In this thesis, spectrum sensing problem for the wideband signals has been discussed. Two different problems were faced while working with the wideband signals and solution to them has been provided respectively.

In Chapter 4, the wavelet edge detection technique was applied on the observed wideband spectrum. This technique generates peaks which contains the frequency band boundaries information. In the presence of noise, the random noisy peaks make it hard to calculate the frequency band boundaries efficiently. A threshold value based on the blind source separation technique was obtained. This value is used to suppress the noisy peaks.

In Chapter 5, a solution for performing spectrum sensing in the wideband regime is provided. Sensing problem is time dependent and in situations it may not be possible for a cognitive radio to acquire the required amount of data. To overcome this problem, spectrum sensing has been performed on the sub-Nyquist rate sampled data. The structure based Bayesian sparse reconstruction (SBBSR) algorithm has been used in this context. Different cases, based on the various assumptions taken in the literature, are considered and analyzed.

## **CHAPTER 2**

### **FUNDAMENTAL CONCEPTS**

In this chapter brief overview of the compressive sensing and blind source separation techniques is given. Recently these techniques have found exciting applications in the field of signal processing and communications. Here we provide a brief description about these techniques.

#### **2.1 COMPRESSIVE SENSING**

Traditional trend in data reconstruction, from the observed signals or images, follows the well-known Nyquist sampling theorem. According to theorem, sampling must be done at least two times faster than the signal bandwidth. This principal is basis for most of the present stage devices like analog to digital convertors, medical imaging or audio and video devices [17]. In some applications samples collected at the Nyquist rate, results in enormous amount of data and require compression before transmission or storage. Theory of compressive sensing – also comes under terminology compressive sampling or sparse recovery – provides an efficient way of data acquisition, that overcomes the

Nyquist criteria. Compressive sensing (CS) captures and represents sparse signals at a rate lower than the Nyquist rate [18].

### **2.1.1 HISTORY**

A precursor to CS was first used in 1970s when the seismologists reconstructed images of reflective layers within the earth based on data that did not seem to satisfy Nyquist criterion [19]. Concept of CS came into picture in 2004 when David Donoho, Emmanuel Candes, Justin Romberg and Terence Tao reconstructed an image based on the data that seems insufficient by Nyquist criteria.

### **2.1.2 MOTIVATION**

Consider a scenario where few sensors (as compared to required amount) are available to acquire the desired information. For instance, it is very expensive to design sensors when performing the imaging in infrared domain. Designing of pixels in the infrared domain is very expensive. So less amount of sensors than required are available [20]. Measurements can also be expensive for example, fuel cell imaging [21]. In fuel cell imaging neutron scattering technique is used. Neutrons are fired at the fuel cells and the scattering patterns are observed. Neutron shooting process is very expensive process.

In medical resonance imaging (MRI), the image of a living tissue is captured. Imaging here means acquiring information about an object by collecting the Fourier coefficients. Acquiring the Fourier coefficients is time consuming process. One has to

spend plenty of time on scanner to collect these coefficients. Problems that can occur during this process are as follows

- 1- Observer starts to move, after a while, so the measurements are not accurate.
- 2- Throughput of scanner is limited.

Figure 2.1 portrays process of the MRI [22]. Figure 2.1a shows the image, to be acquired, in spatial domain and Figure 2.1b shows the frequency domain equivalent of that image. The Fourier coefficients are calculated along the radio lines. Assume Figure 2.1a is  $1000 \times 1000$  pixel image, which according to today imaging is not that large. There are 1 million pixel values and assume there are 22 radio lines in Figure 2.1b. On each radio line 1000 Fourier coefficients are required. Observed problem is an under-determined system of equations i.e. 22000 coefficients are available whereas originally this picture consists of 1 million pixels. So 98% of the information is missing. Question here rises: how to perform reconstruction?

### **2.1.3 THEORY OF COMPRESSIVE SENSING**

Compressive sensing provides reconstruction for sparse signals. Normally the signals are sparse in some domain/basis and hence CS can be used for reconstruction. We wish to acquire a discrete-time signal i.e.  $\mathbf{x} \in \mathbb{C}^N$  ( $N \times 1$  length vector) which is  $K$  sparse in some domain. This can be thought as a digital image with  $N$  pixels and with  $K$  significant coefficients in the wavelet domain [20]. Any signal can be represented in terms of

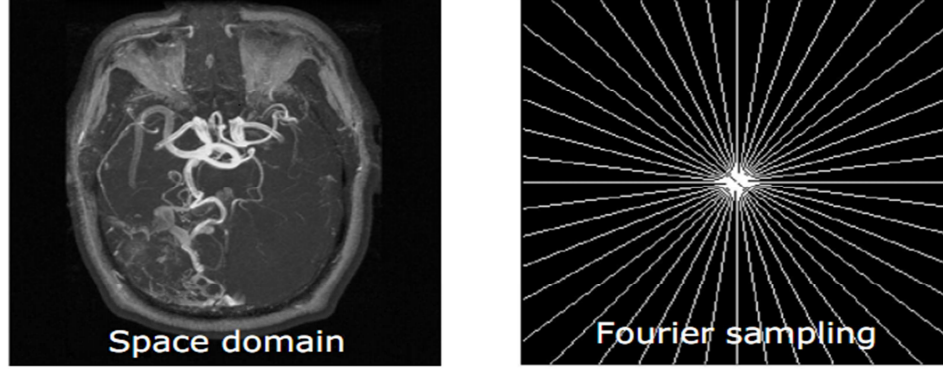


Figure 2.1: Example of MRI a) in space domain b) in Frequency domain

a basis of  $N \times 1$  vectors  $\{\psi\}_{i=1}^N$ . Corresponding basis matrix (of dimension  $N \times N$ ) can be formed as

$$\Psi = [\psi_1 | \psi_2 | \dots | \psi_N] \quad (2.1)$$

Using equation (2.1) any signal  $\mathbf{x}$  can be expressed as

$$\mathbf{x} = \sum_{i=1}^N s_i \psi_i \quad (2.2)$$

or in vector form

$$\mathbf{x} = \Psi \mathbf{s} \quad (2.3)$$

where  $\mathbf{s}$  is the  $N \times 1$  column vector of weighting coefficients. In equation (2.3)  $\mathbf{x}$  and  $\mathbf{s}$  represents the same signal in different domains i.e. one in time and other in  $\Psi$  [23]. CS is applicable to the signals that have sparse representation. Such signal  $\mathbf{x}$  is a linear combination of  $K$  basis vectors ( $K \ll N$ ) i.e. only  $K$  of the  $N$  coefficients in equation (2.2) are nonzero.



### 2.1.3.1 The Sensing Problem

Let's consider the linear measurement process that computes  $M < N$  inner products between  $\mathbf{x}$  and a collection of vectors  $\{\boldsymbol{\phi}_j\}_{j=1}^M$  as in

$$y_j = \langle \mathbf{x}, \boldsymbol{\phi}_j \rangle \quad (2.4)$$

Equation (2.4) can be written in vector form as

$$\mathbf{y} = \boldsymbol{\Phi} \mathbf{x} + \mathbf{n} = \boldsymbol{\Phi} \boldsymbol{\Psi} \mathbf{s} + \mathbf{n} = \boldsymbol{\Theta} \mathbf{s} + \mathbf{n} \quad (2.5)$$

where matrix  $\boldsymbol{\Phi}$  is obtained by stacking the measurement vectors  $\boldsymbol{\phi}_j^T$  as rows.  $\boldsymbol{\Theta}$  is  $M \times N$  sized matrix. Figure 2.2 shows illustration of equation (2.5) [23].

Two fundamental concepts that are basis of compressive sensing are

- 1- Sparsity
- 2- Incoherence

#### **Sparsity**

Consider the image in Figure 2.3a [24]. Observe that it is not sparse in the spatial domain. If it is viewed in appropriate basis then it becomes approximately sparse. Figure 2.3b shows this image in the wavelet domain. Observe that few coefficients contain most of the signal energy and rest coefficients are very small. This image can be regarded as (approximately) sparse in wavelet domain.

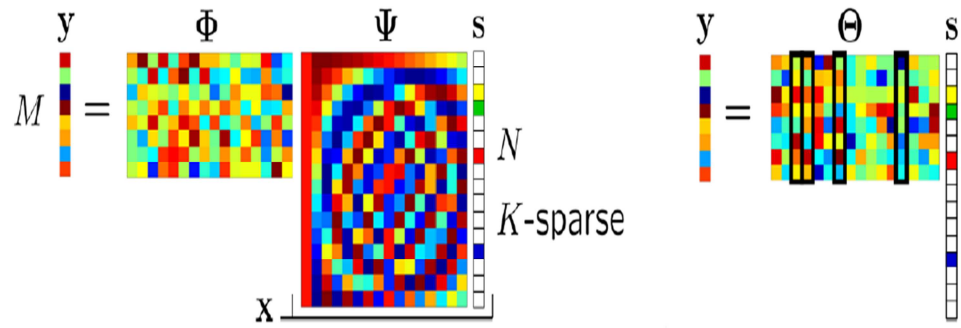


Figure 2.2: Compressive Sensing measurement process

### Incoherence

Basic goal is to reconstruct  $N$  length signal  $\mathbf{x}$  from  $M$  length measurements  $\mathbf{y}$ . There are two different domains i.e. one in which the signal is sparse  $\boldsymbol{\psi}_i$  and other in which the measurements are done i.e.  $\boldsymbol{\phi}_j$ . Coherence between the sparsity and sensing domain is defined as [25]

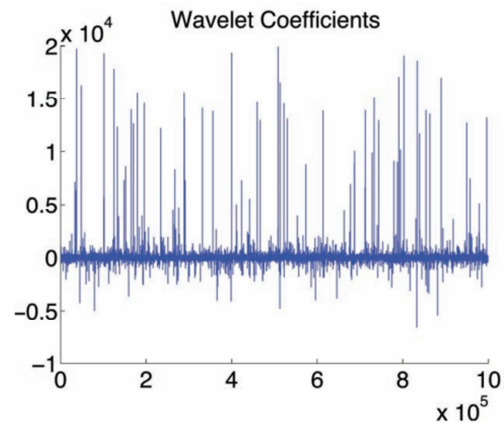


Figure 2.3: a) 1 Megapixel Image b) Wavelet coefficients

$$\mu(\Phi, \Psi) = \sqrt{N} \max_{ij} |\langle \phi_i, \psi_j \rangle| \quad (2.6)$$

whereas correlation values according to linear algebra lies in range

$$1 \leq \mu(\Phi, \Psi) \leq \sqrt{N} \quad (2.7)$$

We are interested in the pairs  $(\Phi, \Psi)$  that are coherent by value of 1 i.e. they are incoherent. For instance, coherence between the time and frequency domain is minimal i.e. equal to 1. Another incoherent pair is wavelets and noise-lets where the coherency is between  $1 \leq \mu(\Phi, \Psi) \leq 3$  [25]. Some favorable distributions to represent  $\Phi$  are [23]

1- Gaussian:  $\phi_{ij} \sim \mathcal{N}\left(0, \frac{1}{M}\right)$

2- Bernoulli:  $\phi_{ij} = \begin{cases} +\frac{1}{M} & \text{with probability } \frac{1}{2} \\ -\frac{1}{M} & \text{with probability } \frac{1}{2} \end{cases}$

3- Database-friendly:  $\phi_{ij} = \begin{cases} +\frac{1}{M} & \text{with probability } \frac{1}{6} \\ 0 & \text{with probability } \frac{2}{3} \\ -\frac{1}{M} & \text{with probability } \frac{1}{6} \end{cases}$

Choosing Gaussian measurement matrix has useful property i.e. matrix  $\Theta$  is also independent and identically Gaussian regardless of the choice of  $\Psi$ .

Restricted isometry property had been proposed by Candes and Tao [26]. This property is used to study the general robustness of measurement matrix  $\Theta$ . According to this property, for each value of  $S = 1, 2, \dots$ , define an isometry constant  $\delta_S$  for measurement matrix  $\Theta$  as the smallest number such that

$$(1 - \delta_S) \|\mathbf{s}\|_2^2 \leq \|\boldsymbol{\Theta} \mathbf{s}\|_2^2 \leq (1 + \delta_S) \|\mathbf{s}\|_2^2 \quad (2.8)$$

holds for all  $S$ -sparse vectors  $\mathbf{s}$ . If this property holds then measurement matrix approximately preserves the Euclidean length of  $S$ -sparse signals.

### 2.1.3.2 Sparse Signal Recovery

Incoherency property defined in previous section ensures that sparse signal can be fully described with  $M$  measurements. But this property does not provide information regarding reconstruction of signal. Reconstruction algorithm helps in recovering  $N$  length signal  $\mathbf{x}$  from  $M$  length  $\mathbf{y}$  measurements.

Problem discussed in equation (2.5) is an under-determined system of equations. An infinite number of solutions can be provided to solve this system. Let's define  $p$ -th power of  $l_p$  norm of vector  $\mathbf{s}$  as

$$(\|\mathbf{s}\|_p)^p = \sum_{i=1}^N |s_i|^p \quad (2.9)$$

If  $p = 0$ , equation (2.9) results in  $l_0$  norm. This norm counts the total number of non-zero entries in a given vector. For instance, a  $K$  sparse signal has  $l_0$  norm of  $K$ . Basic idea behind sparse signal reconstruction is to identify smallest subset of matrix  $\boldsymbol{\Theta}$  whose linear span contains the observations  $\mathbf{y}$  [23].

Various approaches are proposed in the literature to recover the sparse signal. One approach opted greedy search to recover the sparse signal. Some examples for greedy search algorithms are matching pursuit, projection pursuit [27], orthogonal matching

pursuit [28] and tree based matching pursuit [29]. Another approach recursively solves a sequence of iteratively re-weighted linear least squares (IRLS) problems [30].

Total number of measurements required to reconstruct the sparse signal with high probability depends on following parameters

- 1- Length of signal i.e.  $N$ .
- 2- Sparsity level i.e.  $K$  of the signal
- 3- Value of coherence between sparse domain  $\Psi$  and measurement domain  $\Phi$ .

According to [25], if we have a  $N$  length signal  $\mathbf{x}$  i.e.  $K$ -sparse in  $\Psi$  and we select  $M$  measurements uniformly at random in the  $\Phi$  domain as

$$M \geq \mu^2(\Phi, \Psi) \times K \times \log(N) \quad (2.10)$$

than the sparse signal can be recovered with overwhelming probability by solving the  $l_1$ -norm minimization problem.

## 2.2 BLIND SOURCE SEPARATION

The goal of blind source separation (BSS) technique is to recover the source signals from the observed mixture at receiver. Typically observations are obtained at the output of a set of sensors, where each sensor receives a different combination of the source signals. The aim of the BSS technique is to separate source signals from the received mixture of source signals. The adjective “blind” stresses two facts [31]

- 1- Source signals are unknown at the receiver.
- 2- No information is available about the mixing system.

Since its first development, nearly twenty years ago, the BSS has developed into an important signal processing technique. In fact BSS has become a quite important topic of research in many domains like speech enhancement, biomedical engineering, communication, remote sensing system and geophysics etc. Figure 2.4 shows the block diagram for BSS [32].

### **2.2.1 MIXING MODELS FOR BSS TECHNIQUES**

Consider the source signal vector  $[x_1(n), x_2(n), \dots, x_N]^T$ , the mixture vector  $[y_1(n), y_2(n), \dots, y_M]^T$  and the noise signal vector  $[n_1(n), n_2(n), \dots, n_M]^T$ , where  $N$  denotes the number of sources and  $M$  denotes the number of sensors (or mixtures). Figure 2.5 shows the block diagram illustrating BSS technique [33].

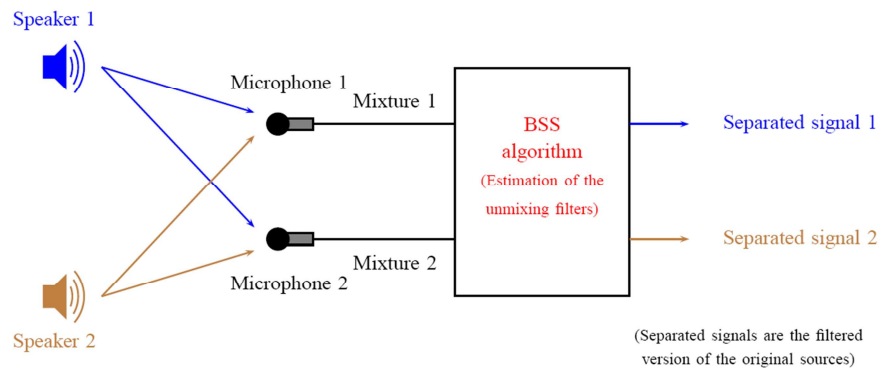


Figure 2.4: Block Diagram for Blind Source Separation

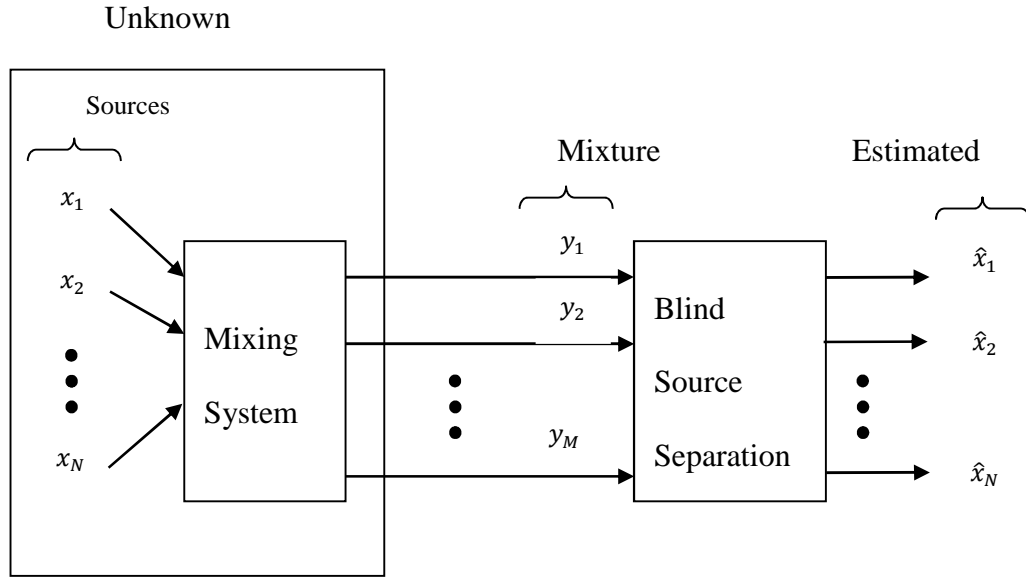


Figure 2.5: Block Diagram illustrating BSS system

There are two types of models considered for mixing of the source signals in BSS

### 1- Instantaneous Mixing Model

### 2- Convolutive Mixing Model

In instantaneous mixing model, observations at time  $n$  are only a linear combination of the sources at the same time  $n$ . Output of the sensor/receiver is called instantaneous mixture and can be described by the following equation [33]

$$y_i(n) = \sum_{j=1}^N a_{ji}(n)x_j(n) \text{ where } i \in \{1, \dots, M\} \quad (2.11)$$

where  $a_{ji}$  represents the element of mixing system. In the presence of noise received signal can be written as

$$y_i(n) = \sum_{j=1}^N a_{ji}(n)x_j(n) + n_i(n) \text{ where } i \in \{1, \dots, M\} \quad (2.12)$$

For the mixing model given in equations (2.11) and (2.12), effects such as inhomogeneities, diffraction of medium and refraction are assumed to be negligible and as a result sources are linearly super imposed by the channels. However from basic concepts of digital signal processing, physical properties of propagation channel are often mathematically modeled as convolution operator and thus a linear time-invariant model may sometimes be more accurate.

Assume FIR filter model for the propagation channel. Convulsive mixtures can be described as

$$y_i(n) = \sum_{j=1}^N \sum_{k=1}^L a_{ji}(k) x_j(n - k) \text{ where } i \in \{1, \dots, M\} \quad (2.13)$$

Where  $a_{ji}(k)$  is the  $k$ -th coefficient of the filter corresponding to the path between sources  $j$  and sensor  $i$ ,  $L$  is the filter length. For the noisy case, the model becomes [33]

$$y_i(n) = \sum_{j=1}^N \sum_{k=1}^L a_{ji}(k) x_j(n - k) + n_i(n) \text{ where } i \in \{1, \dots, M\} \quad (2.14)$$

Convulsive model fits most of the real world scenarios excluding some special cases. For instance, for time varying transfer functions or when some nonlinearity is added to the mixtures.



An important feature of the BSS problem is the relationship between  $N$  and  $M$  i.e. between the number of sources and number of observed mixtures. Three different scenarios can be described as

- 1-  $N = M$ : Problem becomes determined case.
- 2-  $N < M$ : Problem become over determined case.
- 3-  $N > M$ : Problem become under determined case.

These scenarios actually represent two level of difficulty in solving the BSS problem. Determined and over determined represent the easy level while under determined represents higher difficulty level [33].

## 2.3 CONCLUSION

In this chapter we discussed the compressive sensing technique and the blind source separation technique. Compressive sensing provides sub-Nyquist rate sampling solution to the sparse signals. This helps working at less than Nyquist sampling rate. Blind source separation provides a robust solution for separating the observed mixed signals at the receiver. Both techniques had found stimulating applications in signal processing and communications.

## **CHAPTER 3**

### **LITERATURE SURVEY**

Spectrum sensing in the wideband regime requires huge amount of samples. Sensing problem is time dependent and consequently creates burden on analog to digital converters and the digital signal processors. In this chapter previous work done on the spectrum sensing using both Nyquist and sub-Nyquist rate sampling is discussed. In addition a new algorithm for sparse signal reconstruction is also discussed.

#### **3.1 SPECTRUM SENSING TECHNIQUES FOR COGNITIVE RADIO**

In this section some of the most common techniques used for spectrum sensing are discussed. Present literature for the spectrum sensing is still in its early stages of development [12].

##### **3.1.1 ENERGY DETECTION**

Energy detection is the simplest form of signal detection technique. In classical literature it is also given the name of radiometry. This technique measures the presence

of signal by computing the energy of a received signal in a particular frequency band and comparing it with a threshold which depends on the noise floor. Sometimes spectral environment is analyzed in the frequency domain and Power Spectral Density (PSD) of the observed signal is estimated. This approach is referred as periodogram. Figure 3.1 shows the energy detection approach using Welch's periodogram [34].

Some of the challenges involved with the energy based detection are poor performance under low SNR, setting threshold value for the incoming signal and poor efficiency while detecting spread spectrum signals [12].

### **3.1.2 WAVEFORM BASED SENSING**

Some times in the wireless communication system known pattern like preambles, midambles, spread spectrum sequences etc are transmitted with the signal to assist synchronization. Such signals information is recovered by correlating the incoming signal with a known waveform. This type of signal detection is called waveform based sensing where extra information is merged in the signal at the transmitter and then signal is

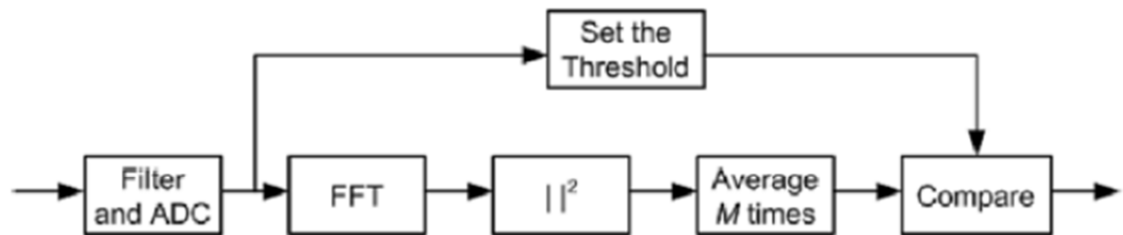


Figure 3.1: Energy Detection using Welch's Periodogram

recovered at receiver with some apriori information. This sort of sensing is only applicable to the systems with known signal patterns. The waveform based sensing is better in both convergence time and reliability than the energy based detection [35].

### **3.1.3 CYCLOSTATIONARITY-BASED SENSING**

Cyclostationarity or feature detection exploits the cyclostationarity feature presents in the incoming signal. Detection of the primary user signal is based on these features. Wireless modulated signals are generally cyclostationary as in the modulation process they are coupled with sine wave carriers, pulse trains, repeating spreading or hopping sequence etc. These processes induce periodicity in the signal making them cyclostationary. The cyclostationary based detection algorithm can differentiate between the noise and the primary transmission. They are also capable of distinguishing between different type of the primary users [12]. This sensing technique outperforms the energy based sensing scheme at low SNR. High accuracy comes with the cost of higher computational complexity. In addition, this technique also requires prior knowledge of cyclic frequencies of primary transmission.

### **3.1.4 MATCHED FILTERING**

Matched filtering is considered as the optimum method for detection of primary user provided the receiver has perfect knowledge of the transmitted signal. This scheme demodulate the receive signal and hence requires the complete knowledge of the

bandwidth, pulse shaping, operating frequency etc. These requirements make the implementation cost of CR quite expensive [12].

### 3.2 SPECTRUM SENSING USING COMPRESSIVE SENSING

In 2007 [16], Z. Tian and G.B. Giannakis performed spectrum sensing using the compressive sensing technique. Observed signal is sparse in the frequency domain. Figure 3.2 shows the frequency response of the observed signal  $\mathbf{x}(t)$ . Assumed signal ( $\mathbf{x}(t)$ ) consists of  $Z$  bands with the frequency spacing between  $Z$  bands is given as  $[f_0, f_1 \dots f_Z]$ . Following assumptions were used to solve the problem

- PSD of each band is almost flat.
- Frequency boundaries of the overall observed spectrum i.e.  $f_0$  and  $f_Z$  are known at cognitive radio.
- Number of bands i.e.  $[f_1, f_2 \dots f_{Z-1}]$  are unknown at cognitive radio.
- Noise effect on the signal is additive and white.

Assume the sensing timing window is defined as  $t \in [0, NT_0]$ .  $T_0$  represents the Nyquist sampling rate. According to the Nyquist theorem,  $N$  samples are required to reconstruct  $\mathbf{x}(t)$  without aliasing. Sampling process at a digital receiver can be expressed as

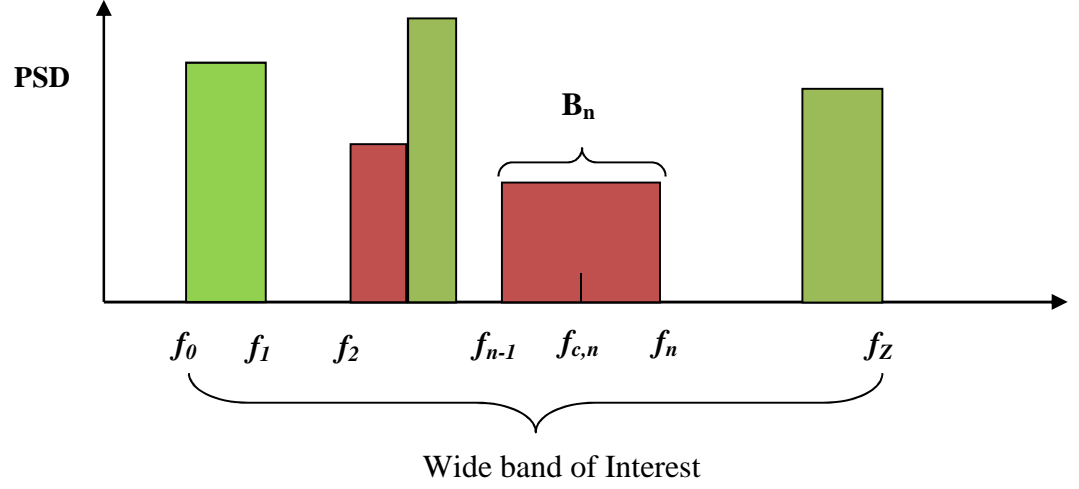


Figure 3.2: PSD of assumed Signal

$$\mathbf{y}(t) = \mathbf{S}_c^T \mathbf{x}(t) \quad (3.1)$$

where  $\mathbf{x}(t)$  represents  $N \times 1$  length vector and  $\mathbf{S}_c^T$  is an  $M \times N$  projection matrix. The process defined in equation (3.1) can be explained as a conversion of continuous domain signal  $\mathbf{x}(t)$  into the discrete sequences  $\mathbf{y}(t) \in \mathcal{C}^M$ , performed by digital receiver. In equation (3.1) when  $M = N$ , Nyquist rate uniform sampling is performed. Using  $M < N$ , performs reduced rate sampling scheme [16]. In the scenario when  $M < N$  is used, reconstruction of the received signal spectrum is performed using compressive sensing

$$\mathbf{x}(f) = \arg \min_{\mathbf{x}(f)} \|\mathbf{x}(f)\|_1, \quad s.t. \quad (\mathbf{S}_c^T \mathbf{F}_N^{-1}) \mathbf{x}(f) = \mathbf{y}_t \quad (3.2)$$

where

$$\mathbf{S}_c^T \mathbf{F}_N^{-1} \mathbf{x}(f) = \mathbf{S}_c^T \mathbf{x}(t) \quad (3.3)$$

where  $\mathbf{S}_c^T$  represents identity matrix of dimensions  $M \times N$  ( $M < N$ ) and  $\mathbf{F}_N$  represents the discrete Fourier transform matrix. This matrix corresponds to the basis matrix in which incoming signal is sparse. Since the observed signal is sparse in the frequency domain so the basis matrix is equivalent to discrete Fourier time (DFT) matrix. Any methodology like basis pursuit or matching pursuit or orthogonal matching pursuit can be used to recover the spectrum [16].

PSD of the incoming signal is flat within each band. Transition occurs at the beginning of a new band. Hence spectrum sensing can be considered as the edge detection problem. These edges provide the information of start and end location of a frequency band. Once the frequency spectrum is reconstructed, next step is to estimate band locations i.e.  $[f_1, f_2, \dots, f_{Z-1}]$  using the wavelet edge detection technique.

Continuous wavelet transform of incoming signal is given as follows

$$\rho_s = y(f) * \varphi_s(f) \quad (3.4)$$

Where  $\varphi_s(f)$  is the dilated wavelet smoothing function,  $*$  defines the convolution operator and  $s$  depicts the dilation factor of the wavelet smoothing function and takes values in terms of power of 2. Common example of the wavelet smoothing function is Gaussian function. For detection of edges first derivative of the wavelet transform can be used which is given as [36]

$$\begin{aligned}
\rho'_s &= s \frac{d}{df} (\mathbf{y} * \boldsymbol{\varphi}_s)(f) \\
&= \mathbf{y}(f) * (s \frac{d}{df} (\boldsymbol{\varphi}_s))(f)
\end{aligned} \tag{3.5}$$

Local maximum of the first derivative provides information of edges which corresponds to the start and end location of a frequency band. It is also mentioned in [36], second derivative of equation (3.5) can be used to detect the frequency band edges.

Once the frequency boundaries i.e.  $\{f_n\}_{n=0}^{Z-1}$  are detected, next step is to calculate the PSD within each band and decide about the presence or absence of primary user. Calculation of the PSD is given as

$$\beta_n = \frac{1}{f_n - f_{n-1}} \int_{f_{n-1}}^{f_n} \mathbf{y}(f) df \tag{3.6}$$

Based on the PSD values and noise variance decision regarding presence or absence of the primary user in a particular frequency band is made.

In 2009, Xi Chen et al. improved the work of Giannakis [16]. Parallel spectrum sensing structure for a cognitive radio is proposed for improved probability of detection. Incoming signal is passed to number of branches. Each branch is provided with its own sensing matrix. Each branch reconstructs its own frequency spectrum of the received signal. Using the wavelet edge detection technique, each branch locates the frequency boundaries present within the received signal. Finally decision regarding presence or absence of primary user is made based on the results from all branches. This technique



shows better probability of detection results in comparison to [16] in the presence of noise. Figure 3.3 portrays this phenomenon [37].

In 2010, V.H. Nassab et al. came with a different approach of using the wideband filters. Assume that the observed spectrum is  $W$  Hz wide. Each primary user needs  $B$  Hz for transmission of their data. Total number of available frequency bands in  $W$  Hz are defined as  $N = \frac{W}{B}$ . Total number of filters, say  $K$ , at a CR are less than number of bands present within a signal i.e.  $K \ll N$ . It is assumed that the number of bands present in incoming signal is fixed. Received signal is convolved with the wideband filters. Energy of each wideband filtered output is calculated. Obtained energy vector is sparse in the

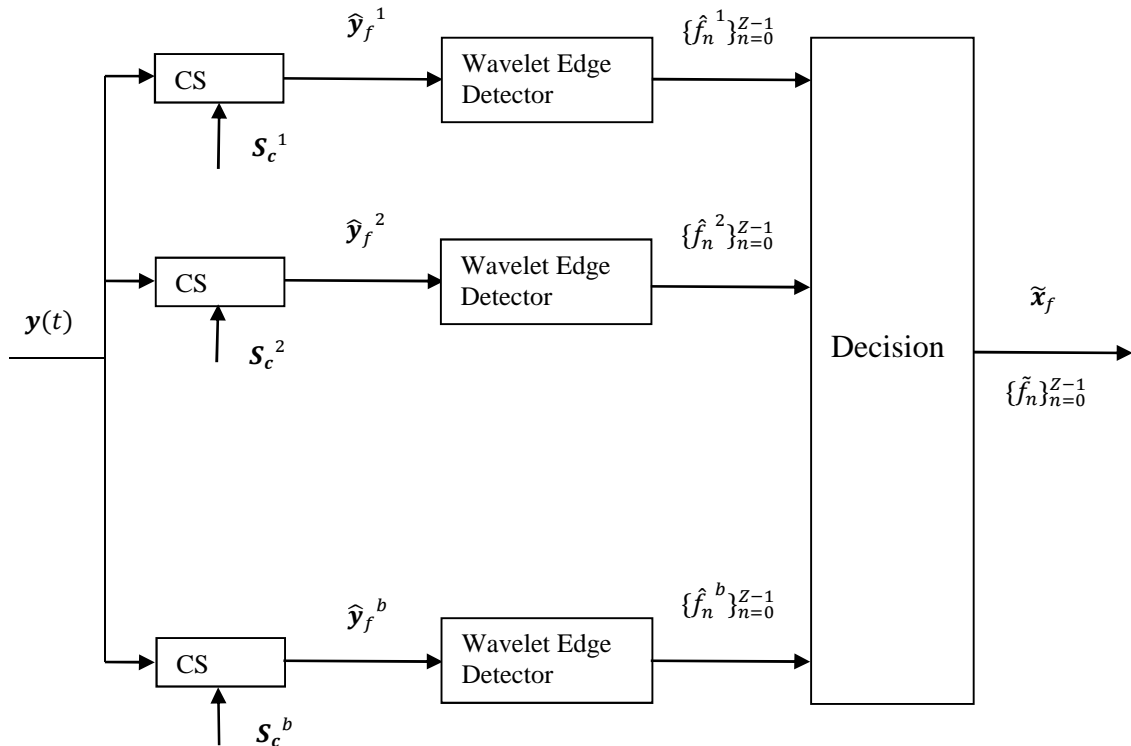


Figure 3.3: A parallel structure for spectrum sensing based on CS

frequency domain. Now from the measurements of energy vector (that are less in number than original energy vector) reconstruction of complete  $N$  length energy vector is done. Based on this reconstructed energy vector decisions are made regarding the presence or absence of primary user. This technique is computationally less complex than aforementioned techniques [38].

In 2010 [39], D. Sundman et al. modified the idea presented in [40]. Autocorrelation vector achieved in [40] deals with the wide-sense stationary (WSS) signals only. However, the signal at the output of AIC is non-WSS. Autocorrelation vector is modified which can deal with the non-WSS signals. Memory based spectral detection concept is also proposed. According to this proposition overall reduction in computational complexity is achieved. It is assumed that mostly wireless signals are static over certain period of time. For instance, TV or radio broadcast is almost static. Since spectrum sensing is performed almost every second so mobile phone calls and wireless internet can also be assumed as static signals. Earlier estimation of the correlation matrix (for instance) requires  $L$  samples. Convex problem of the compressive sensing requires (for instance)  $M$  samples. Thus, each realization of power spectrum requires  $L \times M$  samples which are not much less than total  $N$  samples required for conventional sampling. It is proposed that by calculating spectral detection with memory assumptions these  $L \times M$  samples are reduced in a great percentage over time. Despite of above stated pros there is also a cost associated with this procedure. If error occurs on any realization calculation than this error will be carried on until full procedure is performed again.

In 2010 [41], Y. Liu and Q. Wan used the apriori knowledge of spectrum distribution (within a region) and proposed mixed  $l_2/l_1$  norm de-noising operator. Normally the knowledge of allocated frequency band (to a primary user) can be achieved in advance from regulatory authorities. For instance, information regarding the frequency band occupancy by Global System for Mobile communications (GSM) can be gathered from regulatory authority. According to the algorithm, assuming block sparsity within each primary user frequency band, first calculation of  $l_2$  norm of each block is done. Then minimization of sum of these  $l_2$  norms is performed using  $l_1$  norm. It is concluded that by knowing the band gaps and the block sparsity in advance, proposed technique performance is better when compared to standard mixed  $l_2/l_1$  norm de-noising operator (which do not incorporates the aforementioned information).

### 3.3 DRAWBACKS OF COMPRESSIVE SENSING APPROACH

Compressive sensing provides reconstruction for the sparse signals. Most signals are sparse in some domain/basis and hence CS can be used to reconstruct such signals. In the presence of noise, equation (2.5) can be written as

$$\mathbf{y} = \mathbf{\Phi}\mathbf{x} + \mathbf{n} \quad (3.7)$$

where  $\mathbf{\Phi}$  is  $M \times N$  sensing matrix that is assumed to be incoherent with the domain in which  $\mathbf{x}$  is sparse.  $\mathbf{n}$  is the complex additive white Gaussian noise vector  $\mathcal{CN}(0, \sigma^2_n I)$ . Above posed problem is an under-determined system of equations. An infinite number of solutions can be provided to solve this system. Assuming signal  $\mathbf{x}$  is  $K$  sparse;  $\ell_0$

minimization problem can be used to reconstruct this signal using only  $M \geq 2K$  measurements.

$$\hat{\mathbf{x}} = \min_{\mathbf{x}} \|\mathbf{x}\|_0 \quad \text{subject to} \quad \|\mathbf{y} - \Phi\mathbf{x}\|_2 \leq \epsilon \quad (3.8)$$

where  $\epsilon$  is dependent on  $\sigma_n^2$  i.e. noise variance. Solving the  $\ell_0$  minimization problem is impractical as it is non-deterministic polynomial time hard [42]. Over the years alternative sub-optimal approaches has been presented in the literature. Instead of using  $\ell_0$  minimization, a relaxed  $\ell_1$  minimization has been considered. These algorithms reconstruct the signal  $\mathbf{x}$  with high probability using convex relaxation approaches. The convex relaxation approaches solve the  $\ell_1$  minimization problem using linear programming.

The convex relaxation approaches are good replacement of  $\ell_0$  minimization. Though they reconstruct the signal  $\mathbf{x}$  with high probability but there are also some problems associated with these approaches. Some of these issues are discussed below.

### **3.3.1 COMPUTATIONAL COMPLEXITY**

Convex relaxation approach cannot be used to reconstruct a signal with large dimensions. Linear programming is used to solve the  $\ell_1$  minimization problem. This method has computational complexity of  $\mathcal{O}(M^2 N^{3/2})$  [43]. In literature this problem is solved by using the greedy approaches to solve  $\ell_1$  minimization problem. Computational complexity of the greedy approaches is  $\mathcal{O}(MNR)$  where  $R$  is the number of iterations.

Numerous greedy approaches have been proposed in literature as Orthogonal matching pursuit (OMP) [44], Regularized orthogonal matching pursuit (ROMP) [45] and Compressive sampling matching pursuit (CoSamp) [46].

### **3.3.2 STRUCTURE OF SENSING MATRIX**

Convex relaxation approaches do not use the structure inhibited by sensing matrix. Normally, in practical scenarios, the sensing matrix exhibits some structure, for instance partial DFT matrix or Toeplitz matrix. Best results are generated by convex relaxation approaches when the sensing matrix is random. This requires random sampling which provides a constraint, as currently uniform sampling architectures are being used.

### **3.3.3 EVALUATION OF PERFORMANCE**

Normally it is easy to work with familiar performance quantifying terms like Mean Square Error (MSE) or bias etc [47]. In convex relaxation approaches it is difficult to obtain these estimates.

### **3.3.4 USAGE OF APRIORI INFORMATION**

Convex relaxation approaches do not use the apriori statistical information about the signal support and noise. Sparsity is the only information that is used by these approaches. Any other apriori information is used on the estimates generated by them.

Hence performance is bottlenecked by the reconstruction ability. Every other information can play role to refine the recovered signal. Apriori statistical information has been studied in [48], [49] and [50] in context of Bayesian estimation and belief propagation. In [51] and [52] apriori information have been applied to the cases when signal is Gaussian. Study of the non-Gaussian case is still unsolved question.

### **3.3.5 Bottleneck on Performance**

Traditionally, increasing computational complexity means improvement in the performance. But in convex relaxation approaches this does not happen. Complexity of these algorithms is fixed. To improve performance one has to increase the amount of measurements i.e.  $M$ .

Considering above discussion a suitable sparse signal recovery approach is required that overcomes the shortcoming of convex relaxation approach.

## **3.4 STRUCTURE BASED BAYESIAN SPARSE RECONSTRUCTION**

Structure based Bayesian sparse reconstruction (SBBSR) approach mentioned in [47] is a sparse signal recovery approach based on the Bayesian estimation technique. While reconstructing the signal it uses

- Apriori statistical information
- Apriori sparsity information

- Sensing matrix Structure

Nonetheless like the convex relaxation approaches, apriori sparsity and statistical information can be used while implementing this technique. Assuming the same signal model given in equation (3.2) or (3.3), the sparse vector  $\mathbf{x}_f$  can be modeled as

$$\mathbf{x}(f) = \mathbf{x}_B \odot \mathbf{x}_G \quad (3.9)$$

where  $\odot$  represents dot multiplication between two vectors.  $\mathbf{x}_B$  is an independent and identically distributed (i.i.d) Bernoulli random variable and the entries  $\mathbf{x}_G$  can be drawn from any distribution (like Gaussian). This model of  $\mathbf{x}(f)$  provides a sparse signal. Sparsity information is indulged by i.i.d. Bernoulli random variable and the amplitudes of these observations are drawn from some other distribution.

If the support  $S$  of  $\mathbf{x}(f)$  is known we can write (3.7) as [47]

$$\begin{aligned} \mathbf{y} &= \Phi \Psi \mathbf{x}(f) + \mathbf{n} \\ &= \Theta \mathbf{x}(f) + \mathbf{n} \\ \mathbf{y}|_S &= \Theta_S \mathbf{x}_S(f) + \mathbf{n}_S \end{aligned} \quad (3.10)$$

$\Theta_S$  is the sub-matrix formed from  $\Theta$  containing only those columns represented by  $S$ .

### **3.4.1 ESTIMATION OF SPARSE SIGNAL**

Focus here is to obtain the optimal estimate of observed signal  $\mathbf{x}(f)$ . Estimation of this signal has been done using the SBBSR algorithm [47]. As earlier mentioned, this technique helps us to use the apriori statistical and sparsity information as well as the sensing matrix structure. Normally in convex relaxation approaches such information is neglected. Two different Bayesian parameter estimation techniques have been proposed in [47] for reconstruction of  $\mathbf{x}(f)$ . They are based on minimum mean square error (MMSE) and maximum a posteriori probability (MAP).

In spectrum sensing, information regarding locations of frequency bands which are occupied by primary users is acquired. Traditional approaches like the energy detection or the matched filtering require complete knowledge of signal and that requires a complete spectrum in frequency domain with corresponding PSDs and frequency locations. These traditional approaches are also interested in observing the occupied frequency locations. However in such cases calculation of complete signal information is a necessity. If an algorithm can detect the locations only, it is enough for spectrum sensing purpose. Hence the MAP will suffice our needs. It provided the estimate of occupied locations which helped to find out vacant bands. These vacant bands can be used for transmitting the data of secondary user.

MAP estimate of observed signal  $\mathbf{x}(f)$  can be written as



$$\hat{\mathbf{x}}_{MAP}(f) = \arg \max_S p(\mathbf{y}/S) p(S) \quad (3.11)$$

where  $p(S)$  is the probability of a given support. Assuming the signal model of  $\mathbf{x}(f)$  given previously we can determine the probability of support as

$$p(S) = p^S (1 - p)^{N-S} \quad (3.12)$$

which actually refers to Binomial distribution. Support of signal is dependent on the Binomial distribution so is the corresponding probability.

Now the problem of calculating MAP remains to calculate  $p(\mathbf{y}/S)$ . This probability can be calculated depending on whether the observed signal given support  $\mathbf{x}(f)|S$  is Gaussian or not. Thus, there are two cases; one when the primary user data has Gaussian distribution and second when it has non-Gaussian distribution.

**Case 1:  $\mathbf{x}(f)|S$  is Gaussian**

If the primary user data has Gaussian distribution,  $\mathbf{x}(f)|S$  is Gaussian, then  $\mathbf{y}|S$  will also be Gaussian (because of linear system model) with zero mean and covariance  $\mathbf{\Sigma}_S$ . Corresponding probability is calculated as [47]

$$p(\mathbf{y}/S) = \frac{\exp(-\frac{1}{\sigma_n^2} \mathbf{y}^H \mathbf{\Sigma}_S^{-1} \mathbf{y})}{\det(\mathbf{\Sigma}_S)} \quad (3.13)$$

where covariance matrix is given as

$$\Sigma_S = I + \frac{\sigma_x^2}{\sigma_n^2} \Theta_S \Theta_S^H \quad (3.14)$$

**Case 2:  $\mathbf{x}(f)|S$  is unknown**

If the primary user data distribution is unknown i.e.  $\mathbf{x}(f)|S$  distribution is unknown then no information can be deduced about  $\mathbf{y}|S$ . In such case, the observed signal  $\mathbf{y}$  is acquired from a projection of  $\mathbf{x}$  onto some subspace spanned by the sensing matrix with addition of white Gaussian noise. Corresponding probability is calculated as [47]

$$p(\mathbf{y}|S) = \exp\left(-\frac{1}{\sigma_n^2} \|\mathbf{P}_{\Theta_S}^\perp \mathbf{y}\|^2\right) \quad (3.15)$$

where  $\mathbf{P}_{\Theta_S}^\perp$  is the orthogonal projector onto the orthogonal complement of the subspace spanned by the columns of  $\Theta_S$  and is given by

$$\mathbf{P}_{\Theta_S}^\perp = I - \Theta_S (\Theta_S^H \Theta_S)^{-1} \Theta_S^H \quad (3.16)$$

### **3.4.2 EVALUATION OVER $S$**

Information about the corresponding estimates to recover the sparse signal is available but knowledge about the range of  $S$  on which to evaluate these estimates is unavailable. Possible supports could be present anywhere in the  $N$  length signal. This requires narrowing down the search space in order to reduce complexity. Otherwise, the whole  $N$  length signal will be searched for possible support size. Two possible solutions have been proposed in literature. One suggests using the convex relaxation approaches in

finding the most probable support of the sparse vector [25]. However the other (Fast Bayesian Matching Pursuit (FBMP) [51]), suggests performing a greedy tree search over all the combinations. Convex relaxation approach uses the apriori sparsity information while reconstructing the sparse signal. On contrary, FBMP uses both apriori sparsity and statistical information. None of them had used the structure of sensing matrix to gain more reduction in computational complexity.

Normally sensing matrix bears some structure like the partial DFT matrix or Toeplitz matrix. In [47], in addition to apriori sparsity and statistical information the sensing matrix structure is also used to achieve reduction in computational complexity. Sensing matrix is not orthogonal because of its dimensions  $M \times N$  (where  $M \ll N$ ). However in matrix like partial DFT or Toeplitz an orthogonal matrix of size  $M \times M$  could be found. Remaining  $N - M$  columns usually group around these  $M$  orthogonal columns to form semi-orthogonal clusters. This orthogonality information helps in reducing computational complexity of algorithm.

Assume  $S$  is the possible support of  $\mathbf{x}_f$ . Corresponding  $\Theta_S$  columns can be grouped into  $P^1$  semi-orthogonal clusters i.e.  $\Theta_S = [\Theta_1 \Theta_2 \dots \Theta_P]$ . Using semi-orthogonality the overall likelihood is the product of likelihoods of individual clusters. Hence the corresponding MAP metric for the Gaussian case is given as

---

<sup>1</sup> As  $\|S\|_0$  is a Binomial distribution  $\sim B(N, p)$ , it can be approximated by a Gaussian distribution  $\sim \mathcal{N}(Np, Np(1-p))$  when  $Np > 5$ . Thus in this case,  $P(\|S\|_0 > P) = \frac{1}{2} \text{erfc}\left(\frac{P - N(1-p)}{\sqrt{2Np(1-p)}}\right)$ .  $P$  can be set equal to  $\text{ceil}(\text{erfc}^{-1}(10^{-2})\sqrt{2Np(1-p)} + Np)$  [51].

$$\mathcal{L}_S = p^S (1-p)^{N-S} \exp\left(-\frac{P-1}{\sigma_n^2} \|\mathbf{y}\|^2\right) \prod_{i=1}^P \frac{\exp\left(-\frac{1}{\sigma_n^2} \mathbf{y}^H \boldsymbol{\Sigma}_i^{-1} \mathbf{y}\right)}{\det(\boldsymbol{\Sigma}_i)} \quad (3.17)$$

whereas for the unknown signal distribution case the corresponding MAP estimate is given as [47]

$$\mathcal{L}_S = p^S (1-p)^{N-S} \exp\left(-\frac{P-1}{\sigma_n^2} \|\mathbf{y}\|^2\right) \prod_{i=1}^P \exp\left(-\frac{1}{\sigma_n^2} \|\mathbf{P}_{\boldsymbol{\Theta}_i}^\perp \mathbf{y}\|^2\right) \quad (3.18)$$

### **3.4.3 SIGNAL RECONSTRUCTION METHODOLOGY USING**

#### **SBBSR**

In this section the SBBSR based sparse signal recovery approach is explained. The sub-Nyquist rate sampled signal  $\mathbf{y}$  is correlated with sensing matrix. Based on correlation result clusters are made. Within each cluster the MAP estimates are calculated and decision regarding presence or absence of the primary user is made. Figure 3.4 describes main steps of the SBBSR algorithm.

##### **3.4.3.1 Correlation of Signal and Sensing Matrix**

Assume the signal model given in equation (3.10)

$$\mathbf{y} = \boldsymbol{\Theta} \mathbf{x}(f) + \mathbf{n} \quad (3.19)$$

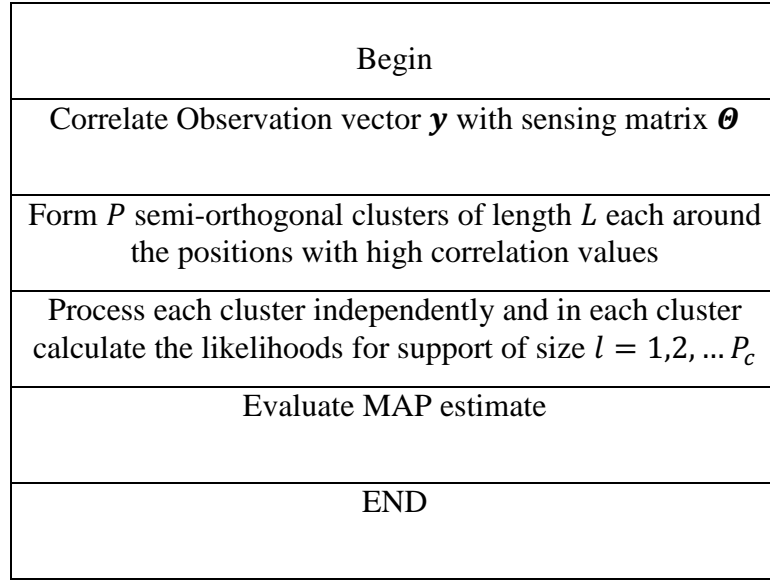


Figure 3.4: Flow Chart of Orthogonal Clustering Algorithm

Correlate signal  $\mathbf{y}$  with the sensing matrix

$$\hat{\mathbf{y}} = \mathbf{y}^T \boldsymbol{\theta} \quad (3.20)$$

where  $\hat{\mathbf{y}}$  represents the correlation result. Maximum values of the correlation result will help in finding the possible locations where support of sparse vector  $\mathbf{x}(f)$  can exist.

#### 3.4.3.2 Semi-Orthogonal Cluster Formulation

From  $\hat{\mathbf{y}}$  select the index which corresponds to the maximum correlation value. Make a cluster of length  $L$  around this location. Cluster length  $L$  is dependent on the correlation between the columns of sensing matrix. This value can be calculated by correlating any column of sensing matrix with the whole sensing matrix. Make  $P$  clusters in the similar fashion.

### 3.4.3.3 Find Supports and Likelihoods

From previous step  $P$  semi orthogonal clusters are attained. Assume  $P_c^1$  denotes the maximum possible support size in a cluster. For each support size  $l = 1, 2 \dots P_c$  calculate the corresponding likelihoods values within a cluster. Repeat this process for all clusters. As a result from each cluster, likelihood vector of length  $P_c$  is acquired.

### 3.4.3.4 Evaluate MAP Estimate

We have  $P$  clusters and  $P_c$  likelihood values (which correspond to the support of size  $l = 1, 2 \dots P_c$ ) within each cluster. To obtain the MAP estimates, multiply each likelihood value with its corresponding probability of support. Select the maximum MAP estimates from each cluster. Corresponding locations of that estimates provides the information for non-zero locations of the sparse signal  $\mathbf{x}(f)$ .

## **3.5 CONCLUSION**

In this chapter, various spectrum sensing algorithms based on both the Nyquist and sub-Nyquist sampling rate were discussed. Sub-Nyquist rate sampling algorithms provide solution to spectrum sensing problem in the wideband regime.

---

<sup>1</sup>  $P_c$  is calculated in the similar way as  $P$ . As support within a cluster is also based on Binomial Distribution  $\sim B(L, p)$ . Thus we set  $P_c = (\text{erfc}^{-1}(10^{-2})\sqrt{2Lp(1-p)} + Lp)$  [47].

## **CHAPTER 4**

### **BLIND SOURCE SEPERATION BASED THRESHOLD**

#### **CALCULATION**

In this chapter, the wideband spectrum sensing using wavelet edge detection technique is addressed. This technique does not require information of frequency bands locations and calculate it from the received wideband signal. Hence dependency on the regulatory authority is waived.

Observed spectrum consists of numerous frequency bands (each band depicts occupancy by primary user). The power spectral density (PSD) within each frequency band is smooth. Transition of the PSD from one band to another band is considered as irregularity in the PSD. Such irregularities can be studied using the wavelet transforms which are capable of characterizing local regularity of a signal [53].

Applying wavelet transform on the incoming signal results in peaks at locations where the signal PSD is irregular. In absence of noise these peaks provides the information of frequency band boundaries. However, in presence of noise these peaks

are accompanied by the random peaks which may corrupt information of the frequency band boundaries. In [36], multiscale wavelet products were used to extract the frequency band boundaries from observed peaks. This technique requires multiplication of various wavelet transform gradients. As a result, peaks representing the frequency band boundaries were exposed whereas random peaks were suppressed. The multiscale wavelet products require apriori knowledge about total number of active frequency bands in a spectrum. This information is normally unknown at the CR. The proposed algorithm in this chapter, calculates a threshold value for the observed peaks at output of wavelet transformed signal. Only those peaks are considered which have amplitude greater than threshold value whereas others are neglected. Blind source separation technique is used to calculate the threshold value.

## 4.1 SYSTEM MODEL

Spectrum sensing approach presented in [36] assumes that a total of  $B$  Hz in the frequency range  $[f_0, f_Z]$  is available for the wideband wireless network and is known to the CR. The frequency bands locations and PSD levels within this  $B$  Hz are unknown. Moreover the number of bands within a time remains same. Frequency response of the incoming signal is flat within each band. Figure 3.2 illustrates the PSD structure of incoming signal. Incoming signal consists of  $Z$  spectrum bands whose frequency location and PSD levels required detection. The received signal PSD can be written as follows



$$y(f) = \sum_{n=1}^Z \alpha_n^2 x_n(f) + S_w(f), \quad f \in [f_0, f_Z] \quad (4.1)$$

Where  $\alpha_n^2$  is defined as the signal power density in corresponding band and  $x_n(f)$  is the normalized power spectral shape within each band and is given as

$$x_n(f) = \begin{cases} 1, & \forall f \in B_n \\ 0, & \forall f \notin B_n \end{cases} \quad (4.2)$$

$S_w(f)$  is the zero mean additive white noise. Time domain equivalent of equation (4.1) is

$$y(t) = \sum_{n=1}^Z \alpha_n x_n(t) + n(t) \quad (4.3)$$

$x_n(t)$  can be a pulse train and is defined as follows

$$x_n(t) = \sum_{k=-\infty}^{\infty} b_k h(t - kT_s) e^{j2\pi f_{c,n}t} \quad (4.4)$$

For the model given above we have to determine the number of frequency bands, their locations and the signal power density i.e.  $Z, \{f_n\}_{n=1}^{Z-1}$  and  $\{\alpha_n^2\}_{n=1}^Z$ .

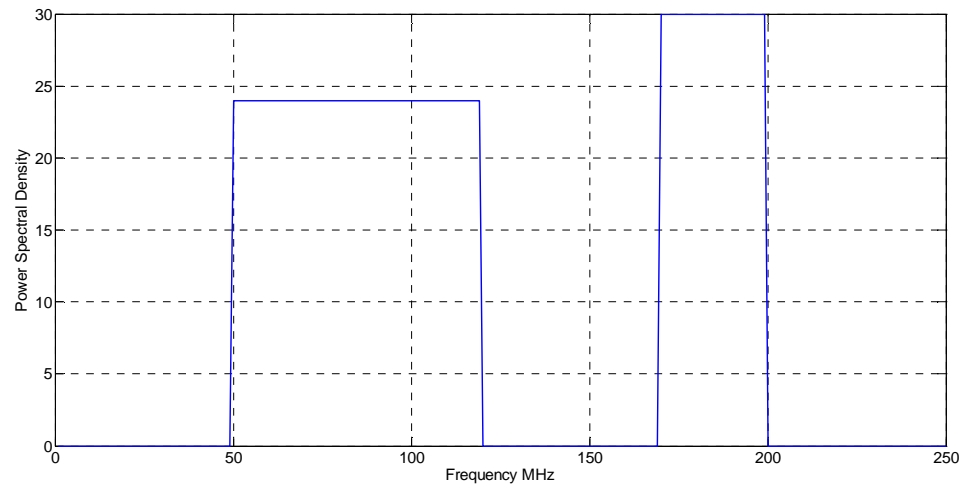
## 4.2 PROBLEM STATEMENT

PSD of the incoming signal is flat within each frequency band. Hence spectrum sensing can be considered as the edge detection problem. These edges provide the information of start and end location of a frequency band. Wavelet transform is applied

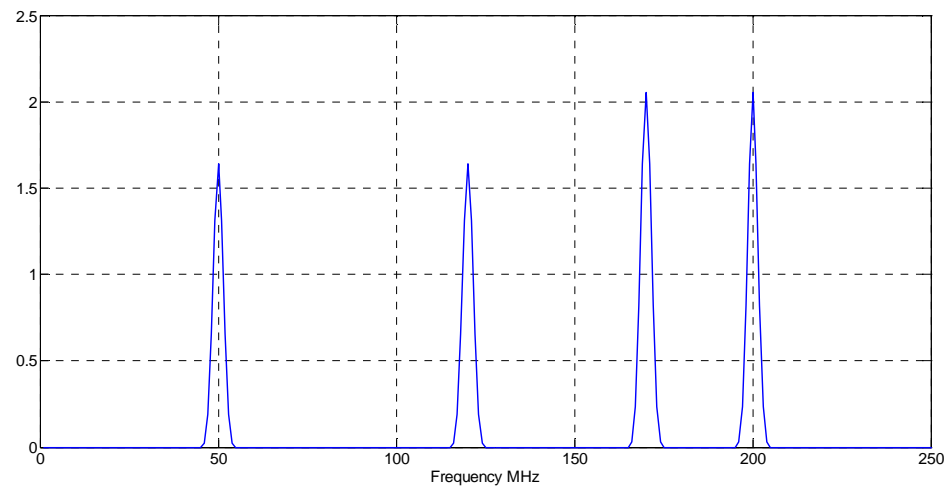
on the received signal using equation (3.4). For detection of edges, first derivative of wavelet transform can be used (as shown in equation (3.5)). Local maxima of first derivative provide the information of edges which corresponds to start and end location of a frequency band. Once frequency boundaries i.e.  $\{f_n\}_{n=0}^{Z-1}$  are detected then next step is to calculate the PSD within each band and decide about presence or absence of a primary user. PSD within each frequency band is calculated using equation (3.6).

The edge detection provides us with knowledge of frequency band boundaries using equation (3.5). For the noiseless case calculation of the frequency band boundaries is simple. Figure 4.1a, illustrates incoming signal PSD for the noiseless case and Figure 4.1b illustrates the corresponding edges located using the edge detection technique.

Now consider the case when the incoming signal is contaminated by noise. Figure 4.2a, illustrates this scenario. Output of the edge detection technique provides us with mixed edges as illustrated in Figure 4.2b. Observe the combination of true peaks and noisy peaks. The frequency boundaries for given bands cannot be determined directly (as in noiseless scenario). In the next section, solution to this problem using blind source separation algorithm has been provided.

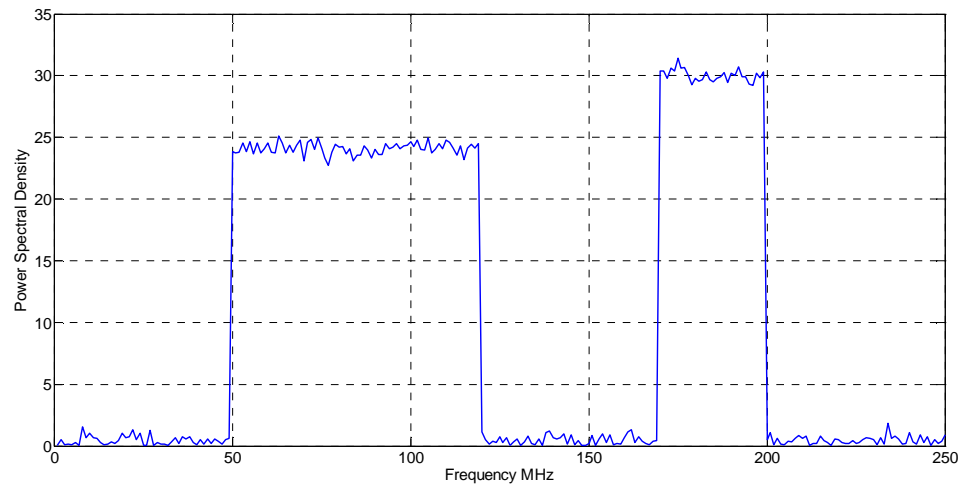


(a)

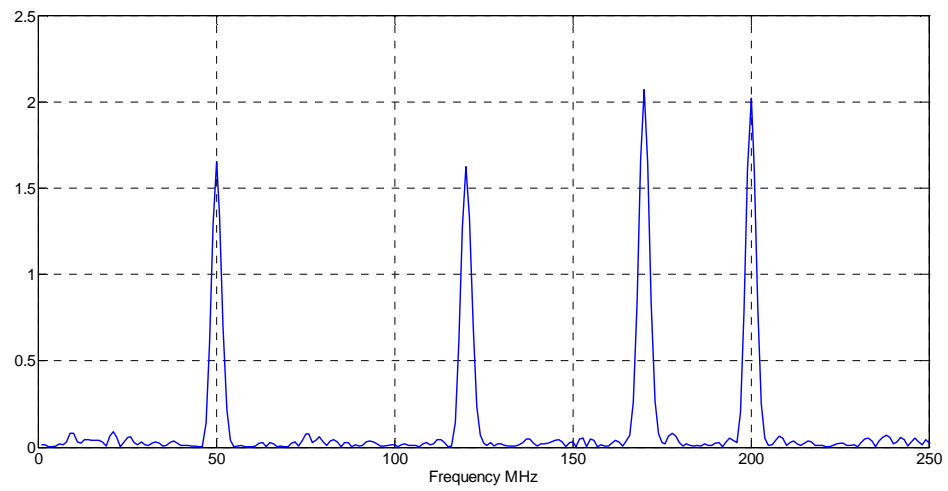


(b)

Figure 4.1: (a) Incoming Signal PSD; (b) Output of Edge Detection technique.



(a)



(b)

Figure 4.2: (a) Incoming Signal PSD; (b) Output of Edge Detection technique.

## 4.3 BLIND SOURCE SEPARATION APPROACH TO EDGE

### DETECTION

Blind source separation has found very useful applications in the area of signal processing and neural networks [54]. The blind source separation does not require the knowledge of the channel and the transmitted signal. In fact its goal is to recover the unobserved signals i.e. ‘source signals’ from a set of observed signals. Term ‘Blind’ refers to following two facts [31]

- Source signals are not observed.
- There is no apriori knowledge available about the mixing system.

Since the development of blind source separation technique many new algorithms have been suggested. Some of these algorithm depend on exploiting the second order statistics and stationary or non-stationary conditions of the received signal, others need higher order statistics and some exploits the time-frequency diversities [55]. All these algorithms obtain cost function through some optimization process which normally is computationally complex.

In [54], the blind source separation algorithm was presented. The maximum signal to noise ratio (SNR) is achieved when the sources are separated completely. Cost function of this algorithm is based on the SNR definition. The algorithm achieved low computational complexity solution based on the instantaneous mixing method. The

assumption was that the source signals come from different sources and could be considered as statistically independent. The received signal can be written as

$$y_i(t) = \sum_{j=1}^n a_{ij}x_j(t) \quad (4.5)$$

where  $a_{ij}$  represents the instantaneous mixing matrix  $(i, j)$  element. In vector form, we can write equation (4.5) as

$$\mathbf{y}(t) = \mathbf{A} \mathbf{x}(t) \quad (4.6)$$

where  $\mathbf{y}(t)$  is a vector of the mixed signals. The BSS algorithms only have information of the mixed signals and statistical independence property of the source signals. Assuming  $\mathbf{W}$  is an un-mixing matrix for the aforementioned problem, the BSS problem can be stated as follows

$$\hat{\mathbf{x}}(t) = \mathbf{W}\mathbf{y}(t) = \mathbf{W} \mathbf{A} \mathbf{x}(t) \quad (4.7)$$

where  $\hat{\mathbf{x}}(t)$  is the estimate of the source signals i.e.  $\mathbf{x}(t)$ . The difference between the original signal and the estimated signal is the noise signal. The SNR may be defined as [54]

$$SNR = 10 \log \frac{\mathbf{x} \cdot \mathbf{x}^T}{\mathbf{e} \cdot \mathbf{e}^T} = 10 \log \frac{\mathbf{x} \cdot \mathbf{x}^T}{(\mathbf{x} - \hat{\mathbf{x}}) \cdot (\mathbf{x} - \hat{\mathbf{x}})^T} \quad (4.8)$$

Optimized processing of equation (4.8) results in the Eigen value problem. The resultant Eigen vector matrix corresponds to the un-mixing matrix  $\mathbf{W}$ . Once un-mixing

matrix is achieved the source signals can be obtained using equation (4.7). The un-mixing matrix is obtained by solving singular value decomposition problem that satisfies

$$(\mathbf{y}\mathbf{y}^T) \times \mathbf{W} = \left( (\mathbf{y}_{MA} - \mathbf{y})(\mathbf{y}_{MA} - \mathbf{y})^T \right) \times \mathbf{W} \times \mathbf{D} \quad (4.9)$$

where  $\mathbf{y}_{MA}$  is the moving average estimate of  $\mathbf{y}$  and  $\mathbf{D}$  is the diagonal matrix of the generalized Eigen values.

In [56], it is mentioned that (for energy detection technique) the received signal can be written in terms of its sample covariance matrix i.e.

$$\mathbf{R}_y(N) = \mathbf{R}_x(N) + \sigma^2 \mathbf{I} \quad (4.10)$$

$$\text{where } \mathbf{R}_y(N) = \left( \frac{1}{N} \sum_{n=0}^{N-1} \mathbf{y}(n)\mathbf{y}^T(n) \right)$$

$$\text{and } \mathbf{R}_x(N) = \left( \frac{1}{N} \sum_{n=0}^{N-1} \mathbf{x}(n)\mathbf{x}(n) \right)$$

are the received and transmitted signal sample covariance matrices, respectively. Also,  $\sigma^2$  is the noise variance. The transmitted signal sample covariance matrix cannot be calculated as no information regarding the transmitted (or source) signal is available. It is given in [56] that the blind source separation algorithm can calculate the un-mixing matrix for the received signal. Using the un-mixing matrix and received signal an estimate of transmitted signal (as shown in equation (4.7)) and its corresponding sample covariance matrix can be acquired. The noise variance can be calculated as

$$\sigma^2 \mathbf{I} = \frac{1}{N} \sum_{n=0}^{N-1} \mathbf{y}(n) \mathbf{y}^T(n) - \frac{1}{N} \sum_{n=0}^{N-1} \mathbf{W} \mathbf{y}(n) \mathbf{y}^T(n) \mathbf{W}^T \quad (4.11)$$

In our case, signal  $\mathbf{y}$  is the output of wavelet edge detection technique ( $\boldsymbol{\rho}'_s$ ) (as in Figure 4.2b). The noise variance is not sufficient to threshold one such signal. In order to calculate exact threshold values, the noise variance have been normalized with the sample mean of received signal (as in Figure 4.2a). Hence the threshold value can be written as

$$T = \frac{\sigma^2}{\frac{1}{N} \sum_{n=0}^{N-1} |\rho'_s(n)|} \quad (4.12)$$

Using  $T$  output of the edge detection technique can be thresholded and hence can calculate the frequency edges locations.

Based on aforementioned discussion we can summarize the whole algorithm as

- Calculate  $\boldsymbol{\rho}'_s$  by applying the wavelet edge detection technique to the received signal.
- Apply the blind source separation technique on  $\boldsymbol{\rho}'_s$  to calculate  $\mathbf{W}$ .
- Calculate the noise variance using equation (4.11).
- Calculate the sample mean of  $\boldsymbol{\rho}'_s$ .
- Calculate the threshold value  $T$  using equation (4.12).
- Threshold the output of edge detection technique  $\boldsymbol{\rho}'_s$  using  $T$ .



- Compute the frequency band boundary locations (i.e. start and end) iteratively from the output of previous step.
- Compute the PSD within these frequency band boundaries.

Figure 4.3 shows above steps in flow chart form for proposed algorithm.

## 4.4 SIMULATION

Here it is assumed that the observed wideband signal of interest lies in the range of  $[0, 1000]\Delta$  Hz, where  $\Delta$  is the frequency resolution. During the transmission there are total of  $N = 11$  bands in the wideband signal with frequency boundaries  $\{f_n\}_{n=0}^{10} = [0, 100, 119, 300, 319, 500, 519, 700, 719, 900, 919, 1000]$ . Out of these 11 bands only 5 bands are carrying the primary user transmission and rest 6 bands are available for secondary user i.e. they are spectrum holes. In simulation, the Gaussian wavelet is used for edge detection technique. The effect of noise on the spectrum sensing performance has been studied.

Success ratio and probability of detection curves were obtained over range of SNR. Success ratio is defined as probability of accurately detecting the frequency band boundaries. Probability of detection is defined as accurately detecting the whole frequency band. Figure 4.4 shows the calculated success ratio over the range of SNR values and its comparison with the multiscale wavelet products technique. The proposed

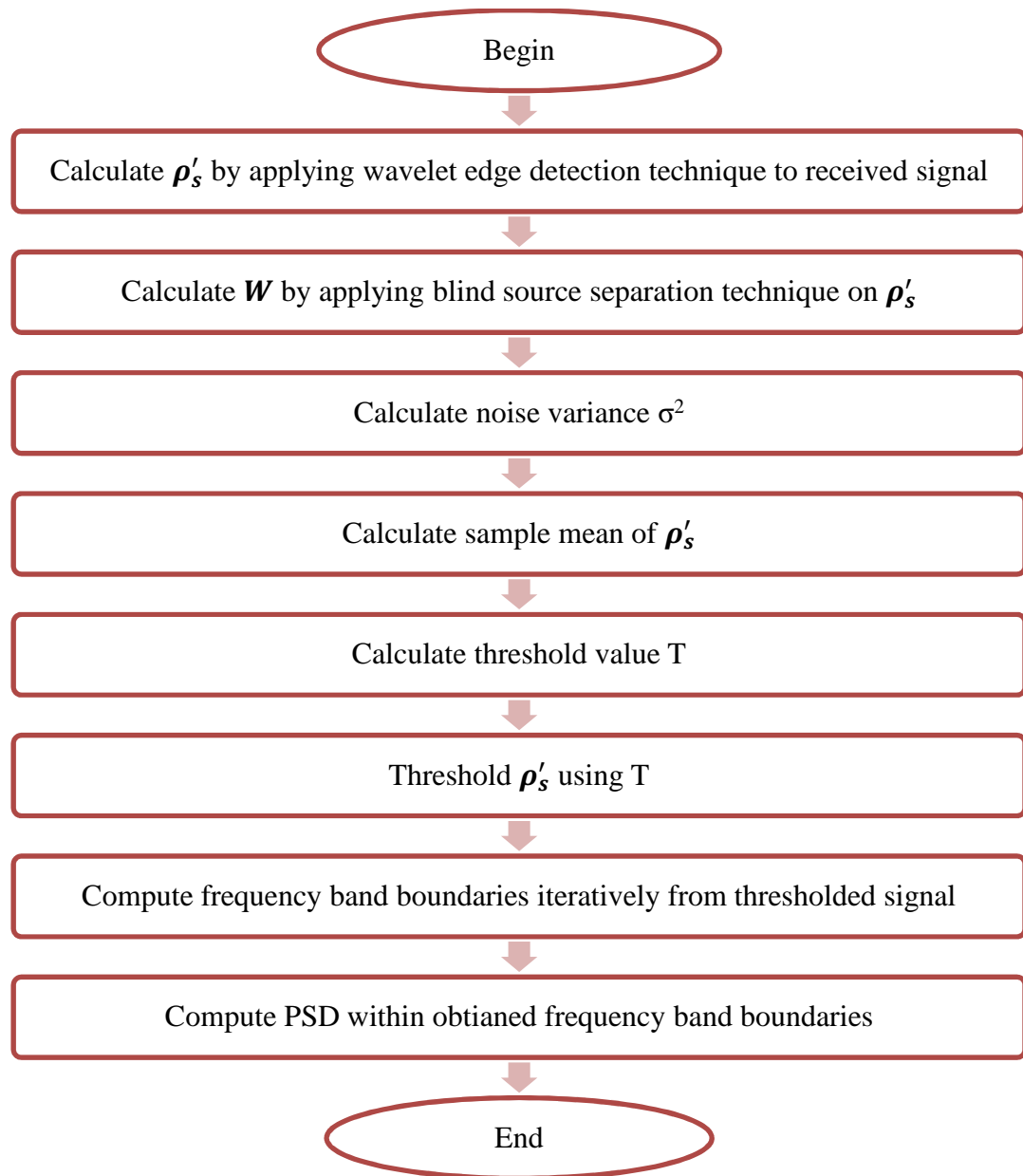


Figure 4.3: Flowchart of proposed algorithm

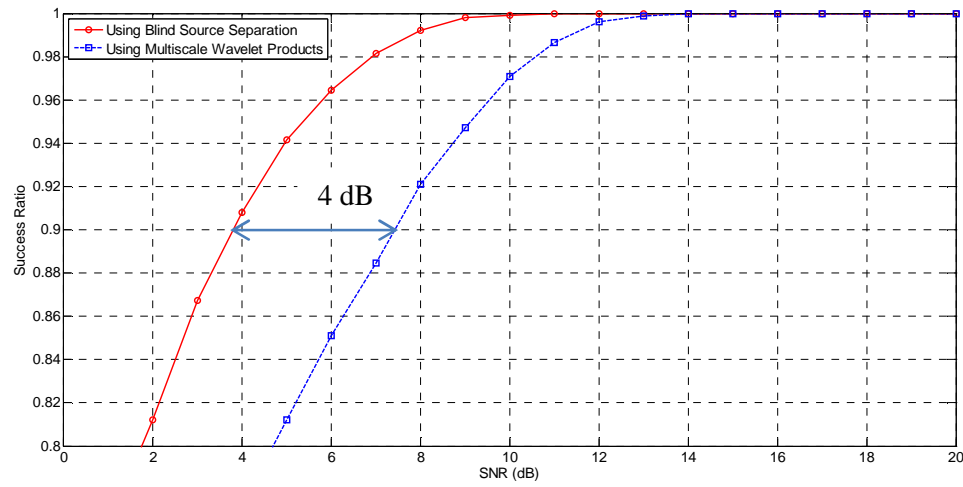


Figure 4.4: Success ratio versus SNR

technique had shown improvement of 4 dB for the success ratio plot. Figure 4.5 shows the probability of detection over range of SNR values. This result shows that proposed technique gained 8dB improvement for the probability of detection plot.

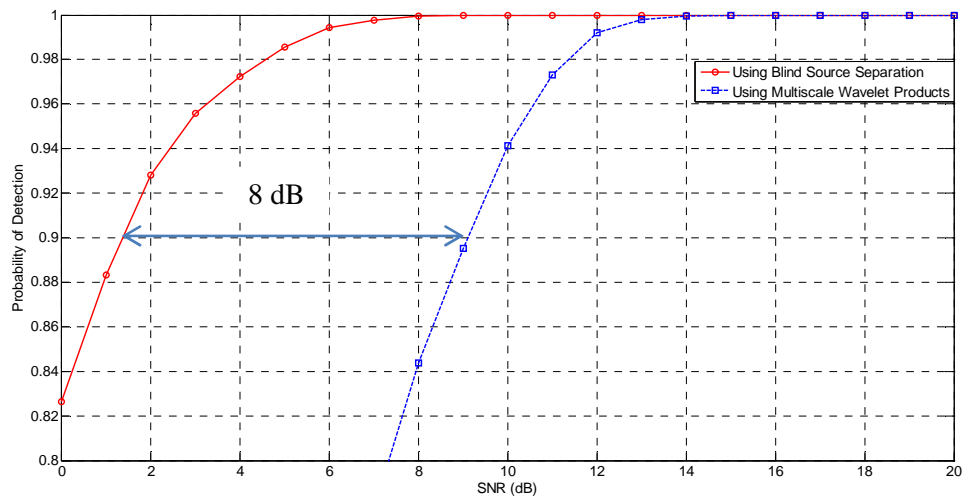


Figure 4.5: Probability of Detection versus SNR

## 4.5 CONCLUSION

In this chapter, a threshold value is proposed for detecting true peaks from the signal obtained at the output of wavelet edge detection technique. The noisy peaks are suppressed by thresholding the signal. This procedure directly affects the performance of spectrum sensing process. The proposed algorithm gained 4 dB improvements in terms of success ratio and 8 dB improvements in terms of probability of detection when compared with multiscale wavelet product technique. Proposed algorithm improves the performance of spectrum sensing process using the low complexity blind source separation algorithm.

## **CHAPTER 5**

### **SPECTRUM SENSING USING SBBSR APPROACH**

In this chapter, spectrum sensing problem has been addressed using the SBBSR algorithm. In section 3.2, the compressive sensing based algorithms for spectrum sensing were discussed. The compressive sensing based algorithm used apriori sparsity information. Performance of these algorithms is dependent on number of measurements. The sensing matrix structure is not used in implementation of these algorithms. Efficient results are generated when the sensing matrix structure is random. This requires random sampling techniques which provides a constraint, as currently uniform sampling architectures are being used. The SBBSR algorithm uses apriori statistical and sparsity information. In addition the sensing matrix structure is also used. The sensing matrix structure proved helpful in reduction of computational complexity. The SBBSR algorithm provides much flexible implementation in comparison to the CS based techniques. Taking advantage of this flexible implementation different condition has been imposed on the SBBSR algorithm and corresponding results are analyzed.

## 5.1 SBBSR APPROACH FOR SPECTRUM SENSING

The SBBSR algorithm is based on Bayesian estimation approach for reconstruction of sparse signals. As discussed in section 3.4, this algorithm uses apriori statistical and sparsity information as well as the sensing matrix structure. Section 3.4.3 provides detailed description of the algorithm. In this section, spectrum sensing using the SBBSR algorithm is discussed.

Assume the case when the transmitted signal (primary user signal) distribution is known and is Gaussian. The sensing matrix in case of spectrum sensing is a partial inverse discrete Fourier transform (IDFT) matrix and is given as

$$\Theta = \mathbf{S}_c^T \mathbf{F}_N^{-1} \quad (5.1)$$

where  $\mathbf{S}_c$  is the identity matrix of size  $N \times M$  and  $\mathbf{F}_N^{-1}$  is the IDFT matrix of size  $N \times N$ . In this case the observation vector can be written as

$$\mathbf{y} = \mathbf{S}_c^T \mathbf{F}_N^{-1} \mathbf{x}(f) + \mathbf{n} \quad (5.2)$$

Here it is assumed that the wideband signal of interest lies in the range of  $[0, 100]\Delta$  Hz, where  $\Delta$  is frequency resolution. Spectrum occupancy is sparse and has a sparsity level of 6%, 6 out of 100 coefficients are non zero. Assume that non-zero coefficients are the frequency locations where the transmission is being done by primary user and rest is the vacant band. Here, goal is to sense this signal and inform secondary

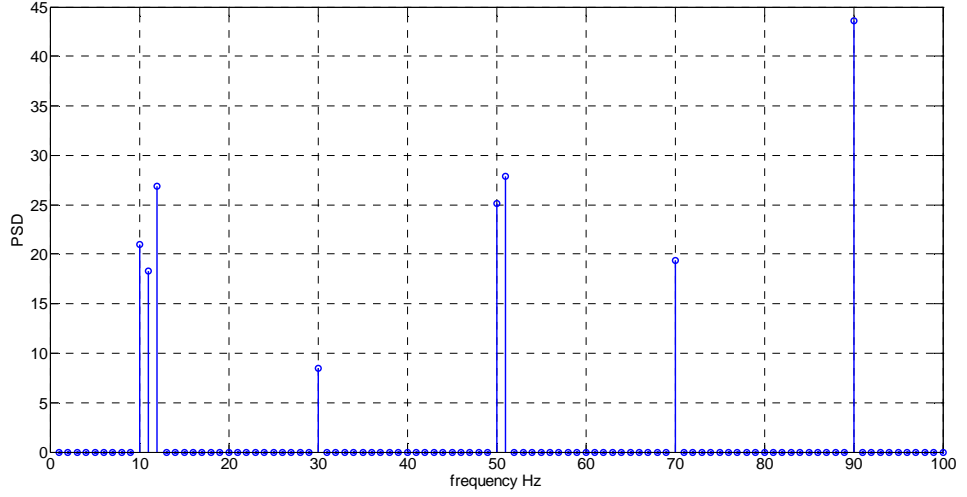


Figure 5.1: Received Signal at CR

user which locations are vacant for transmission of data. Figure 5.1 shows the signal discussed above. This signal is modeled as a Bernoulli-Gaussian (as described in section 3.4).

The length of observed signal  $\mathbf{y}$  is  $M = \frac{N}{\ell}$  (where  $\ell$  is 2). Cluster length  $L$  is observed from the correlation among the columns of the sensing matrix and equals 3. The number of clusters  $P$  equals 9 and the support size  $P_c$  equals 2. Number of clusters and support size are calculated using Binomial to Gaussian assumption described in section 3.4.3. The signal is corrupted using AWGN noise model with SNR of 30 dB. Observe columns  $j \in 0, \ell, 2\ell, \dots, (M-1)\ell$  of sensing matrix correspond to the orthogonal matrix  $\Theta_M$ .

Figure 5.2 shows the correlation among the columns of sensing matrix. The 50<sup>th</sup> column of sensing matrix is correlated with the sensing matrix itself. Column 50 is in fact  $25\ell$  and is orthogonal with column 52 (which is  $26\ell$ ) and 48 (which is  $24\ell$ )

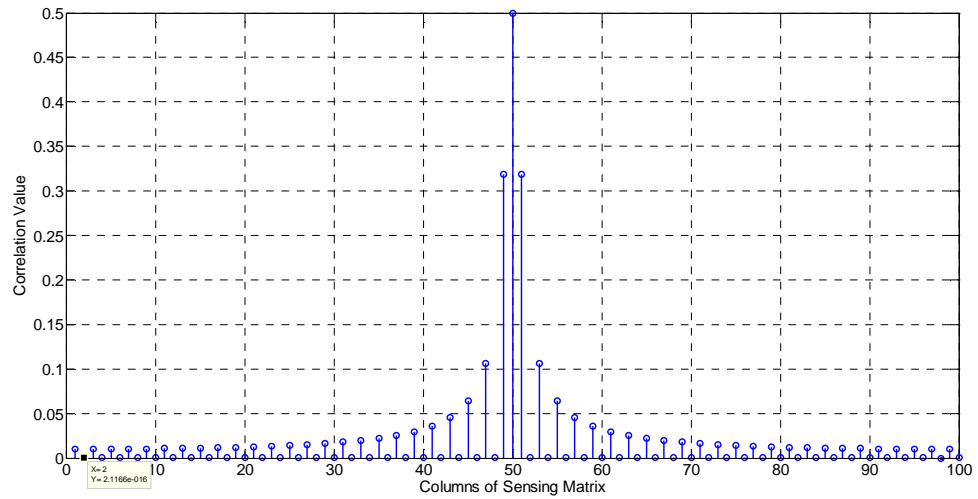


Figure 5.2: Correlation among Columns of Sensing Matrix

which entails the fact that columns  $j \in 0, \ell, 2\ell, \dots, (M-1)\ell$  of the sensing matrix are orthogonal.

Figure 5.3 shows the correlation result of observed signal with the sensing matrix.

This figure shows the sorted result of correlation. On y- axis it is representing the

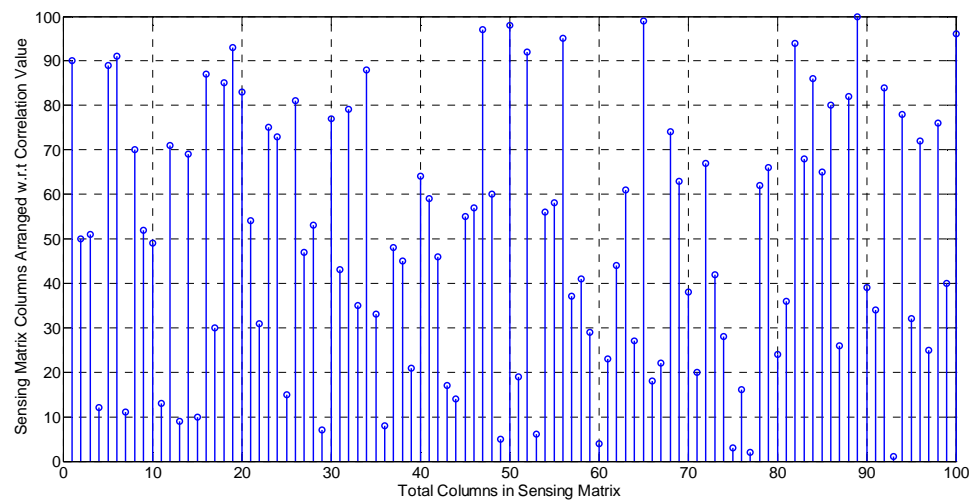


Figure 5.3: Correlation of Observed Signal with Sensing Matrix



column number of sensing matrix and on  $x$ -axis it is representing the total number of columns. Recall that, the sensing matrix is of size  $M \times N$  and the result of correlation is a vector of size  $1 \times N$ . The correlation result is displayed in descending order. Hence index 1 represents column of the sensing matrix which has highest correlation, index 2 represents the column which has next maximum correlation value and so on.

Since information of (column) indexes corresponding to the high correlation values is available, we can make  $P$  clusters around them and calculate the corresponding likelihoods and the MAP estimates within each of them. TABLE 5-1 shows the indexes which fall into clusters.

Index corresponding to the highest correlation value is the center of cluster 1. Next, look at the index corresponding to second highest correlation value. If this index is

TABLE 5-1: CLUSTER INFORMATION

Cluster Number	Indexes Covered by Cluster	Useful Index in Cluster
1	[89 90 91]	90
2	[49 50 51]	50 and 51
3	[11 12 13]	11 and 12
4	[69 70 71]	70
5	[52 53]	None
6	[8 9 10]	10
7	[86 87 88]	None
8	[29 30 31]	30
9	[84 85]	None

already present in the previous cluster discard this index and move to the next. In this way,  $P$  clusters have been created. These clusters could have variable lengths or a fixed length depending on the availability of correlating indexes. Also, there are some clusters which do not contain any true location like clusters 5, 7 and 9 in TABLE 5-1.

After creating the clusters, calculation of likelihoods and the MAP estimate of each cluster is required. Calculation of the likelihoods/MAP estimates for the support of size 0, 1, 2 ...  $P_c$  within each cluster is required. Here,  $P_c$  equal 2 so estimates for supports of size 0, 1, 2 has been calculated within each cluster. TABLE 5-2 shows the corresponding MAP estimates for these support sizes.

The MAP estimate of support being zero is also required. Observe from TABLE 5-1, clusters 5, 7 and 9 do not contain any useful information. The MAP estimate of zero support helped in limiting the search over only those clusters which contain true locations. Observe from TABLE 5-2, the MAP estimate of support zero for cluster 5 is larger than other estimates within same cluster.

Searching of true locations inside clusters is quite simple. An example for calculation of true locations in cluster 1 is given as follows.

1. Find the maximum estimate value in cluster 1 from all support sizes (-1581.1 from support of size 1).
2. Compare this estimate value with that (estimate value) of zero support (compare -1581.1 with -2532.2).

TABLE 5-2: MAP ESTIMATES FOR CORRESPONDING SUPPORT SIZES

Cluster	Likelihood of Support = 0	Likelihood of Support = 1	Likelihood of Support = 2
1	-2532.2	[-2102.2 -1581.1 -2201.4] [89 90 91]	[-1585.8 -1771.5 -1585.0] [89,90 89,91 90,91]
2	-2532.2	[-2292.1 -1676.3 -1963.1] [49 50 51]	[-1643.6 -1723.0 -1615.6] [49,50 49,51 50,51]
3	-2532.2	[-2308.0 -2297.6 -2432.2]	[-2290.9 -2348.0 -2398.0]
4	-2532.2	[-2369.4 -2267.2 -2514.7]	[-2337.8 -2351.9 -2357.1]
5	-2532.2	[-2685.0 -2576.7 -2532.2]	[-2582.2 -2532.2 -2532.2]
6	-2532.2	[-2436.1 -2377.7 -2339.9]	[-2444.8 -2343.8 -2311.2]
7	-2532.2	[-2521.8 -2484.0 -2535.3]	[-2353.5 -2524.9 -2478.9]
8	-2532.2	[-2537.2 -2310.7 -2540.6]	[-2497.4 -2545.6 -2499.0]
9	-2532.1	[-2515.2 -2537.3 -2532.1]	[-2516.8 -2532.1 -2532.1]

3. If it is greater than estimate value of zero support, it means that corresponding cluster contains true locations. The corresponding indexes of maximum estimate provides true locations information. (-1581.1 is greater than -2532.2 and corresponding true index is 90)

The MAP estimate for zero support can be calculated as

$$\mathcal{L}_0 = (1 - p)^L \exp\left(-\frac{1}{\sigma_n^2} \|\mathbf{y}\|^2\right) \quad (5.3)$$

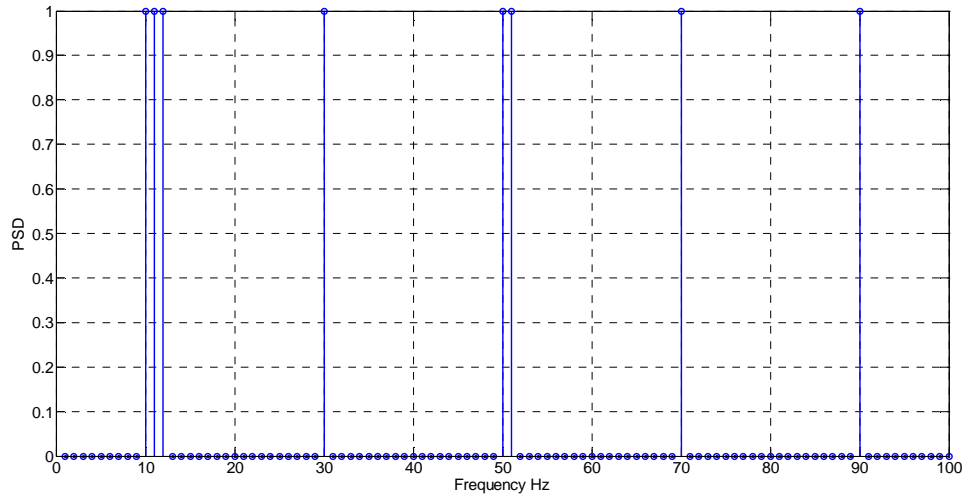


Figure 5.4: Recovered Spectrum

Figure 5.4 shows the recovered sparse signal  $\mathbf{x}(f)$ . Indexes obtained from the SBBSR algorithm corresponds to occupancy by the primary users with in observed frequency spectrum.

## 5.2 SIGNAL MODEL FOR SIMULATION

In the following simulations the wideband signal model is same as defined in equation (5.2) and displayed in Figure 3.2. Choosing this model for the spectrum definition proves fruitful while performing comparison analysis between the SBBSR algorithm and the compressed sensing based spectrum sensing. Active frequency bands can be designed as nonzero mean Gaussian signal. Since equations (3.13), (3.14), (3.15) and (3.16) mentioned in section 3.4.2 are defined for zero mean Gaussian signal. Modification of equation (3.13) and (3.14) for the nonzero mean Gaussian signal is

necessary whereas equation (3.15) and (3.16) are designed for the cases when signal distribution is unknown. So, whether the transmitted signal is Gaussian with zero mean or nonzero mean does not affects its performance. Hence these equations do not require modification. Corresponding (modified) equations for (3.13) and (3.14) are

$$p(\mathbf{y}/S) = \frac{\exp(-\frac{1}{\sigma_n^2} (\mathbf{y} - \mathbf{\Theta}\mu_x)^H \mathbf{\Sigma}_S^{-1} (\mathbf{y} - \mathbf{\Theta}\mu_x))}{\det(\mathbf{\Sigma}_S)} \quad (5.4)$$

and

$$\mathbf{\Sigma}_S = \mathbf{I} - \frac{\mu_x}{\sigma_n^2} \mathbf{\Theta}_S \mathbf{\Theta}_S^H + \frac{\sigma_x^2}{\sigma_n^2} \mathbf{\Theta}_S \mathbf{\Theta}_S^H \quad (5.5)$$

Correspondingly calculation of likelihood for the zero support is given as

$$\mathcal{L}_0 = (1 - p)^L \exp(-\frac{1}{\sigma_n^2} \|\mathbf{y} - \mathbf{\Theta}\mu_x\|^2) \quad (5.6)$$

The sensing matrix structure is same (a partial IDFT matrix) as defined in equation (5.1). Here it is assumed that the wideband signal of interest lies in the range of  $[0, 1000]\Delta$  Hz, where  $\Delta$  is frequency resolution. The observed spectrum is sparse and has a sparsity level of 6%. Figure 5.5 shows above discussed wideband signal. In addition to the wideband spectrum mentioned in Figure 5.5, spectrum sensing is also performed for the spectrum designed using zero mean Gaussian signal as shown in Figure 5.6. This signal specification is same as for the wideband spectrum shown in Figure 5.5.

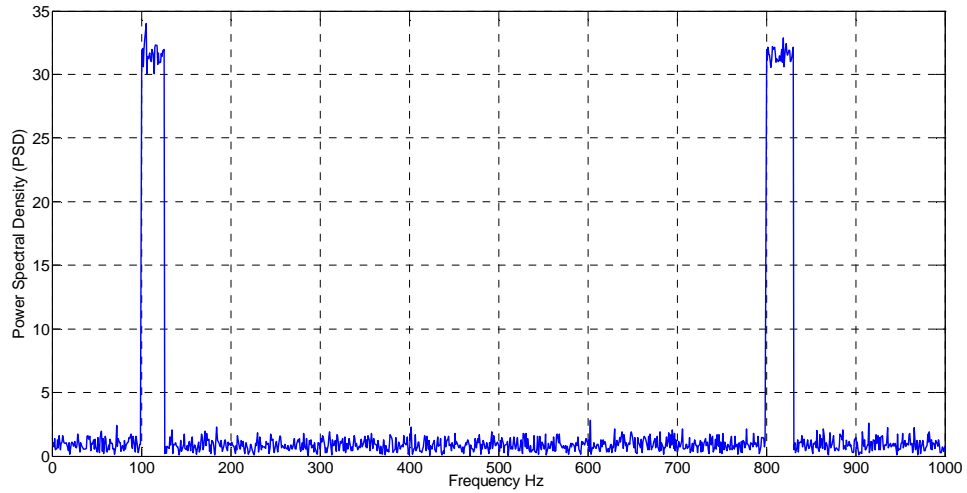


Figure 5.5: Assumed Wideband Signal – Flat PSD

### 5.3 SIMULATION RESULTS

In this section, discussion on simulation results of the spectrum sensing using the SBBSR algorithm has been carried out. Contributions added to the SBBSR algorithm are also explained along with simulations. Simulations are divided into two parts based on following cases:

- When the transmitted signal distribution is known and is Gaussian
- When the transmitted signal distribution is unknown.

Separate simulations and discussion on aforementioned cases have been done. The SBBSR algorithm performance is compared with the compressive sensing based spectrum sensing. It was assumed in [16] that the PSDs of received signal at the CR

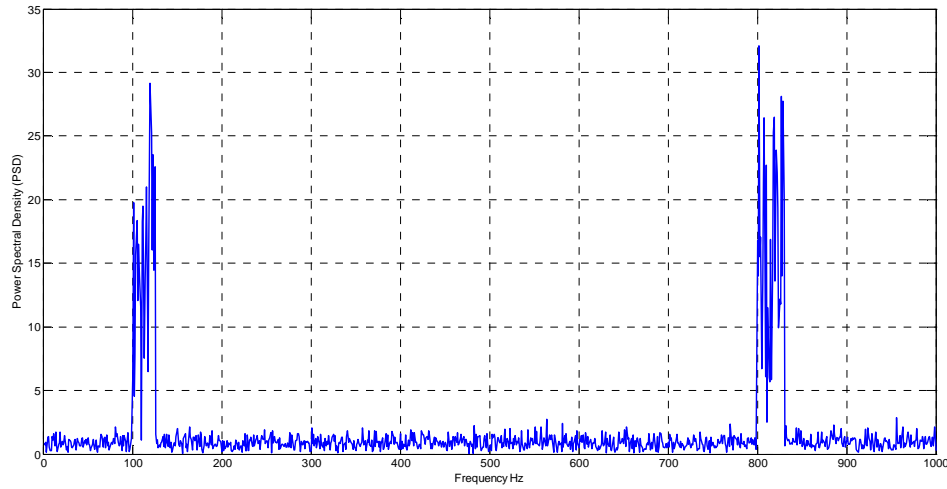


Figure 5.6: Assumed Wideband Signal - Non Flat PSD

should be flat. The spectrum was recovered from sub-Nyquist rate samples using the  $l_1$  minimization approach. The wavelet edge detection technique was applied on the recovered spectrum to obtain the frequency band edges. The PSD is calculated within these frequency bands and decision regarding presence or absence of the primary user was made. The wideband signal shown in Figure 5.5 has been considered.

### **5.3.1 TRANSMITTED SIGNAL DISTRIBUTION IS KNOWN**

Consider the scenario where the transmitted signal, or the primary user signal, distribution is known and is Gaussian. In order to recover the locations where transmission is done by primary user we used the SBBSR algorithm. The SBBSR algorithm supports flexible implementation (as discussed in upcoming text). Numerous

conditions can be imposed to enhance sensing ability of a CR. Based on these conditions corresponding simulations can be described as

- Case 1: Performing spectrum sensing using the SBBSR algorithm without any condition on the received signal.
- Case 2: Performing spectrum sensing using the SBBSR algorithm considering fixed (same) length frequency bands in the received signal.
- Case 3: Performing spectrum sensing using the SBBSR algorithm considering variable length frequency band in the received signal.

#### 5.3.1.1 Case 1

In this case following apriori information (regarding the received signal) is considered

- Received signal is sparse.
- Received signal distribution is known.

Consider the wideband signal shown in Figure 5.5. There are two primary users present in the observed spectrum. Goal of spectrum sensing is to recover the locations of these two primary users.

The SBBSR algorithm provides sub-Nyquist rate sampling solution. The observation (the  $M$  length vector)  $\mathbf{y}$  is sub-Nyquist rate sampled signal. Ratio of Nyquist to sub-Nyquist rate sampling is  $M = \frac{N}{4}$ , where  $N$  is the number of samples required according to the Nyquist rate sampling. Since here we have the block sparse signals so we made some changes in the SBBSR algorithm to make it compatible with the block sparse signals. The



spectrum sensing problem discussed here is same as described in section 5.1. In section 5.1 block sparsity was not taken into consideration however here the block sparse signal is considered. Solution to the problem is somewhat same but there are minor changes as described in following steps.

- 1- Make a fixed length cluster based on correlation between the clusters of sensing matrix as

$$\hat{L} = \frac{N}{M} + 1 \quad (5.7)$$

If working with variable measurement sizes ( $M$ ) than choose maximum possible value of  $\hat{L}$  and fix it for all  $M$ . After choosing  $\hat{L}$  make clusters as mentioned in section 3.4.3.2.

- 2- Instead of calculating likelihoods for support of size  $0,1,2, \dots P_c$  calculate them for  $0,1,2, \dots \hat{P}_c$  where  $\hat{P}_c$  is defined as

$$\hat{P}_c = 2\hat{L} - 1 \quad (5.8)$$

- 3- Instead of making  $P$  clusters, form  $\hat{P}$  clusters of length  $\hat{L}$  where  $\hat{P}$  is defined as

$$\hat{P} = P \times \hat{P}_c \times p \quad (5.9)$$

where  $p$  is the probability of support as defined in equation (3.12). Using above methodology the modified SBBSR algorithm is explained in Figure 5.7.

We are dealing with block sparse signal as shown in Figure 5.5 and Figure 5.6. Instead of explaining each step, as did earlier in section 5.1, required values are explained

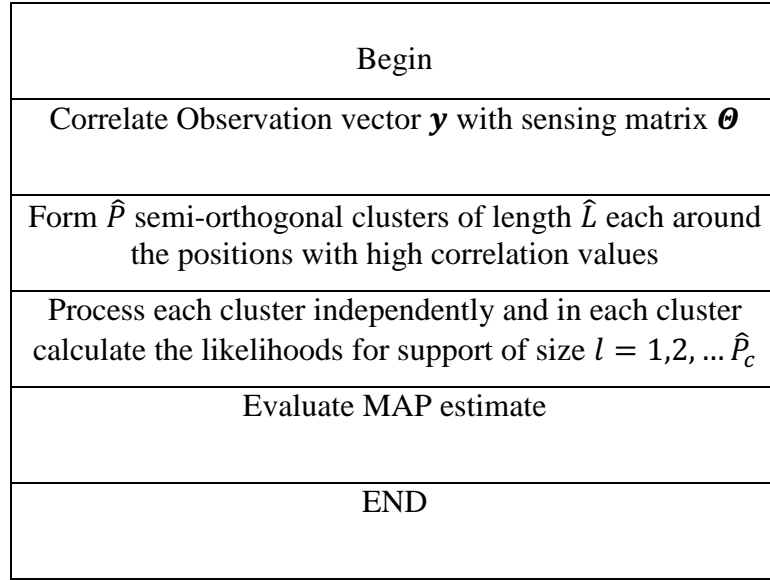


Figure 5.7: Flow Chart of Modified SBBSR Algorithm

in tabular form. Spectrum sensing is performed using the modified SBBSR algorithm as mentioned in Figure 5.7. Corresponding values for performing spectrum sensing on the wideband signals are mentioned in TABLE 5-3. Instead of showing recovery of one signal we opted for probability of detection curves. As described earlier in section 4.4, probability of detection plots explains the probability of detecting true occupied locations by the primary users over range of SNR.

TABLE 5-3: REQUIRED VALUES BY SBBSR ALGORITHMS FOR CASE 1

Observation Vector Size	Number of Clusters	Maximum Support Size	Cluster Size
$M$	$\hat{P}$	$\hat{P}_c$	$\hat{L}$
$\frac{N}{4}$	29	9	9

Probability of detection curves for both Figure 5.5 and Figure 5.6 are shown in Figure 5.8. Corresponding result for spectrum sensing performed using the compressive sensing is also shown in this figure.

### Discussion of Results

IEEE has defined a standard IEEE 802.22 for wireless regional area network (WRAN) devices [57]. According to this standard, probability of detection should be higher than 90% for the WRAN devices to work. Working ranges for aforementioned results (according to IEEE 802.22 standard) are shown in TABLE 5-4. Observe from TABLE 5-4, spectrum sensing results for the SBBSR algorithm (in flat PSDs case) is better than the compressive sensing technique. Former case shows improvement of more than 5dB.

Spectrum sensing based on the sub-Nyquist rate samples is useful when we have high

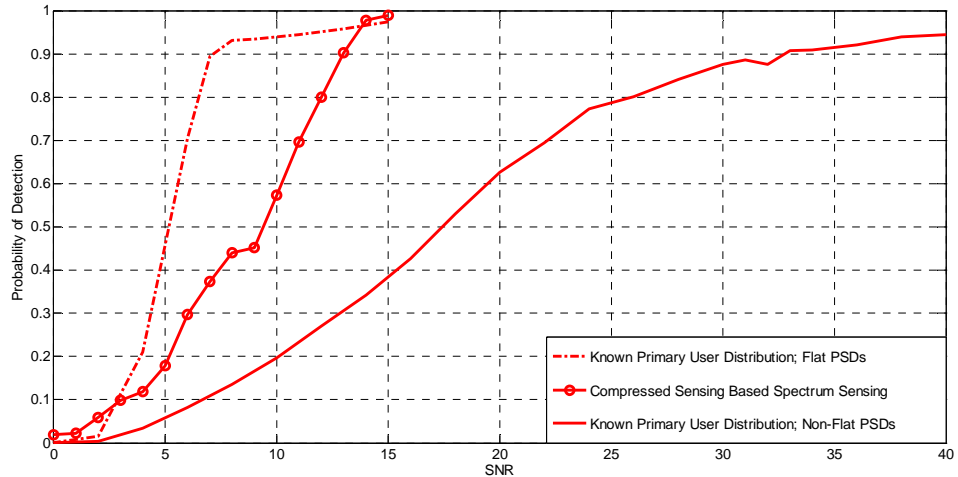


Figure 5.8: Probability of Detection for Known Primary User Distribution - Case 1

TABLE 5-4: WORKING RANGE FOR KNOWN PRIMARY USER  
DISTRIBUTION - CASE 1

Observation Vector Size $M$	Working Range for Figure 5.8		
$\frac{N}{4}$	$SNR \geq 7.1dB$	$SNR \geq 32.75dB$	$SNR \geq 12.95dB$

SNR available. Though sensing problem is solved using four times less measurements (than required) but we are trading it off at the cost of performance. Hence these algorithms are applicable to the sensing problems where high SNR is available but we have timing constraint to perform spectrum sensing. Limited time means limited amount of measurements. Traditional spectrum sensing algorithms will not be able to work under such circumstances and will give poor performance. However, proposed procedure gives good results with limited measurements. At low SNR, signal loses its sparsity because of the high amplitude noise samples. So it is difficult to provide recovery at low SNR.

#### 5.3.1.2 Case 2

Let us assume the scenario in which apriori information about Primary user's band length (or bandwidth) is available. As mentioned in [41], the primary/licensed users have been assigned frequencies based on static spectrum allocation scheme. For instance, the bands 1710-1755 MHz and 1805-1850 MHz are allotted to GSM 1800. This also gives a hint that on certain frequency band the primary users will appear in the form of clusters. So for a certain band these details can be gathered apriori from regulatory authority. Here it is assumed that on a given spectrum all primary users have been assigned known

(fixed) length bands. As mentioned earlier, the SBBSR algorithm has capability of including apriori statistical and sparsity information. Band length information is considered as apriori length information regarding incoming signal bands. In this section, this information is exploited and corresponding probability of detection plots are analyzed.

Small changes have been made to the SBBSR algorithm mentioned in Figure 3.4. Since apriori knowledge of primary user band length is present so calculation of the MAP/Likelihood estimates for various support sizes i.e.  $l = 1, 2, \dots P_c$  is not required. Actually the support size is already known so the MAP estimates are only calculated for that particular support size. Modified procedure for the SBBSR algorithm is described below and shown in Figure 5.9.

- 1- Correlate observation vector  $\mathbf{y}$  with sensing matrix  $\boldsymbol{\theta}$ .
- 2- Make clusters of known (fixed) length  $L$  around maximum correlation values.
- 3- Compute likelihood for known length within each cluster.
- 4- Calculate corresponding MAP estimates of each cluster.

One key advantage is the reduction of computational complexity. Earlier calculation of estimates for various support sizes  $l = 1, 2, \dots P_c$  was required. So  $2^{P_c}$  estimates were calculated. Now with the band length knowledge estimates for various support sizes is not required. One estimate is calculated for each cluster.

Consider the signal at the input of a CR as described in Figure 5.5 and Figure 5.6. Assume that both primary users have same band length. Here spectrum sensing have been

Begin
Correlate Observation vector $\mathbf{y}$ with sensing matrix $\mathbf{\Theta}$
Form $P$ semi-orthogonal clusters of known length $L$ each around the positions with high correlation values
Process each cluster independently and in each cluster calculate the likelihood for support of a known size
Evaluate MAP estimate
END

Figure 5.9: SBBSR Algorithm for apriori Length Knowledge

performed for these fixed length frequency bands. Steps followed here are same as discussed in section 5.1. Corresponding required values of cluster size, observation vector, number of cluster and support size for performing spectrum sensing on the wideband signals (shown in Figure 5.5 and Figure 5.6) are shown in TABLE 5-5. Instead of showing recovery of the spectrum we focused at the corresponding probability of detection

TABLE 5-5: REQUIRED VALUES BY SBBSR ALGORITHMS FOR CASE 2

Observation Vector Size	Number of Clusters	Maximum Support Size	Cluster Size
$M$	$P$	$P_c$	$L$
$\frac{N}{4}$	79	1	31

curves. Probability of detection curves are obtained by averaging the result of 100 Monte Carlo realizations as shown in Figure 5.10.

### Discussion of Results

Observe from Figure 5.10, apriori knowledge showed promising results for both cases i.e. flat and non-flat PSDs in comparison to the compressive sensing technique. Acceptable working ranges according to IEEE 802.22 standard are given in TABLE 5-6.

Improvement in working range of the algorithm is not the only key advantage. Incorporating the length information also results in reduction of computational complexity. A simple example would be: Earlier (in Case 1) various support sizes  $l = 1, 2, \dots, P_c$  were considered inside a cluster to calculate the MAP estimates. Now with the apriori length information we don't have to calculate these estimates for various

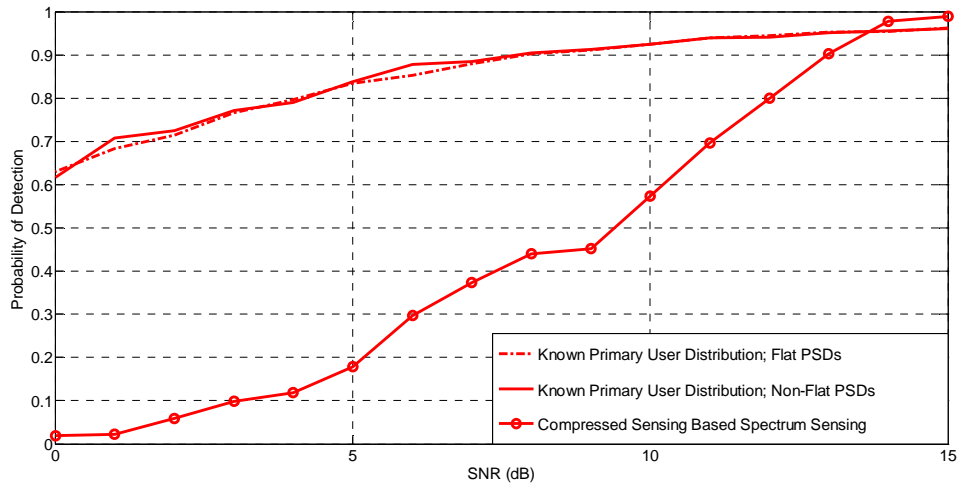


Figure 5.10: Probability of Detection for Known Primary User Distribution - Case 2

TABLE 5-6: WORKING RANGE FOR KNOWN PRIMARY USER  
DISTRIBUTION - CASE 2

Observation Vector Size $M$	Working Range for Figure 5.10		
$\frac{N}{4}$	$SNR \geq 7.8dB$	$SNR \geq 7.8dB$	$SNR \geq 12.95dB$

support sizes. Only one estimate is calculated for known length. Hence computation complexity while calculating estimates is reduced by  $P_c$ .

In summary, apriori knowledge regarding length of primary user's band helped in achieving reduction in computational complexity as well as gain in probability of detection.

#### 5.3.1.3 Case 3

In section 5.3.1.2, it was assumed the received signal at CR consists of fixed length frequency bands. Now assume that in the observed spectrum, variable length frequency bands are present. Length of these frequency bands is assigned based on some probability distribution function. Assume that this apriori length information is also known at the receiver.

This case is quite similar to Case1 where no information regarding the bandwidth of primary users is available. In Case1, the maximum support size was dependent on  $P_c$ . Estimates were calculated corresponding to support sizes of  $l = 1, 2 \dots P_c$  within a cluster. This procedure was repeated for the  $P$  clusters. Corresponding indexes of maximum



valued estimates provides the information regarding occupancy of frequency locations by the primary user. Now, in this section estimate calculation is only done for known support sizes within each cluster.

This apriori information helped in achieving reduction in computational complexity in comparison to Case 1. Earlier in Case1, calculation of the estimates for support sizes  $l = 1, 2 \dots P_c$  within a cluster was required. Now the estimates are only calculated for known lengths within a cluster. This apriori knowledge provides reduction in computational complexity.

Consider Figure 5.5 and Figure 5.6 as the received signals at CR. Both signals contain variable length primary users. Assume that these lengths are based on the Rayleigh distribution. Rayleigh distribution is also known at the CR and so are the corresponding lengths of each primary user. This information has been used while calculating the MAP estimates. Same steps, except one, have been followed for performing spectrum sensing as described in section 5.1. Instead of calculating estimates for support sizes  $l = 1, 2 \dots P_c$  calculate them for the known support sizes. Corresponding required values of cluster size, observation vector, number of cluster and support size for performing spectrum sensing on the wideband signals (shown in Figure 5.5 and Figure 5.6) are shown in TABLE 5-7. Resultant probability of detection curves, averaged over 100 Monte Carlo realizations, for Figure 5.5 and Figure 5.6 have been shown in Figure 5.11

TABLE 5-7: REQUIRED VALUES BY SBBSR ALGORITHMS FOR CASE 3

Observation Vector Size	Number of Clusters	Maximum Support Size	Cluster Size
$M$	$P$	$P_c$	$L$
$\frac{N}{4}$	79	3	[25 31]

### Discussion of Results

Observe from Figure 5.11, considerable improvements have been achieved for both the flat and non-flat PSD cases in contrast to the compressive sensing result. Acceptable working ranges according to IEEE 802.22 standard are given in TABLE 5-8. Apriori knowledge regarding bandwidth of the primary users showed considerable improvement in the performance of the SBBSR algorithm based spectrum sensing. This knowledge also helped in reducing computational complexity of algorithm.

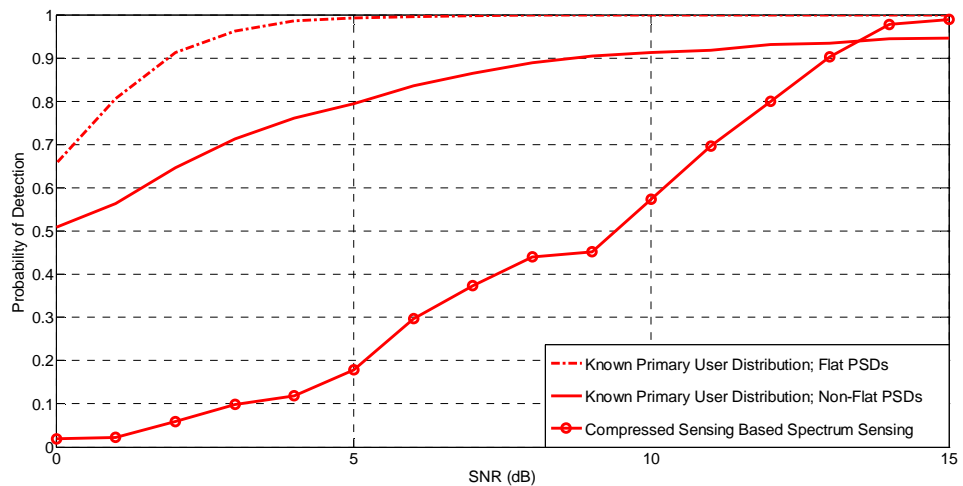


Figure 5.11: Probability of Detection for Known Primary User Distribution - Case 3

TABLE 5-8: WORKING RANGE FOR KNOWN PRIMARY USER  
DISTRIBUTION - CASE 2

Observation Vector Size $M$	Working Range for Figure 5.11		
$\frac{N}{4}$	$SNR \geq 1.8dB$	$SNR \geq 8.5dB$	$SNR \geq 12.9dB$

### **5.3.2 TRANSMITTED SIGNAL DISTRIBUTION IS UNKNOWN**

Earlier in section 5.3.1, it was assumed that the transmitted signal distribution is known at the receiver. Now in this section no knowledge regarding the transmitted signal distribution is available. Equation (3.18) provides the corresponding MAP estimate for current scenario.

Numerous cases (as considered earlier) can be described as follows

- Case 1: Performing spectrum sensing using the SBBSR algorithm without any condition on the received signal.
- Case 2: Performing spectrum sensing using the SBBSR algorithm considering fixed (same) length frequency bands in the received signal.
- Case 3: Performing spectrum sensing using the SBBSR algorithm considering variable length frequency band in the received signal.

### 5.3.2.1 Case1

This case is same as defined in section 5.3.1.1. Only sparsity is considered as the apriori information. Consider the wideband signal shown in Figure 5.5 and Figure 5.6. There are two primary users present in the observed spectrums. Goal of spectrum sensing is to recover the locations of these two primary users. Here spectrum sensing is performed using the modified SBBSR algorithm as mentioned in Figure 5.7. Steps followed here are same as described in section 5.1. For likelihood calculation equation (3.15) has been used. Corresponding values for performing spectrum sensing on the wideband signals (shown in Figure 5.5 and Figure 5.6) are same as mentioned in TABLE 5-3. Corresponding probability of detection plots have been shown in Figure 5.12. Discussion of results as in section 5.3.1.1 is applicable to this section also. Spectrum sensing using the SBBSR algorithm showed considerable improvement when compared

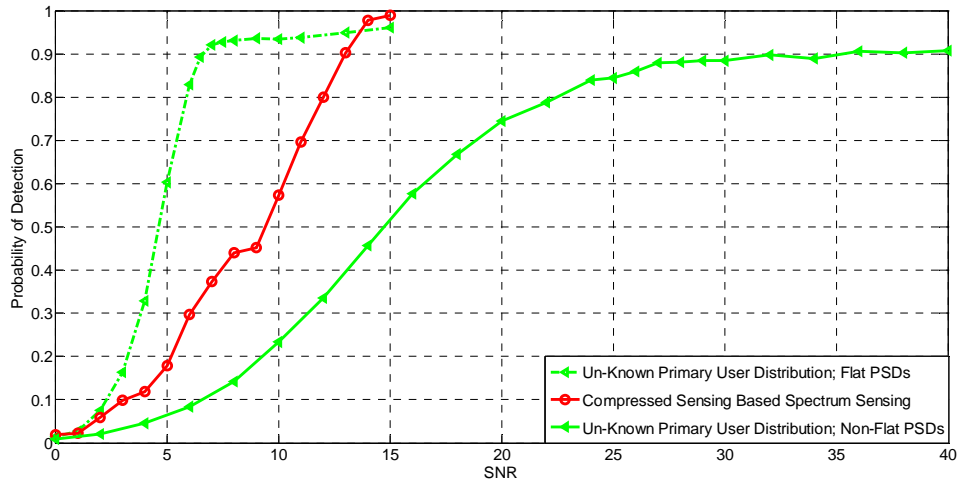


Figure 5.12: Probability of Detection for Un-Known Primary User Distribution - Case 1

with the compressive sensing based results. This proves the fact that the SBBSR algorithm formulation for the case when we don't know about the signal statistics is equally good. TABLE 5-9 provides working ranges according to IEEE 802.22 standard.

#### 5.3.2.2 Case 2

This case is same as defined in section 5.3.1.2. Here it is assumed that on a given spectrum all primary users have been assigned known (fixed) length bands. As mentioned earlier, the SBBSR algorithm has capability of including apriori statistical and sparsity information. Band length information is considered as the apriori length information regarding the incoming signal frequency bands. In this section, this information is exploited and corresponding probability of detection plots are analyzed.

Consider Figure 5.5 and Figure 5.6 as the received signal at a CR. Spectrum sensing performed here is same as defined in section 5.3.1.2 and explained in Figure 5.9. Same assumptions were taken as in section 5.3.1.2. Corresponding required values of cluster size, observation vector, number of cluster and support size for performing spectrum sensing on the wideband signals (shown in Figure 5.5 and Figure 5.6) are same and

TABLE 5-9: WORKING RANGE FOR UN-KNOWN PRIMARY USER  
DISTRIBUTION - CASE 1

Observation Vector Size $M$	Working Range for Figure 5.12		
$\frac{N}{4}$	$SNR \geq 6.5dB$	$SNR \geq 35.3dB$	$SNR \geq 12.9dB$

mentioned in TABLE 5-5. Corresponding probability of detection plots, for Figure 5.5 and Figure 5.6, averaged over 100 Monte Carlo realizations are shown in Figure 5.13. Working ranges according to IEEE 802.22 standard are shown in TABLE 5-10.

Observe the probability of detection curve shown in Figure 5.13 and compare them to case when no knowledge regarding the signal and length of primary user is available, as shown in Figure 5.12. The apriori length knowledge helped in improving the probability of detection. In Figure 5.12 at SNR of 0dB we have poor probability of detection whereas in Figure 5.13 we still have reasonable probability of detection. Another advantage is the reduction in computational complexity. Results obtained in this section are quite similar to section 5.3.1.2. In conclusion, apriori knowledge of length helped in lesser computational complexity and better probability of detection.

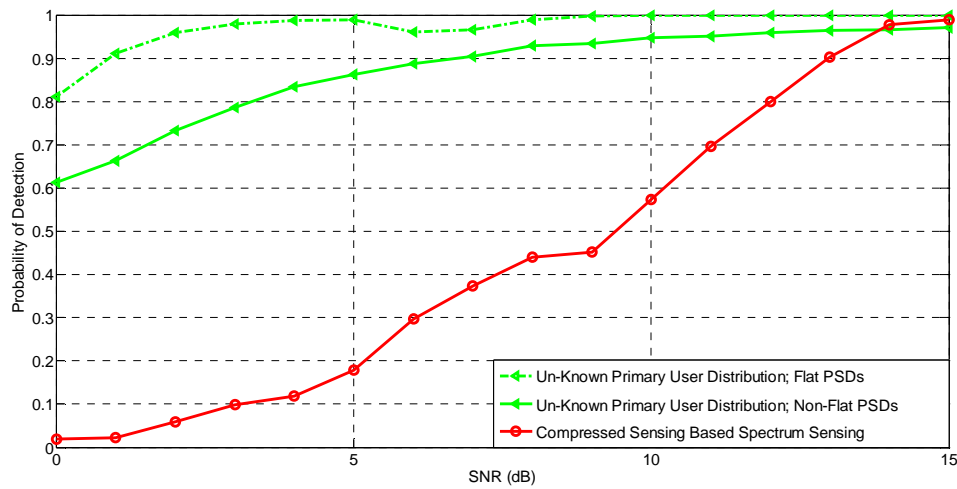


Figure 5.13: Probability of Detection for Un-Known Primary User Distribution - Case 2

TABLE 5-10: WORKING RANGE FOR UN-KNOWN PRIMARY USER  
DISTRIBUTION - CASE 2

Observation Vector Size $M$	Working Range for Figure 5.13		
$\frac{N}{4}$	$SNR \geq 0.9dB$	$SNR \geq 6.8dB$	$SNR \geq 12.9dB$

### 5.3.2.3 Case3

In this section a more generalized scenario is discussed in comparison to the previous scenario. Earlier, it was assumed that the CR is sensing a spectrum in which multiple primary users were present. Each primary user has same (fixed) length bandwidth and is known at the CR. Now assume that multiple primary users are present in observed spectrum and they have variable (length) bandwidth. These lengths are assigned based on some probability distribution function. Assume knowledge of these lengths and probability distribution function is also available at the CR.

This case is similar to the case described in 5.3.1.3. We perform spectrum sensing of the received spectrums shown in Figure 5.5 and Figure 5.6. Assumptions taken and steps performed for spectrum sensing here are same as described in section 5.3.1.3. Corresponding required values of cluster size, observation vector, number of cluster and support size for performing spectrum sensing on the wideband signals are also same and shown in TABLE 5-7. Probability of detection curves averaged over 100 Monte Carlo realizations are shown in Figure 5.14. Working range according to IEEE 802.22 standard

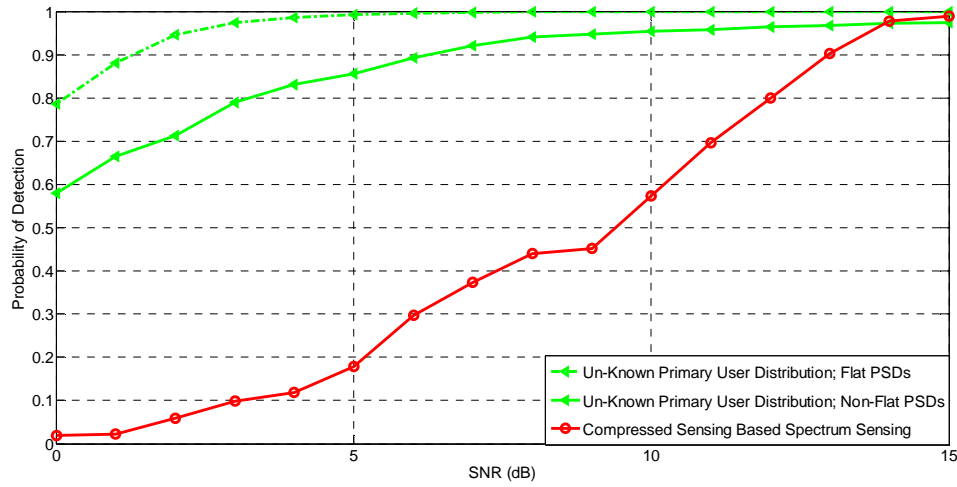


Figure 5.14: Probability of Detection for Un-Known Primary User Distribution - Case 3

are shown in TABLE 5-11. Inculcating apriori knowledge regarding length helped us in improving the performance of algorithm. Comparing current scenario results with Case 2 (section 5.3.2.2) leads us to same conclusion. In fact current scenario is generalization of the same (fixed) length scenario and hence their performance should be same.

Another advantage of using the apriori knowledge is reduction in computational complexity. Earlier estimates were calculated for the various support sizes  $l = 1, 2 \dots P_c$  and now they are only calculated for the fixed and known support sizes.

Summing up, the apriori knowledge of length helped in lesser computational complexity and better probability of detection.



TABLE 5-11: WORKING RANGE FOR UN-KNOWN PRIMARY USER  
DISTRIBUTION - CASE 3

Observation Vector Size $M$	Working Range for Figure 5.14		
$\frac{N}{4}$	$SNR \geq 1.3dB$	$SNR \geq 6.3dB$	$SNR \geq 12.9dB$

## 5.4 CONCLUSION

In this chapter spectrum sensing was performed using the SBBSR algorithm. Observed spectrum is block sparse. Accordingly few modifications were made in the SBBSR algorithm to make it work for the block sparse signals. Based on signal knowledge at the receiver different cases were dealt. The apriori information regarding frequency band length proved helpful. Comparisons were made to the compressed sensing based spectrum sensing approach. In all cases more than (approximately) 6dB improvement was achieved. In addition, lesser computational complexity proved a big edge.

## **CHAPTER 6**

### **SPECIAL CASE: OFDM SIGNAL**

In this chapter spectrum sensing is performed on a real time signal model. It is considered that the primary users are using the Digital Video Broadcasting-Terrestrial (DVB-T) OFDM system for the transmission of their data. Spectrum sensing is performed using the modified SBBSR algorithms as described in Chapter 5. Different cases are dealt based on the knowledge regarding the incoming signal at a CR. Corresponding probability of detection curves are obtained and analyzed.

#### **6.1 DIGITAL VIDEO BROADCASTING-TERRESTRIAL OFDM**

##### **SYSTEM**

The digital video broadcasting (DVB) is a European standard for the broadcast transmission of the digital terrestrial television (DTV). The DVB standard is first published in 1997 [58] and the first transmission using this standard was done in 1998, UK. IEEE has established a group named Wireless Regional Area Network (WRAN) and

had given it a standard IEEE 802.22. This group is established to create standards for the CR Physical/MAC interfaces. These standards will be used by the CR to operate in licensed spectrum of the DTV [59].

Let's review the DVB-T OFDM System. In [60] expression for one OFDM symbol, starting at  $t = t_s$  is given as

$$x(t) = \begin{cases} Re \left\{ \sum_{i=-\frac{N_s}{2}}^{\frac{N_s}{2}-1} d_{i+\frac{N_s}{2}} \exp \left( j2\pi \left( f_c - \frac{i+0.5}{T} \right) (t - t_s) \right) \right\}, & t_s \leq t \leq t_s + T \\ 0, & t < t_s \text{ or } t > t_s + T \end{cases} \quad (6.1)$$

where,

$d_i$  are complex modulation symbols

$N_s$  are the number of sub-carriers

$f_c$  is the carrier frequency

$T$  is the symbol duration

Similar expression for the generalized OFDM system based on the DVB-T system is given in [61] as

$$x(t) = Re \left\{ e^{j2\pi f_c t} \sum_{m=0}^{\infty} \sum_{l=0}^{67} \sum_{k=K_{min}}^{K_{max}} c_{m,l,k} \Psi_{m,l,k}(t) \right\} \quad (6.2)$$

where,

$$\Psi_{m,l,k}(t) = \begin{cases} \exp(j2\pi \frac{k'}{T_u}(t - \Delta - lT_s - 68mT_s)), (l + 68m)T_s \leq t \leq (l + 68m + 1)T_s \\ 0, \text{ else} \end{cases} \quad (6.3)$$

Corresponding variables in equation (6.2) and (6.3) are explained in TABLE 6-1. Equation (6.2) represents a working system that has been used and tested since March, 1997. For one symbol i.e. from  $t = 0$  to  $t = T_s$  equation (6.2) becomes [61]

$$x(t) = Re \left\{ e^{j2\pi f_c t} \sum_{k=K_{min}}^{K_{max}} c_{0,0,k} e^{j2\pi k'(t-\Delta)/T_u} \right\} \quad (6.4)$$

TABLE 6-1: DESCRIPTION OF VARIABLES FOR GENERALIZED DVB-T SYSTEM

VARIABLE	DESCRIBES
$k$	Carrier number
$l$	OFDM symbol number
$m$	Transmission frame number
$K$	Number of transmitted carriers
$T_s$	Symbol duration
$T_u$	Inverse of carrier spacing
$\Delta$	Guard interval
$f_c$	Carrier frequency
$k'$	Carrier index relative to the center frequency i.e. $k' = k - \frac{K_{max}+K_{min}}{2}$
$c_{m,i,k}$	Complex symbol for carrier $k$ of the data symbol number $i$ in frame number $m$

There are two modes of the DVB-T standard i.e.  $2k$  and  $8k$ . Here  $2k$  mode is considered. This mode is intended for the mobile reception of a standard definition DTV. Other specification regarding OFDM symbol in DVB-T  $2k$  mode are given in TABLE 6-2 [61].

For our simulation work we considered only one OFDM symbol. We used a scaled down version of the DVB-T  $2k$  mode i.e. based on  $2k$  mode but has specifications

TABLE 6-2: NUMERICAL VALUES FOR OFDM SYMBOL IN DVB-T  $2k$  MODE

Parameter	DVB-T $2k$ Mode			
Elementary Period $T$	$\frac{7}{64} \mu sec$			
Number of carriers $K$	1705			
Value of carrier number $K_{min}$	0			
Value of carrier number $K_{max}$	1704			
Duration $T_u$	224 $\mu sec$			
Carrier spacing $\frac{1}{T_u}$	4,464 Hz			
Spacing between carriers $K_{min}$ and $\frac{K_{max}(K-1)}{T_u}$	7.61 MHz			
Allowed Guard Interval	$\frac{1}{4}$ ,	$\frac{1}{8}$ ,	$\frac{1}{16}$ ,	$\frac{1}{32}$
Duration of Symbol part $T_u$	$2048 \times T$			
	224 $\mu sec$			
Duration of Guard Interval $\Delta$	$512 \times T$	$256 \times T$	$128 \times T$	$64 \times T$
	56 $\mu sec$	28 $\mu sec$	14 $\mu sec$	7 $\mu sec$
Symbol Duration $T_s = \Delta + T_u$	$2560 \times T$	$2304 \times T$	$2176 \times T$	$2112 \times T$
	280 $\mu sec$	252 $\mu sec$	238 $\mu sec$	231 $\mu sec$

that take smaller duration to compute. These scaled down specifications have been shown in TABLE 6-3. The input signal (observed spectrum) at a CR may consist of single primary user or multiple primary users. Input signal generation is shown in Figure 6.1.

TABLE 6-3: SIMULATED OFDM SYMBOL IN DVB-T 2k MODE

Parameter	DVB-T 2k Mode			
Elementary Period $T$	1.4 msec			
Number of carriers $K$	32			
Value of carrier number $K_{min}$	0			
Value of carrier number $K_{max}$	31			
Duration $T_u$	22.4 msec			
Carrier spacing $\frac{1}{T_u}$	44.64 Hz			
Spacing between carriers	1.4285 KHz			
Allowed Guard Interval	$\frac{1}{4}'$	$\frac{1}{8}'$	$\frac{1}{16}'$	$\frac{1}{32}$
Duration of Symbol part $T_u$	$\left(\frac{K}{2}\right) \times T$			
	22.4 msec			
Duration of Guard Interval $\Delta$	$\left(\frac{0.5K}{4}\right) \times T$	$\left(\frac{0.5K}{8}\right) \times T$	$\left(\frac{0.5K}{16}\right) \times T$	$\left(\frac{0.5K}{32}\right) \times T$
	5.6 msec	2.8 msec	1.4 msec	0.7 msec
Symbol Duration $T_s = \Delta + T_u$	$(0.5K + \left(\frac{0.5K}{4}\right)) \times T$	$(0.5K + \left(\frac{0.5K}{8}\right)) \times T$	$(0.5K + \left(\frac{0.5K}{16}\right)) \times T$	
	28 msec	25.2 msec	23.8 msec	

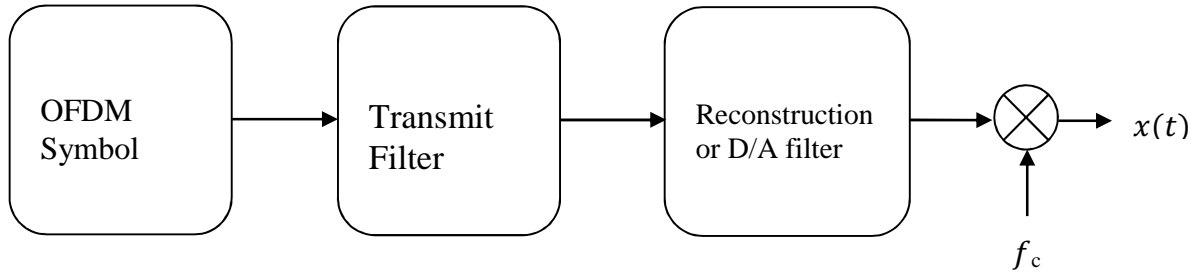


Figure 6.1: OFDM Signal Generation

## 6.2 SIMULATION RESULTS

In this section spectrum sensing using the SBBSR algorithm is performed. Primary users in the observed spectrum are using DVB-T 2k mode for transmission of their data. Parameters of this mode are described in TABLE 6-3. In following text, a detailed description for performing spectrum sensing using the SBBSR algorithm (considering the DVB-T system) is given.

### 6.2.1 SPECTRUM SENSING USING SBBSR ALGORITHM

The observed spectrum consists of one active primary user. Assume the situation where single primary user is present in the observed spectrum. Total available spectrum is 14.28 KHz where the primary user is centered at 7.14 KHz. Primary user is using the same signal model as described in TABLE 6-3. Cyclic prefix is of length  $(\frac{T_u}{4})$ . The primary user band extends from 6.52 – 7.95 KHz and uses QAM modulation scheme. Figure 6.2 shows the observed spectrum which consists of a primary user at 7.14 KHz.

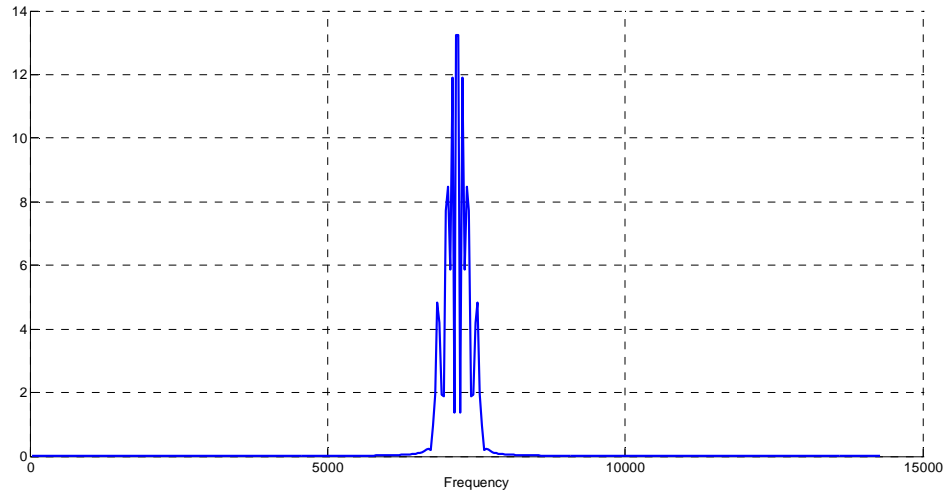


Figure 6.2: Observed Spectrum

Same steps are considered as described in section 5.1. First, correlate the received signal with the sensing matrix. Observed vector at a CR  $\mathbf{y}$  has length of  $M = \frac{N}{2}$ . Upper bound on cluster length  $L$  is 3. Total number of the clusters  $P$  and maximum number of the supports  $P_c$  are 41 and 2. Sparsity level is set to 10%. On linear scale occupied locations correspond to indexes 181, 182 ... 219, 220.

Make  $P$  clusters around high correlation values. TABLE 6-4 provides the cluster information. Since the total numbers of clusters are huge, only few are displayed to illustrate the concept. Observe, some of the clusters contain no useful information for sparse recovery. Next compute the MAP estimate corresponding to the support of sizes  $l = 0, 1, 2$  within each cluster. TABLE 6-5 provides this information.



TABLE 6-4: CLUSTER INFORMATION FOR DVB-T SYSTEM

Cluster Number	Indexes Covered by Cluster	Useful Index in Cluster
1	[210 211 212]	All
2	[191 192 193]	All
3	[206 207 208]	All
4	[195 196 197]	All
.	.	.
.	.	.
.	.	.
40	[357 358 359]	None
41	[123 124 125]	None

Since complete information regarding the MAP estimates is achieved, find the largest estimates and compare them and deduce information regarding the true location (as did in section 5.1). Figure 6.3 shows the transmitted OFDM signal and the recovered OFDM signal.

### **6.2.2 PRIMARY USER SIGNAL DISTRIBUTION IS KNOWN**

Here same scenario is considered as described in section 5.3.1, where the primary user signal distribution is known. In order to recover the locations where transmission is done by primary user the SBBSR algorithm is used. The SBBSR algorithm supports

TABLE 6-5: MAP ESTIMATES FOR CORRESPONDING SUPPORT SIZES -  
DVB-T SYSTEM

Cluster Number	Likelihood of Support = 0	Likelihood of Support = 1	Likelihood of Support = 2
1	-7636.5	[-6283.2 -6097.8 -6931.2] [210 211 212]	[-5422.9 -5579.6 -5609.1] [210,211 210,212 211,212]
2	-7636.5	[-6998.3 -6220.9 -6401.7] [191 192 193]	[-5798.3 -5765.2 -5633.6] [191,192 191,193 192,193]
3	-7636.5	[-6711.6 -6535.3 -7434.0]	[-6321.4 -6511.2 -6463.3]
.	.	.	.
.	.	.	.
.	.	.	.
40	-7636.5	[-7645.5 -7644.1 -7646.3]	[-7653.9 -7655.3 -7653.7]
41	-7636.5	[-7.6449 -7.6441 -7.6468]	[-7.6536 -7.6552 -7.6509]

flexible implementation. As in section 5.3.1, numerous conditions have been imposed to enhance the sensing ability of a CR. Based on these conditions corresponding simulations can be described as

- Case 1: Performing spectrum sensing using the SBBSR algorithm without any condition on the received signal.
- Case 2: Performing spectrum sensing using the SBBSR algorithm considering fixed (same) length frequency bands in the received signal.

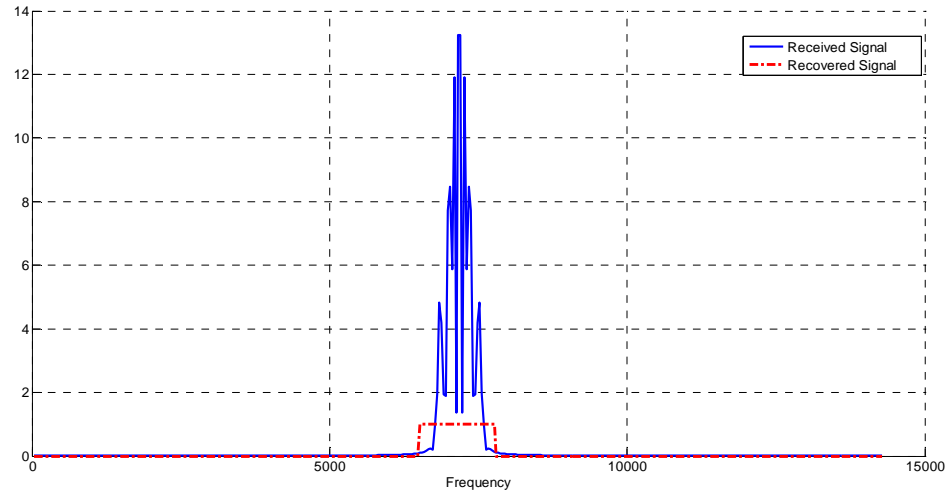


Figure 6.3: Reconstruction of Spectrum - DVB-T System

Here (and in next section), the signal model shown in TABLE 6-3 has been considered. Earlier in Figure 6.2 the observed spectrum has only one active primary user. Now consider the case where multiple primary users are present in the observed spectrum. Assume there are two primary users exploiting the spectrum. The observed spectrum is of bandwidth 28.571 KHz. User 1 is centered on 7.1426 KHz and user 2 is centered on 21.43 KHz. Both users have the same bandwidth i.e. 1.428 KHz. Both users are using the OFDM modulation for transmission. Sparsity level is set to 10%. For both users the cyclic prefix length is same and equals  $\frac{T_u}{4}$ . Figure 6.4 describes the aforementioned scenario.

#### 6.2.2.1 Case 1

In this case no additional apriori information regarding the received signal other than sparsity is considered. Consider the spectrum shown in Figure 6.4. There are two

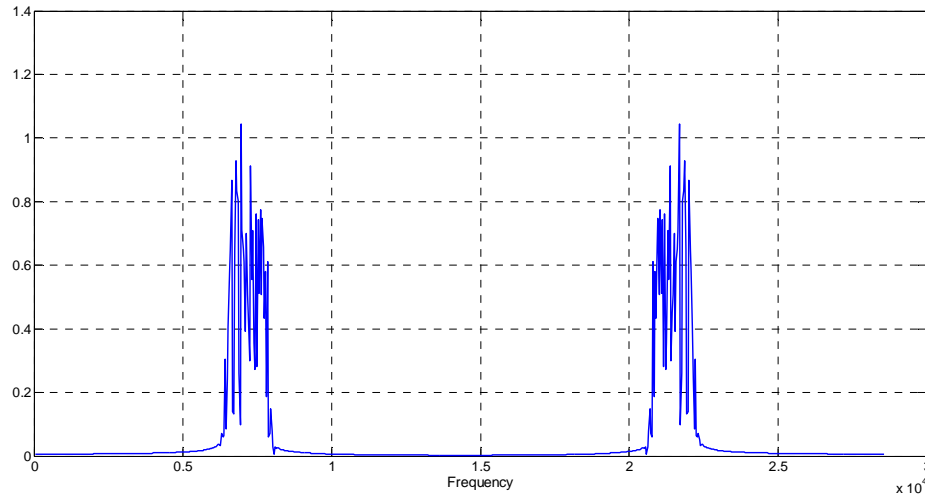


Figure 6.4: Observed Spectrum with Multiple Primary Users – DVB-T System

primary users present in the observed spectrum. This case is exactly similar to the case discussed in section 5.3.1.1. Spectrum sensing is performed using the modified SBBSR algorithm as mentioned in Figure 5.7. The steps followed here are same as described in section 6.2.1. Corresponding values for performing spectrum sensing on the observed spectrum are mentioned in TABLE 6-6. Probability of detection curve for sensing primary users in the observed spectrum (as shown in Figure 6.4) are shown in Figure 6.5. Here we cannot compare our results with that of the compressed sensing based spectrum sensing as PSDs in observed spectrum are not flat. This also provides us a fact that spectrum sensing based on the SBBSR algorithm can handle more realistic cases in contrast to [16]. Working range according to IEEE 802.22 standard is for SNR greater than 36 dB.

TABLE 6-6: REQUIRED VALUES BY SBBSR ALGORITHM – DVB-T Case 1

Observation Vector Size	Number of Clusters	Maximum Support Size	Cluster Size
$M$	$\hat{P}$	$\hat{P}_c$	$\hat{L}$
$\frac{N}{4}$	72	9	9

#### 6.2.2.2 Case 2

Assume the scenario in which apriori information about the primary user's band length (or bandwidth) is available. Assume that in a given spectrum all primary users have been assigned known (fixed) length bands. Band length information is considered as apriori length information regarding the incoming signal bands. In this section, this information is exploited and corresponding probability of detection plots are analyzed.

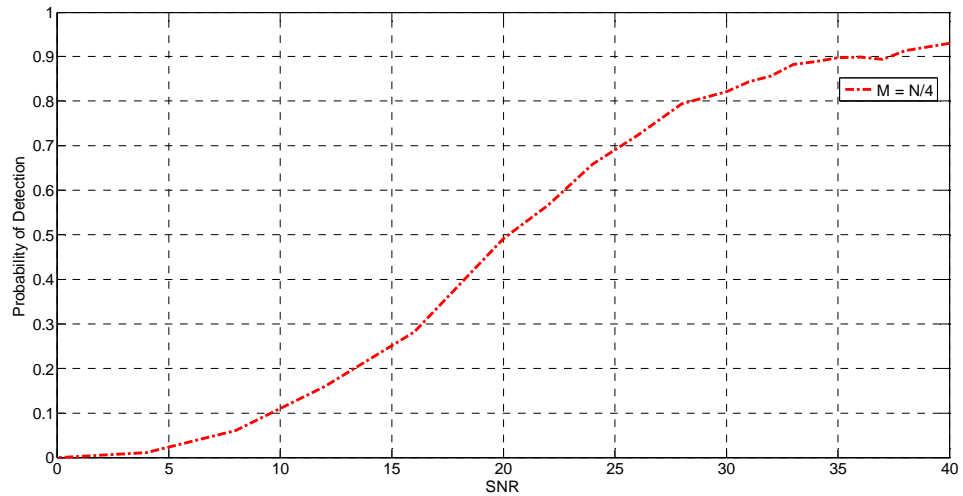


Figure 6.5: Probability of Detection for Known Primary User Distribution – DVB-T

Case 1

As described earlier, this apriori information helps in achieving reduction in computational complexity.

Consider the spectrum shown in Figure 6.4. Spectrum sensing here is performed using the modified SBBSR algorithm as described in Figure 5.9. Steps followed here are same as discussed in section 6.2.1 except few changes as discussed in Figure 5.9. Corresponding required values of the cluster size, observation vector, number of cluster and support size for performing spectrum sensing on the observed spectrum are shown in TABLE 6-7. Probability of detection curve has been achieved by averaging the result of 100 Monte Carlo realizations as shown in Figure 6.6. Observe, working range according to IEEE 802.22 standard is for SNR greater than 12 dB.

Observe the apriori knowledge improved the performance of the SBBSR algorithm by 22dB. Also observe, apriori length knowledge provides better probability of detection than spectrum sensing performed using the compressed sensing (Figure 5.10). The algorithm described in [16], is only applicable for the spectrum where we have flat PSD's whereas the SBBSR algorithm can handle both cases. This proves the fact that spectrum sensing based on the SBBSR algorithm can accommodate, with better probability of detection, real time scenarios in contrast to the compressed sensing based technique.

TABLE 6-7: REQUIRED VALUES BY SBBSR ALGORITHM – DVB-T Case 2

Observation Vector Size $M$	Number of Clusters $P$	Maximum Support Size $P_c$	Cluster Size $L$
$\frac{N}{4}$	103	1	40

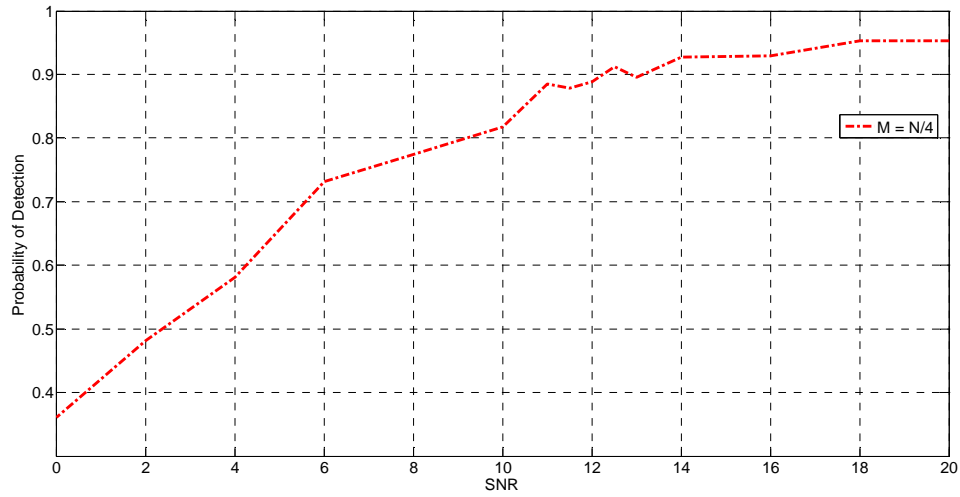


Figure 6.6: Probability of Detection for Known Primary User Distribution – DVB-T

Case 2

### **6.2.3 PRIMARY USER SIGNAL DISTRIBUTION IS UN-KNOWN**

In this section, assume no knowledge about the transmitted signal distribution is available. Equation (3.18) provides the corresponding MAP estimate for current scenario.

In this section we consider the same spectrum as shown in Figure 6.4. Various cases can be described as follows

- Case 1: Performing spectrum sensing using the SBBSR algorithm without any condition on the received signal.
- Case 2: Performing spectrum sensing using the SBBSR algorithm considering fixed (same) length frequency bands in the received signal.

### 6.2.3.1 Case1

This case is same as defined in section 5.3.1.1. Only sparsity of the signal is considered as apriori information. Consider the observed spectrum as shown in Figure 6.4. There are two primary users present in the observed spectrums. Here for spectrum sensing purpose the modified SBBSR algorithm as mentioned in Figure 5.7 has been used. Steps followed here are same as described in section 6.2.1. For likelihood calculation equation (3.15) is used. Corresponding values for performing spectrum sensing on the spectrum shown in Figure 6.4 are same as mentioned in TABLE 6-6. Probability of detection plot for the observed spectrum (shown in Figure 6.4) is shown in Figure 6.7. Observe the working range according to IEEE 802.22 standard is for SNR greater than 33dB.

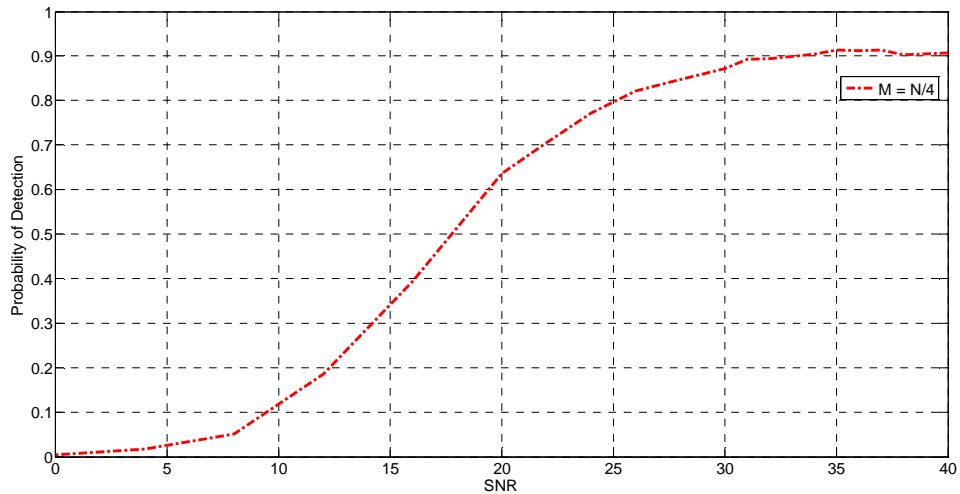


Figure 6.7: Probability of Detection for Un-Known Primary User Distribution –  
DVB-T Case 1



### 6.2.3.2 Case 2

This case is same as defined in section 5.3.1.2. Here it is assumed that on a given spectrum all primary users have been assigned known (fixed) length bands. Band length information is considered as apriori length information regarding the incoming signal bands. In this section, this information is exploited and corresponding probability of detection plots are analyzed.

Consider Figure 6.4 as the observed spectrum at a CR. The spectrum sensing performed here is same as defined in section 5.3.1.2 and explained in Figure 5.9. Corresponding required values of the cluster size, observation vector, number of cluster and support size for performing spectrum sensing on the observed spectrum are same and shown in TABLE 6-7. Probability of detection plot, for the observed spectrum averaged

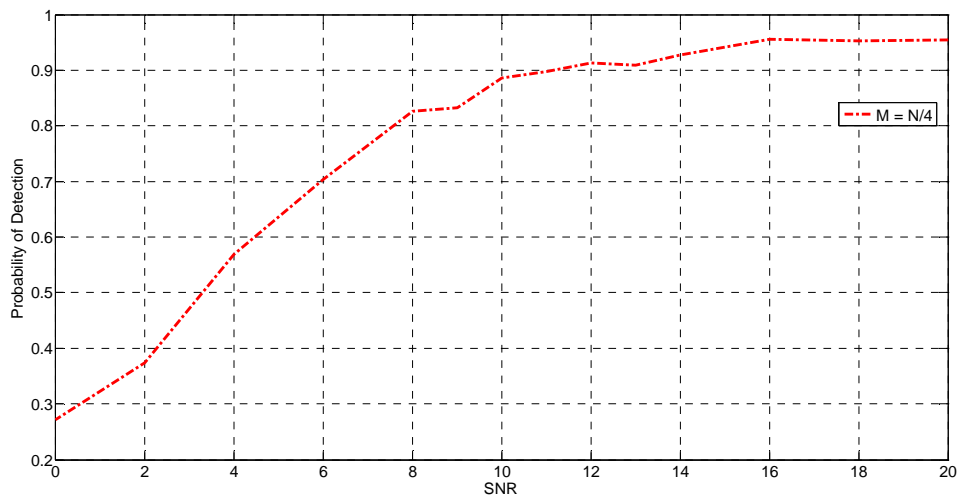


Figure 6.8: Probability of Detection for Un-Known Primary User Distribution –  
DVB-T Case 2

over 100 Monte Carlo realizations is shown in Figure 6.8. Working range according to IEEE 802.22 standard is for SNR greater than 11dB. Apriori knowledge improved the performance of the SBBSR algorithm by 22 dB. Observe that performance under apriori knowledge provides better probability of detection than spectrum sensing performed using the compressed sensing technique. The algorithm described in [16], is only applicable for the spectrum with flat PSDs. This proves the fact that spectrum sensing based on the SBBSR algorithm can accommodate, with better probability of detection, real time scenarios in contrast to the compressed sensing based technique.

### 6.3 CONCLUSION

In this chapter spectrum sensing was performed using the SBBSR algorithm. A more realistic signal model (Digital Video Broadcasting-Terrestrial) was assumed for the primary user. Transmission done by the primary user in observed spectrum is block sparse. The modified SBBSR algorithm was used while performing spectrum sensing. Based on the signal knowledge at the receiver different cases were dealt. Apriori information regarding the frequency band length proved helpful in all cases. The compressed sensing based spectrum sensing approach cannot handle such realistic scenario as PSDs of the frequency bands (in observed spectrum) are not flat. The cases considering apriori knowledge showed better results compared to the compressive sensing based spectrum sensing approach. In all the cases more than (approximately) 1dB improvement was achieved. In addition, lesser computational complexity proved a big edge.

## **CHAPTER 7**

### **CONCLUSION AND FUTURE WORK**

#### **7.1 CONCLUSION**

Efficient utilization of radio spectrum has gained recent attention. It has been observed that utilization of spectrum by the licensed wireless systems, for instance TV broadcasting, is quite low. Some of the frequency bands are overcrowded and some are barely used. Cognitive radio seems a tempting solution to resolve the perceived bandwidth scarcity versus under-utilization dilemma. Spectrum sensing is used to locate the unoccupied frequency bands or spectrum holes.

In Chapter 4, wavelet transform was applied on the received wideband signal at cognitive radios. The wavelet transform generates peaks at the locations where transmission is done by the primary users. In absence of noise, these peaks are sufficient to calculate the frequency band edges information whereas in presence of noise these peaks are accompanied by the noisy peaks as well. A threshold value was calculated using blind source separation technique. This value helped in suppressing the noisy peaks.

In Chapter 5, spectrum sensing for the wideband signal was performed using the structure based Bayesian sparse reconstruction algorithm (SBBSR). The SBBSR algorithm provides sub-Nyquist rate sampling solution to the wideband spectrum sensing problem. Spectrum sensing was performed for various cases using both, the SBBSR algorithm and the compressed sensing based technique. Results obtained from the SBBSR algorithm showed better performance compared to results obtained from the compressed sensing based spectrum sensing technique. In Chapter 6, it was assumed that the primary users are using the DVB-T OFDM system for transmission of their data. Spectrum sensing was performed using the SBBSR algorithm and better probability of detection results were achieved compared to the compressed sensing based spectrum sensing technique.

## **7.2 FUTURE WORK**

There is a possibility that a single cognitive radio may suffer from the multipath or shadowing effects. In such situation, results generated by spectrum sensing may cause interference between the cognitive radio and the primary user. Cooperative communication between the multiple cognitive radios can provide a solution to this problem. In such environment, multiple cognitive radios work together and improve the sensing performance. The proposed work in this thesis is based on the autonomous cognitive radio. This work can be extended to cooperative communication environment and hence sensing performance of all the cognitive radios can be improved.

## REFERENCES

- [1] S. M. Mishra, A. Sahai, and R. W. Brodersen, "Cooperative Sensing among Cognitive Radios," *IEEE International Conference on Communications*, pp. 1658-1663, 2006.
- [2] Federal Communications Commission - First Report and Order and Further Notice of Proposed Rulemaking, "Unlicensed operation in the TV broadcast bands," *FCC 06-156*, 2006.
- [3] Shared Spectrum Company, "Spectrum occupancy measurements." [Online]. Available: [www.sharespectrum.com](http://www.sharespectrum.com).
- [4] M. A. McHenry, "NSF spectrum occupancy measurements project summary," *Shared Spectrum Company Report*, 2005.
- [5] F. K. Jondral, "Cognitive Radio: A Communications Engineering View," *IEEE Wireless Communications*, pp. 28-33, 2007.
- [6] J. Mitola III and G. Maquire, "Cognitive Radio: Making Software Radios More Personal," *IEEE Pers. Comm.*, pp. 13-18, 1999.
- [7] Federal Communications Commission, "Spectrum Policy Task Force, Report ET Docket No. 02-135: November 2002."
- [8] S. Haykin, "Cognitive radio: brain-empowered wireless communications," *IEEE Journal on Selected Areas in Communications*, vol. 23, no. 2, pp. 201-220, Feb. 2005.
- [9] G. Y. Li, "Signal Processing in Cognitive Radio," *Proceedings of the IEEE*, vol. 97, no. 5, pp. 805-823, May 2009.
- [10] Mitola IIIJ, "Cognitive Radio: an integrated agent for software defined radio. PhD Thesis Computer communication laboratory," Royal Institute of Technology (KTH), 2000.

- [11] M. E. Sahin and H. Arslan, "System Design for Cognitive Radio Communications," in *2006 1st International Conference on Cognitive Radio Oriented Wireless Networks and Communications*, 2006, pp. 1-5.
- [12] T. Yucek and H. Arslan, "A survey of spectrum sensing algorithms for cognitive radio applications," *IEEE Communications Surveys & Tutorials*, vol. 11, no. 1, pp. 116-130, 2009.
- [13] G. Ganesan, "Agility improvement through cooperative diversity in cognitive radio," in *GLOBECOM '05. IEEE Global Telecommunications Conference, 2005.*, 2005, p. 5 pp.-2509.
- [14] D. Cabric, S. M. Mishra, and R. W. Brodersen, "Implementation issues in spectrum sensing for cognitive radios," in *Conference Record of the Thirty-Eighth Asilomar Conference on Signals, Systems and Computers, 2004.*, vol. 1, pp. 772-776.
- [15] R. Chen and J.-M. Park, "Ensuring Trustworthy Spectrum Sensing in Cognitive Radio Networks," in *2006 1st IEEE Workshop on Networking Technologies for Software Defined Radio Networks*, 2006, pp. 110-119.
- [16] Z. Tian and G. B. Giannakis, "Compressed Sensing for Wideband Cognitive Radios," in *2007 IEEE International Conference on Acoustics, Speech and Signal Processing - ICASSP '07*, 2007, p. IV-1357-IV-1360.
- [17] M. Unser, "Sampling-50 years after Shannon," *Proceedings of the IEEE*, vol. 88, no. 4, pp. 569-587, Apr. 2000.
- [18] R. G. Baraniuk, "Compressive Sensing," *Proceeding of IEEE Signal Processing Magazine*, pp. 118-124, 2007.
- [19] B. Hayes, "The Best Bits," *American Scientist*, 2009.
- [20] P. Sen and S. Darabi, "A novel framework for imaging using compressed sensing," in *2009 16th IEEE International Conference on Image Processing (ICIP)*, 2009, pp. 2133-2136.
- [21] "http://nuit-blanche.blogspot.com/2007/03/while-reading-compressive-radar-imaging.html." [Online]. Available: <http://nuit-blanche.blogspot.com/2007/03/while-reading-compressive-radar-imaging.html>.
- [22] E. J. Candes, J. Romberg, and T. Tao, "Robust uncertainty principles: exact signal reconstruction from highly incomplete frequency information," *IEEE Transactions on Information Theory*, vol. 52, no. 2, pp. 489-509, Feb. 2006.

- [23] Y. Lamelas Polo, "Compressive Wideband Spectrum Sensing for Cognitive Radio Applications," Delft University of Technology, 2008.
- [24] J. Romberg and M. Wakin, "Tutorial on Compressive Sensing," *IEEE Statistical Signal Processing Workshop*, 2007.
- [25] E. J. Candes and M. B. Wakin, "An Introduction To Compressive Sampling," *IEEE Signal Processing Magazine*, vol. 25, no. 2, pp. 21-30, Mar. 2008.
- [26] E. Candes and J. Romberg, "Sparsity and incoherence in compressive sampling," *Inverse Problems*, vol. 23(3), pp. 969-985, 2007.
- [27] P. J. Huber, "Projection pursuit," *The Annals of Statistics*, vol. 13, pp. 435-475, 1985.
- [28] Y. C. Pati, R. Rezaifar, and P. S. Krishnaprasad, "Orthogonal matching pursuit: recursive function approximation with applications to wavelet decomposition," in *Proceedings of 27th Asilomar Conference on Signals, Systems and Computers*, pp. 40-44.
- [29] C. La and M. Do, "Signal reconstruction using sparse tree representations," *SPIE Wavelets XI*, vol. 5914, 2005.
- [30] I. F. Gorodnitsky and B. D. Rao, "Sparse signal reconstruction from limited data using FOCUSS: a re-weighted minimum norm algorithm," *IEEE Transactions on Signal Processing*, vol. 45, no. 3, pp. 600-616, Mar. 1997.
- [31] J.-F. Cardoso, "Blind signal separation: statistical principles," *Proceedings of the IEEE*, vol. 86, no. 10, pp. 2009-2025, 1998.
- [32] V. G. REJU, "Blind Separation of Speech Mixtures," PhD Thesis, Nanyang Technological University, 2009.
- [33] M. Abbas, T. Ballal, and N. Gbric, "Blind Source Separation Using Time-Frequency Masking," *Radioengineering*, vol. 16, pp. 96-100, 2007.
- [34] H. Sarvanko, M. Mustonen, A. Hekkala, A. Mammela, M. Matinmikko, and M. Katz, "Cooperative and noncooperative spectrum sensing techniques using Welch's periodogram in cognitive radios," in *2008 First International Workshop on Cognitive Radio and Advanced Spectrum Management*, 2008, pp. 1-5.
- [35] H. Tang, "Some physical layer issues of wide-band cognitive radio systems," in *First IEEE International Symposium on New Frontiers in Dynamic Spectrum Access Networks, 2005. DySPAN 2005.*, 2005, pp. 151-159.

- [36] Z. Tian and G. B. Giannakis, "A Wavelet Approach to Wideband Spectrum Sensing for Cognitive Radios," in *2006 1st International Conference on Cognitive Radio Oriented Wireless Networks and Communications*, 2006, pp. 1-5.
- [37] X. Chen, L. Zhao, and J. Li, "A modified spectrum sensing method for wideband cognitive radio based on compressive sensing," in *2009 Fourth International Conference on Communications and Networking in China*, 2009, pp. 1-5.
- [38] V. Havary-Nassab, S. Hassan, and S. Valaee, "Compressive detection for wide-band spectrum sensing," in *2010 IEEE International Conference on Acoustics, Speech and Signal Processing*, 2010, pp. 3094-3097.
- [39] D. Sundman, S. Chatterjee, and M. Skoglund, "On the use of compressive sampling for wide-band spectrum sensing," in *The 10th IEEE International Symposium on Signal Processing and Information Technology*, 2010, pp. 354-359.
- [40] Y. L. Polo, A. Pandharipande, and G. Leus, "Compressive wide-band spectrum sensing," in *2009 IEEE International Conference on Acoustics, Speech and Signal Processing*, 2009, no. 3, pp. 2337-2340.
- [41] Y. Liu and Q. Wan, "Compressive Wideband Spectrum Sensing for Fixed Frequency Spectrum Allocation," *Science And Technology*, p. 21, May 2010.
- [42] E. Candes, J. Romberg, and T. Tao, "Stable signal recovery from incomplete and inaccurate measurements," *Communications on Pure and Applied Mathematics*, vol. 59, no. 8, pp. 1207-1223, 2006.
- [43] Y. Ye, "Interior-Point Polynomial Algorithms in Convex Programming (Y. Nesterov and A. Nemirovskii)," *SIAM Review*, vol. 36, no. 4, p. 682, 1994.
- [44] J. A. Tropp and A. C. Gilbert, "Signal Recovery From Random Measurements Via Orthogonal Matching Pursuit," *IEEE Transactions on Information Theory*, vol. 53, no. 12, pp. 4655-4666, Dec. 2007.
- [45] D. Needell and R. Vershynin, "Uniform Uncertainty Principle and Signal Recovery via Regularized Orthogonal Matching Pursuit," *Foundations of Computational Mathematics*, vol. 9, no. 3, pp. 317-334, Jun. 2008.
- [46] J. A. Tropp, "A comparison principle for functions of a uniformly random subspace," *Probability Theory and Related Fields*, Apr. 2011.
- [47] T. Y. Al-naffouri and A. A. Quadeer, "Structure Based Bayesian Sparse Reconstruction," *IEEE Transactions on Signal Processing*, 2011.
- [48] S. Ji, Y. Xue, and L. Carin, "Bayesian Compressive Sensing," *IEEE Transactions on Signal Processing*, vol. 56, no. 6, pp. 2346-2356, Jun. 2008.



- [49] X. Tan and J. Li, "Computationally Efficient Sparse Bayesian Learning via Belief Propagation," *IEEE Transactions on Signal Processing*, vol. 58, no. 4, pp. 2010-2021, Apr. 2010.
- [50] A. Montanari, B. Prabhakar, and D. Tse, "Belief Propagation Based Multi-User Detection," *Allerton Conf. on Communications, Control and Computing*, 2005.
- [51] P. Schniter, L. C. Potter, and J. Ziniel, "Fast bayesian matching pursuit," in *2008 Information Theory and Applications Workshop*, 2008, pp. 326-333.
- [52] E. G. Larsson and Y. Selen, "Linear Regression With a Sparse Parameter Vector," *IEEE Transactions on Signal Processing*, vol. 55, no. 2, pp. 451-460, Feb. 2007.
- [53] S. Mallat and W. L. Hwang, "Singularity detection and processing with wavelets," *IEEE Transactions on Information Theory*, vol. 38, no. 2, pp. 617-643, Mar. 1992.
- [54] J. Ma and X. Zhang, "Blind Source Separation Algorithm Based on Maximum Signal Noise Ratio," in *2008 First International Conference on Intelligent Networks and Intelligent Systems*, 2008, no. 60672184, pp. 625-628.
- [55] S. D. Jadhav and A. S. Bhalchandra, "Blind Source Separation: Trends of New Age – a Review," *IET International Conference on Wireless, Mobile and Multimedia Networks*, 2008., pp. 251-254, 2008.
- [56] Y. Zheng, X. Xie, and L. Yang, "Cooperative spectrum sensing based on blind source separation for cognitive radio," in *2009 First International Conference on Future Information Networks*, 2009, pp. 398-402.
- [57] C. R. Stevenson, C. Cordeiro, E. Sofer, and G. Chouinard, "Functional requirements for the 802.22 WRAN standard," *IEEE 802.22-05/0007r46*, 2005.
- [58] ETS 300 744, "Digital broadcasting systems for television, sound and data services; framing structure, channel coding, and modulation for digital terrestrial television," *European Telecommunication Standard, Doc. 300 744*, 1997.
- [59] H.-S. Chen, W. Gao, and D. G. Daut, "Spectrum Sensing for OFDM Systems Employing Pilot Tones and Application to DVB-T OFDM," *IEEE International Conference on Communications, 2008. ICC '08.*, pp. 3421 - 3426, 2008.
- [60] R. V. Nee and R. Prasad, *OFDM Wireless Multimedia Communications*. Norwood, MA: Artech House, 2000.
- [61] M. A. Ingram and G. Acosta, "OFDM Simulation Using Matlab," Georgia Institute of Technology, 2000.

## VITA

**Nationality:** Pakistan

**Present Address:** P.O.Box 8648, Dhahran, 31261, Saudi Arabia

**Permanent Address:** House No. 194, Street No. 12, Sector G-15/4, Islamabad, Pakistan

**Email Address:** zahidsaleem\_1987@hotmail.com

**Mobile Number:** +966-542-759418

**Zahid Saleem** received his B.S. degree in Telecommunication Engineering from National University of Computer and Emerging Sciences, Islamabad, Pakistan, in 2009. He is currently pursuing his M.S. degree in Electrical Engineering from King Fahd University of Petroleum and Minerals, Dhahran, Saudi Arabia. His research interest lies in signal processing techniques for cognitive radios and noise cancellation techniques.